
**Advanced Multicomponent Seismic Software**

# Analysis of seismic data recorded in August 2025 by network C8 (stations SV1S-SV5S) at Aquistore test site

Report AQ-2025-08-IM

December 08, 2025

Igor Morozov

igor.morozov@usask.ca

***Contents***

## *1. Station performance*

Station performance for August 2025 is summarized in Figure 1, and state-of-health data are shown in Figure 2. Of the previously noted performance issues, only poor data quality from station SV3S still persists, apparently due to a faulty sensor cable.

### Data recovery

Except for station SV2S which had a non-operational modem, data recovery from all channels was nearly 100% (Figure 1).

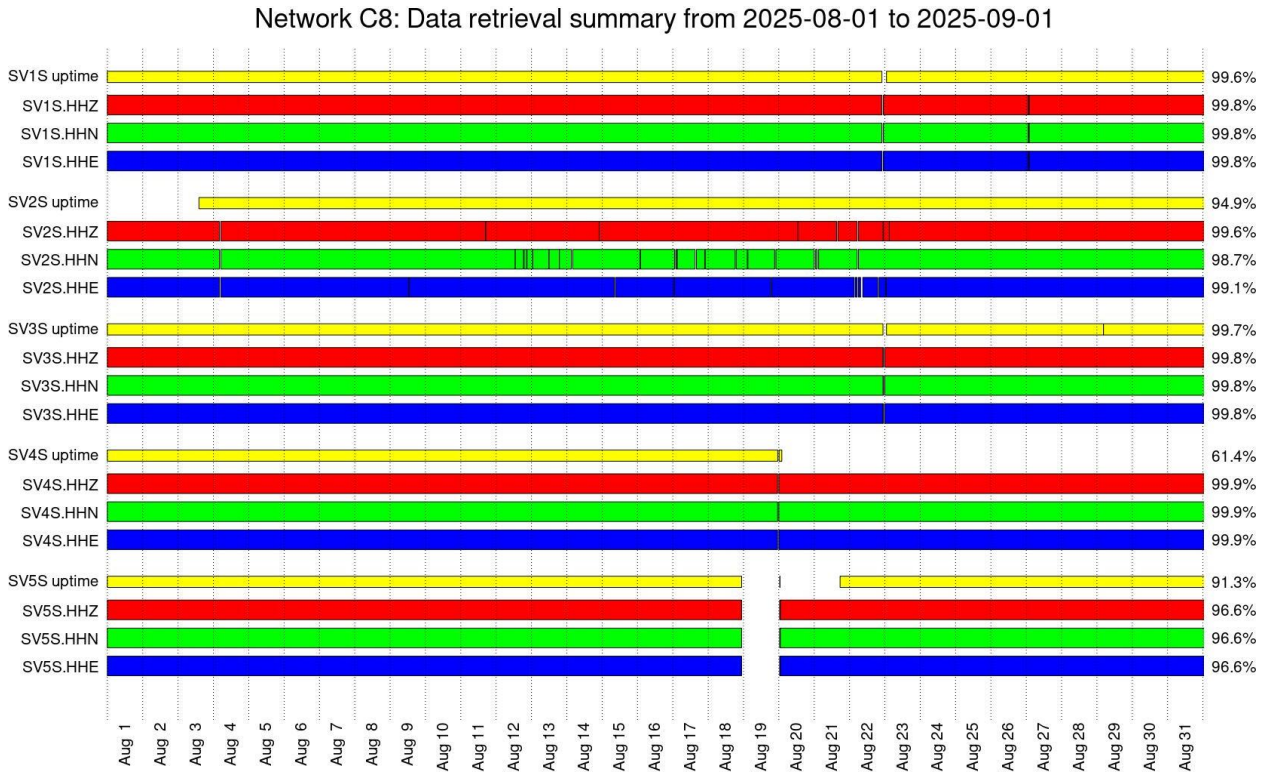


Figure 1. Retrieved data intervals for all channels (red, green, and blue bars) and uptimes (yellow). Total percentages of measured uptime and data retrieval are shown on the right.

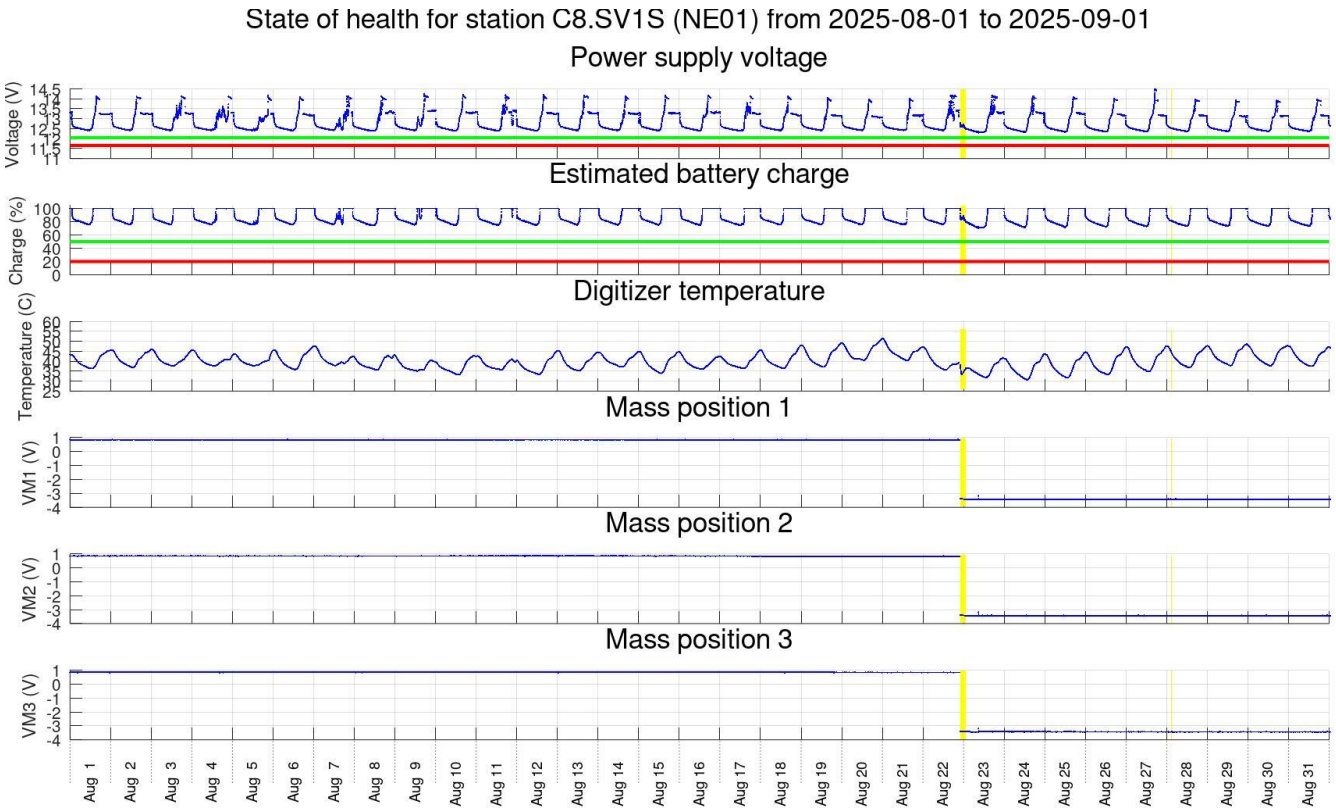


Figure 2. State of health parameters for each station (SV1S here). Image headings: power supply voltage, estimated battery charge levels, temperature on board, voltages measuring mass positions. The abrupt change in “mass positions” was due to replacing the sensor cable.

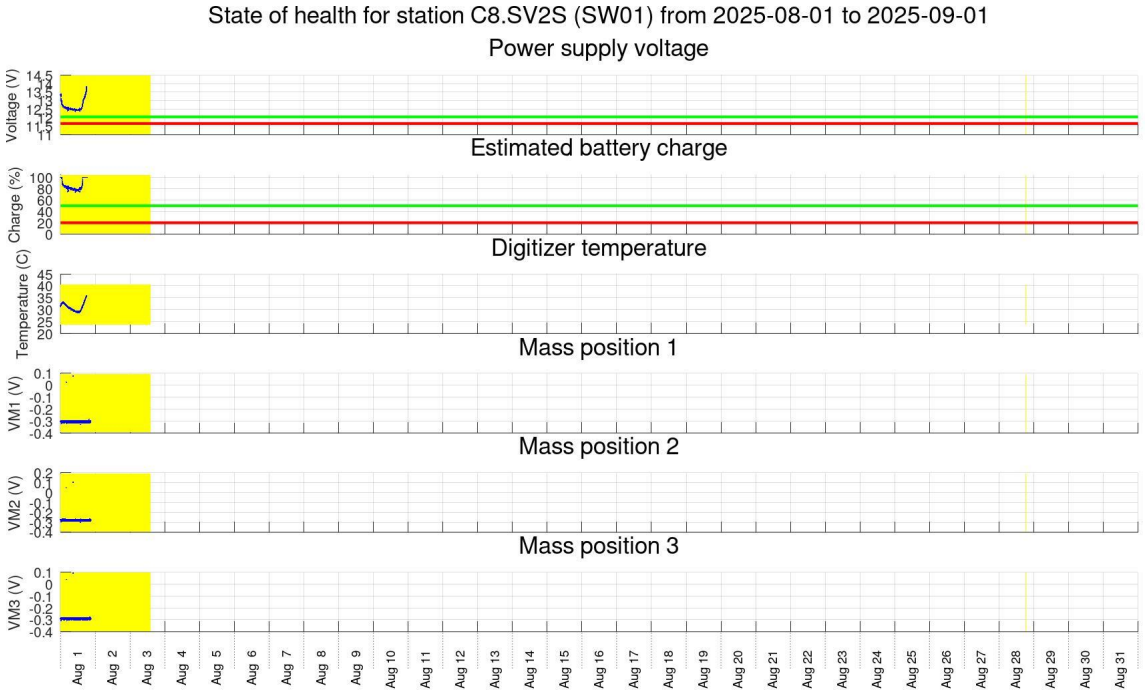


Figure 2, continued, station SV2S. Absence of data was due to an unfortunate lapse in my manual log downloading procedure

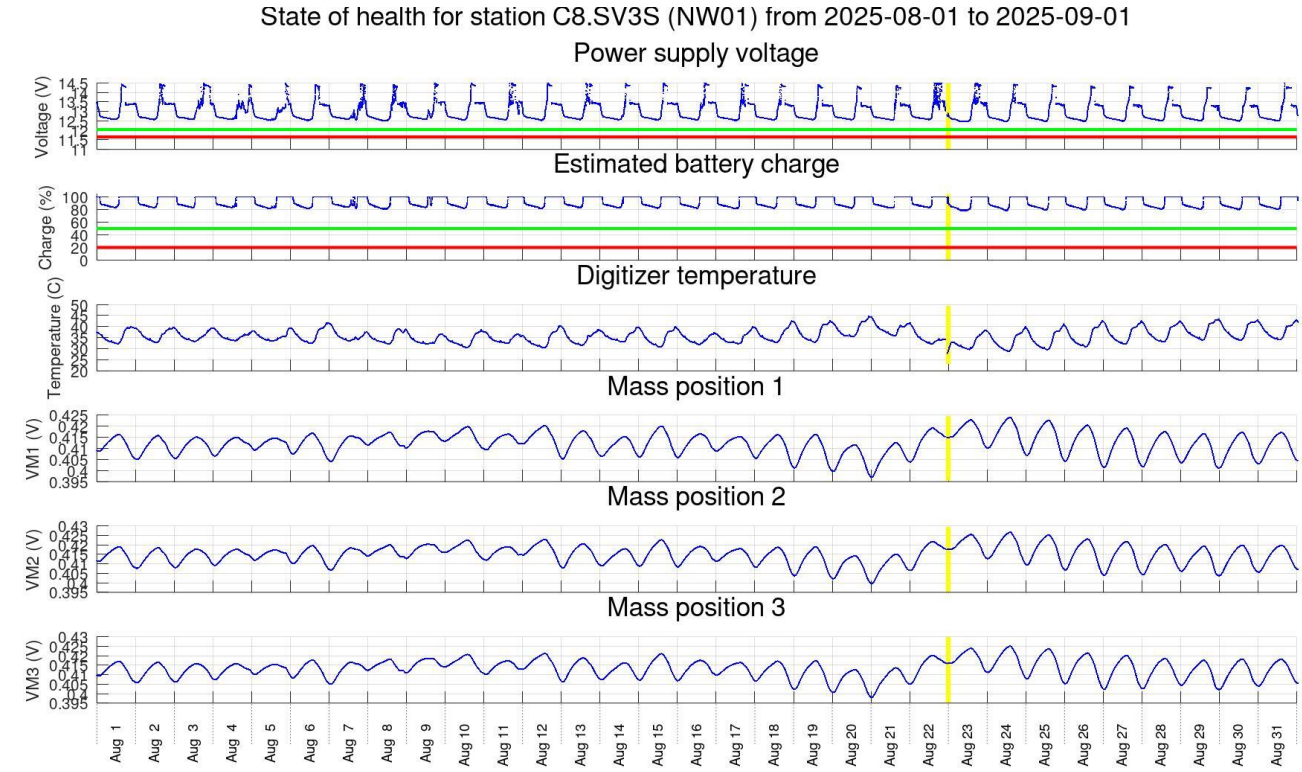


Figure 2, continued, station SV3S.

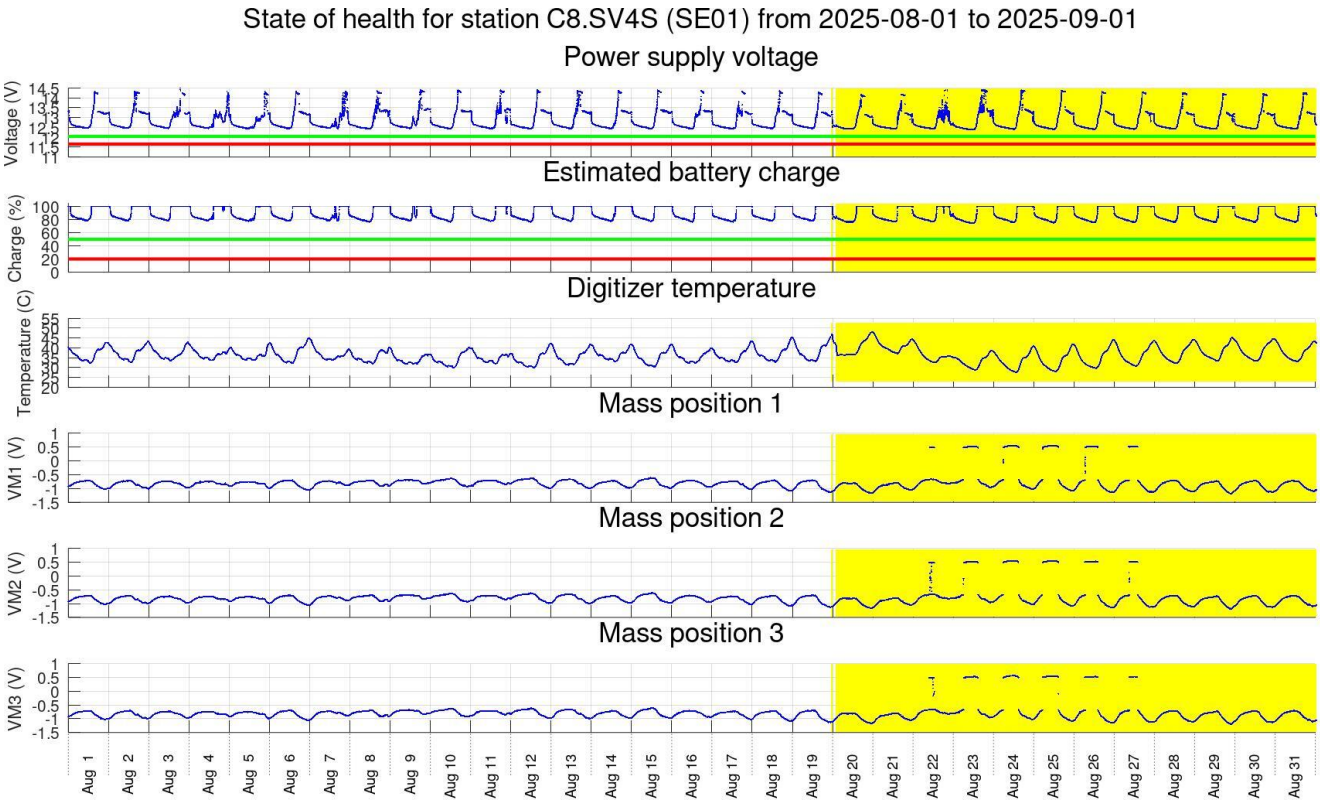


Figure 2, continued, station SV4S.

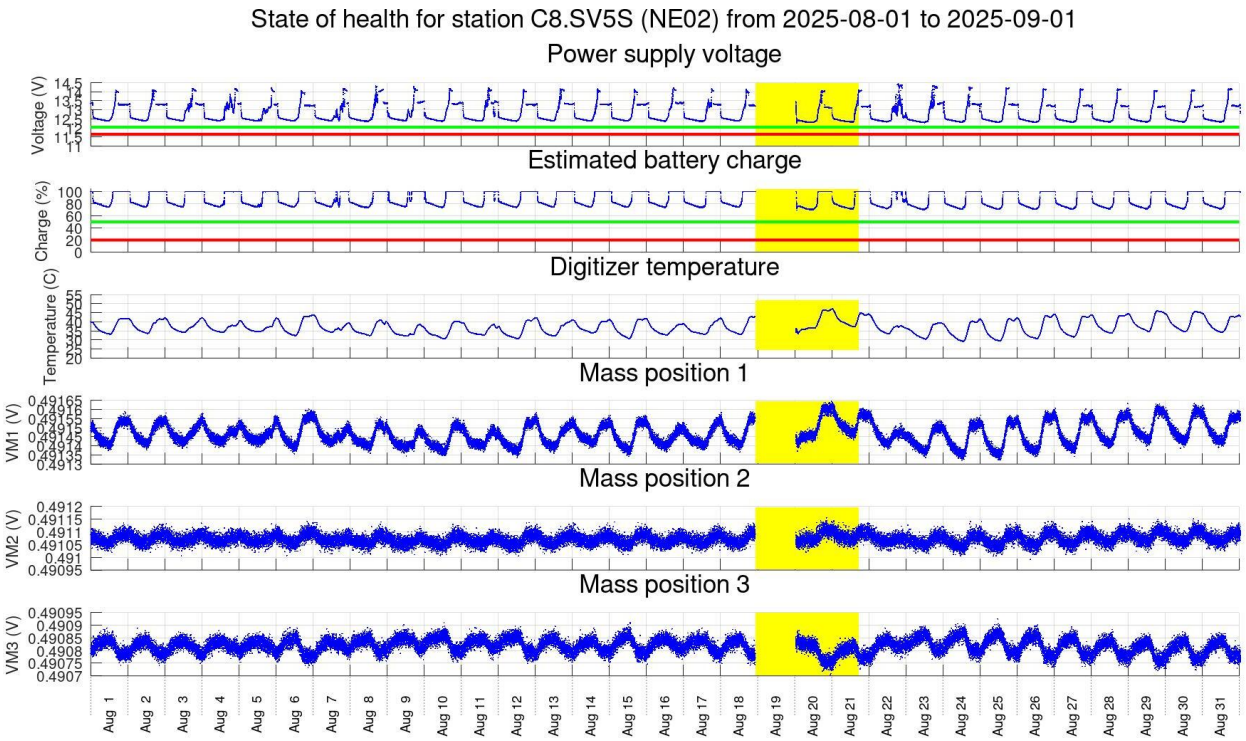

Figure 2, continued, station SV5S.

## 2. *Data quality*

Figure 3 shows two measures of data quality evaluated for each channel:

1) Numbers of spikes and tears (sharp changes of DC level) within 1-hour time intervals;
2) 1-hour root-mean square (RMS) average amplitudes in each channel.

From station SV2S, no data were received, and it is not shown in Figure 3 .

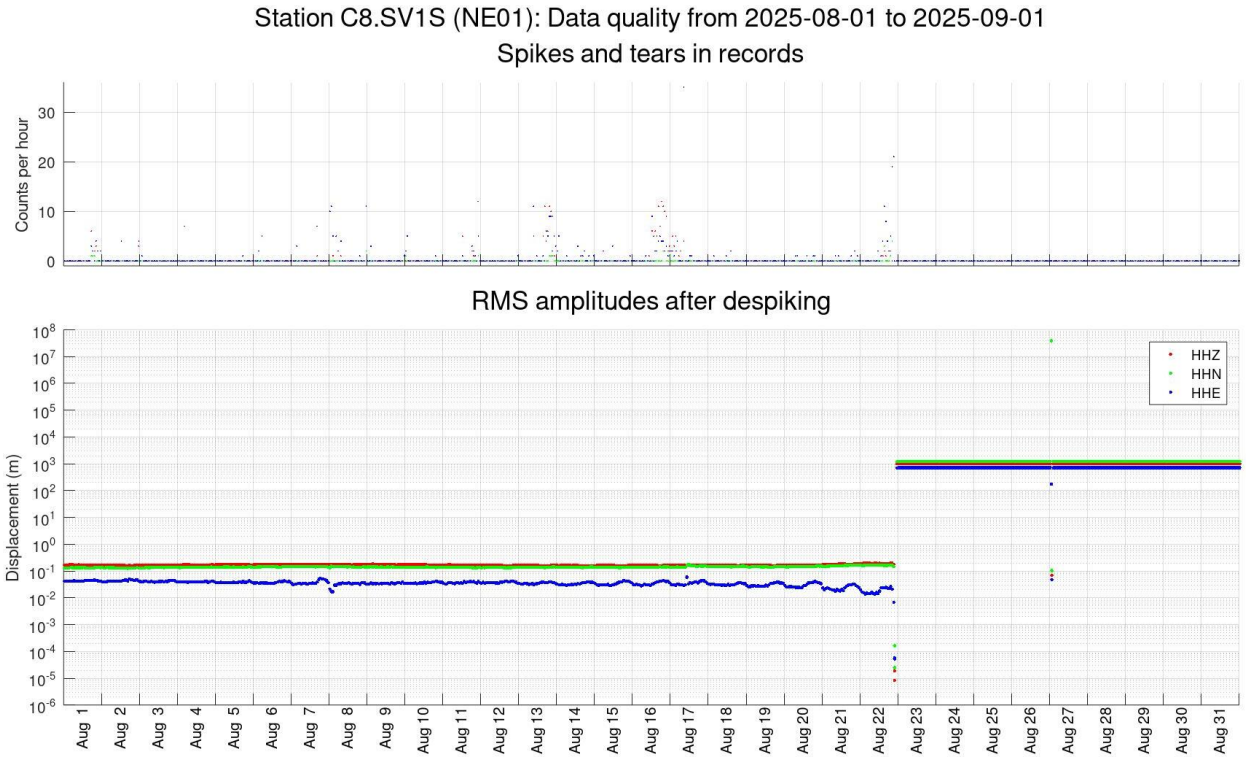


Figure 3. Measures of data quality in hour-long intervals. Station names and time intervals are indicated in plot headings (SV1S in this plot). Red, green, and blue colors correspond to channels HHZ, HHN, and HHE, respectively (as in Figure 1). The jump in amplitudes (apparently to normal values) occurred after replacing the sensor cable.

***Top panels***: Numbers of spikes and tears per hour auto-detected in data records.

***Bottom panels***: RMS ground displacements (meters).

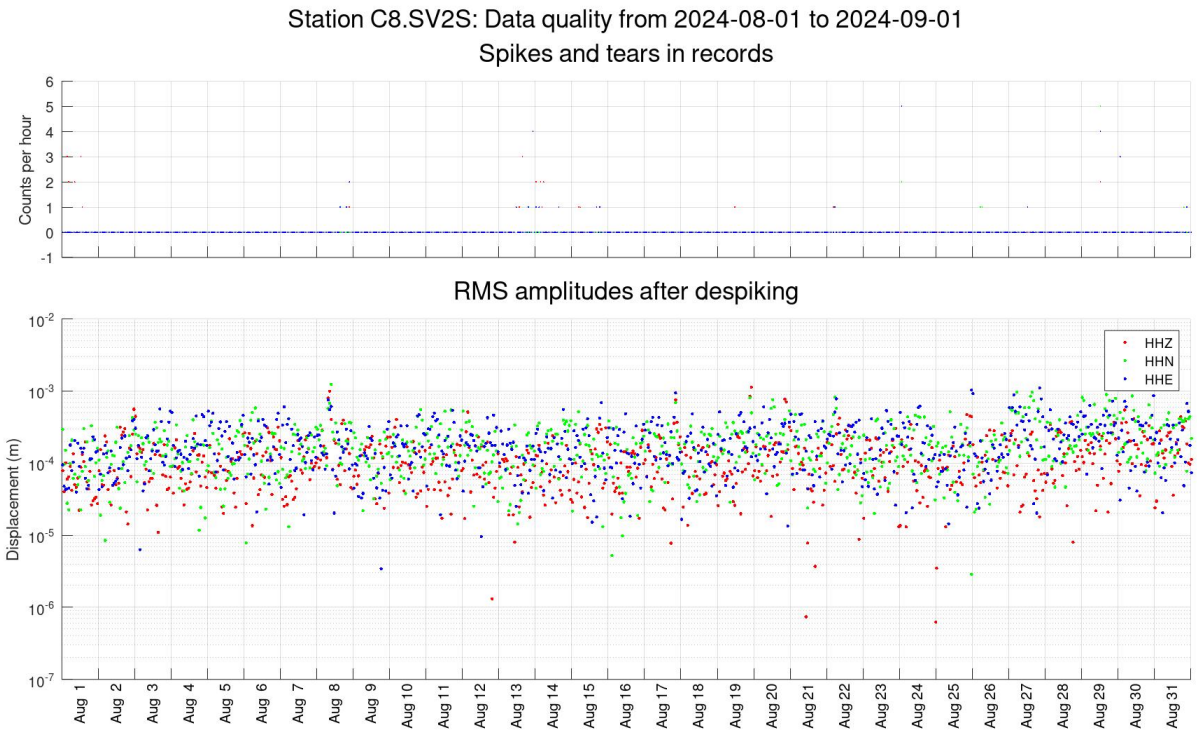


Figure 3, continued. Station SV2S.

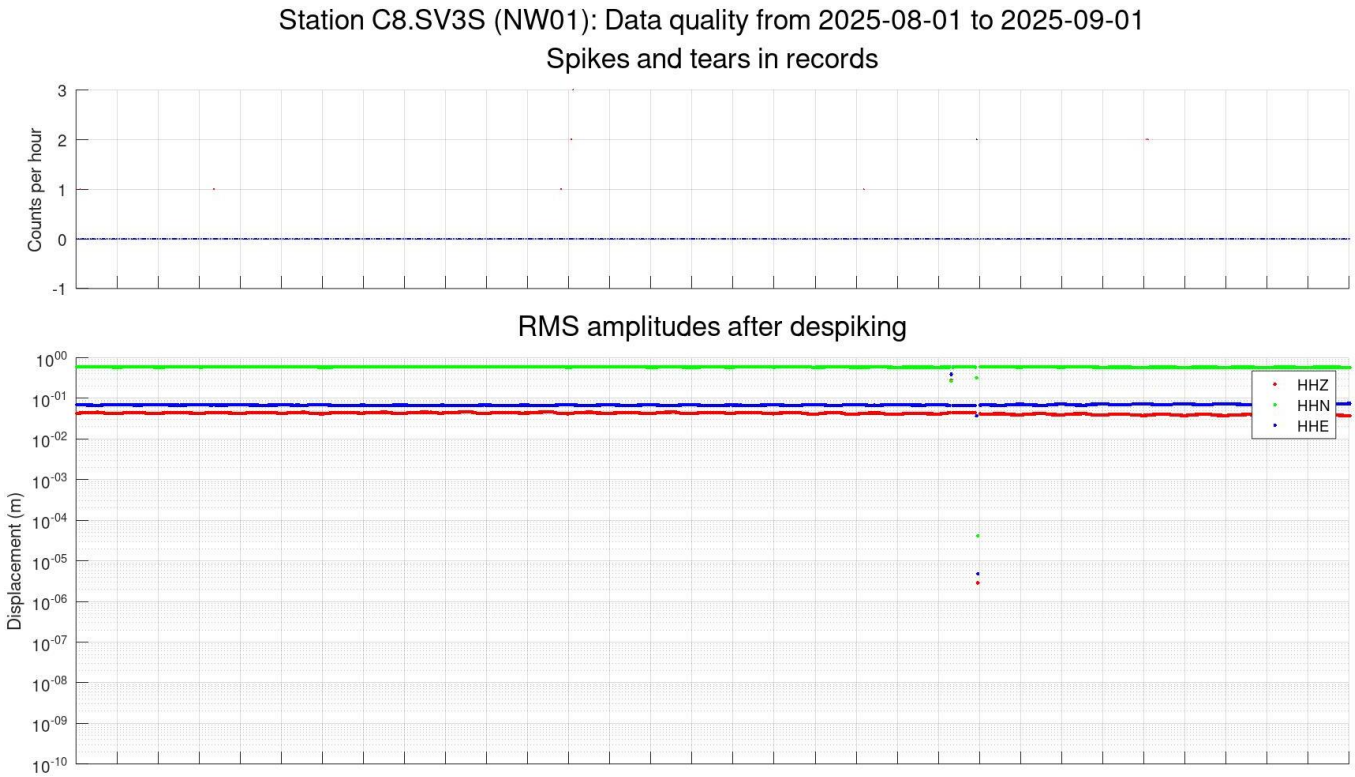


Figure 3, continued. Station SV3S.

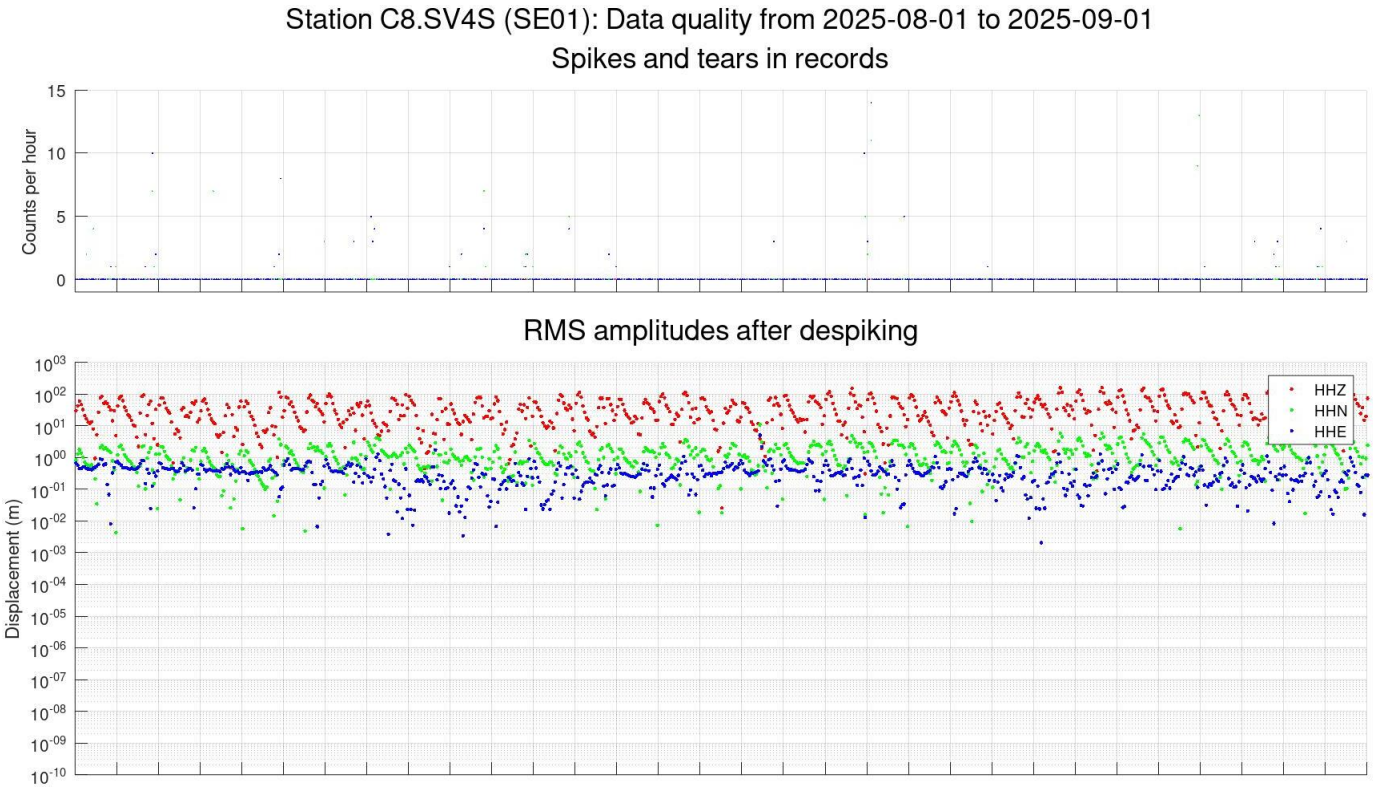


Figure 3, continued. Station SV4S.

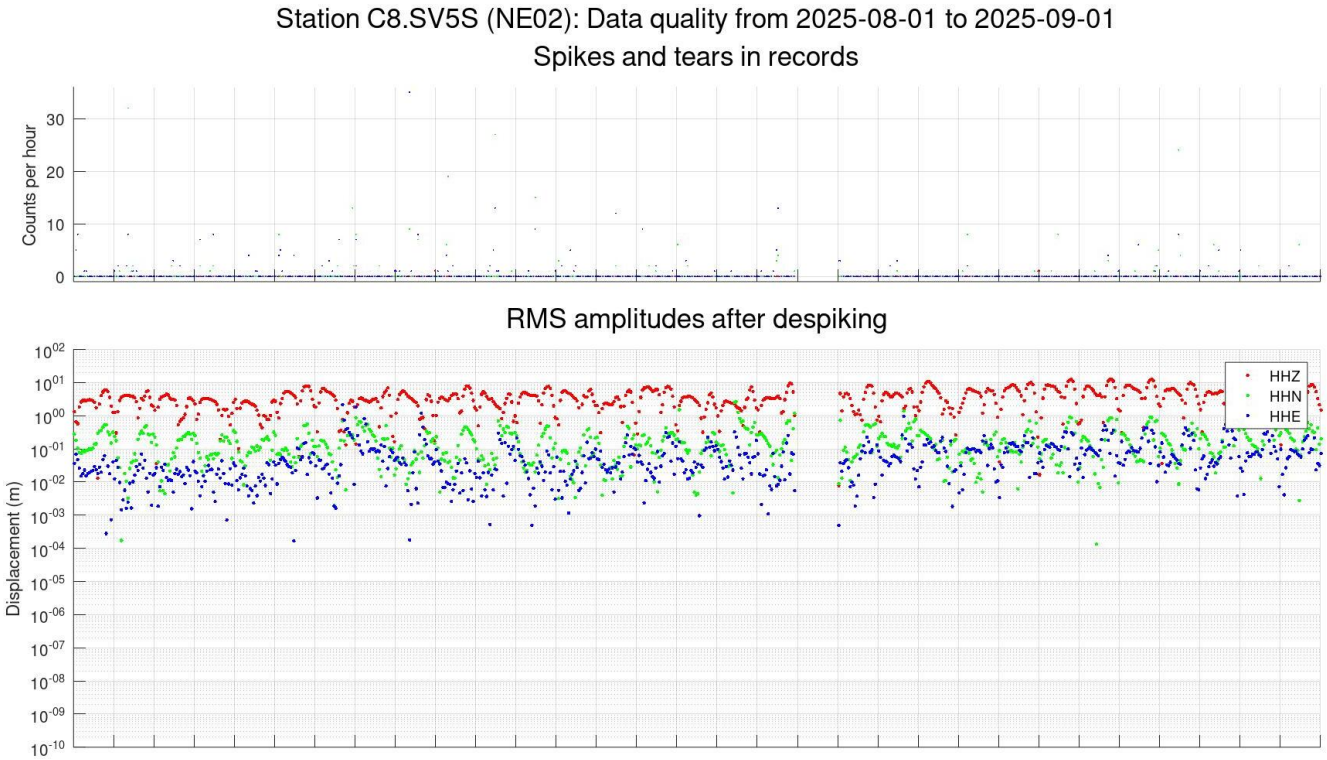


Figure 3, continued. Station SV5S

## 3. Processing procedure and parameters

The data processing procedure was described in previous reports. Parameters of the STA/LTA algorithm in two frequency bands are shown in Table 1. Only one frequency band (#1) is currently used.

Table 1. STA/LTA algorithm parameters

| Parameter | For regional events | For local and target events |
|---|---|---|
| Filter band 1 | 0.5 – 10 Hz | 3 – 20 Hz |
| Filter band 2 | 3 – 50 Hz | 10 – 50 Hz |
| STA window | 3 s | 0.2 s |
| LTA window | 15 s | 2 s |
| Floor on normalized STA/LTA ratio | 0.5 | 0.6 |
| Maximum accepted STA/LTA ratio | 0.99 | 0.99 |
| Relative level of triggering | 0.5 | 0.5 |
| Relative level of detriggering | 0.5 | 0.5 |
| Number of channels for triggering | 3 | 3 |

## 4. Seismic event detection

The classification of seismic events used in these reports and the corresponding numbers of events detected in August 2025 are shown in Table 2.

Table 2. Classification of seismic events detected at Aquistore broadband seismic array

| Event class code | Class name | Identification criteria | Number of detections in this report |
|---|---|---|---|
| 1 | Teleseismic | Hypocentral distance $D > 1000$ km, presence in catalogues | 35 |
| 2 | Regional | $100 < D < 1000$ km, presence in catalogues | 1 |
| 3 | Local | Approx. $4 < D < 100$ km | ---------- |
| 3a | Possible mine blasts | Characteristic waveforms, amplitudes, back-azimuths east of Aquistore, | 13 |

| | | | |
|---|---|---|---|
| | | *D* about 12-15 km | |
| 3b | Mining-related | Low frequencies,<br>extended repeated wavetrains<br>low arrival velocities related to surface waves | 6 (selected from numerous occurrences) |
| 4 | Proximity (close local) | D < 3-4 km, deviation of array moveouts from plane-wave patterns, high frequency | ---------- |
| 4a* | Surface sources near array | Large travel-time moveouts,<br>variable back-azimuths | 6* |
| 4b* | Target zone | Source at recognizable nonzero depth, small travel-time moveouts, high frequency | 0* |

*) Because of using only three stations, classes 4a and 4b are not differentiated in current report.

## Automatic detections

The procedure of multichannel automatic detections is currently being revised and not shown in the present report.

## Event bulletins

Earthquake data bulletins for the period of this report were obtained from NEIC (USGS) and NRCan web services (Figure ). Events larger than magnitude 2.5 were taken from USGS, and all available events obtained from NRCan. Events with magnitudes above the selected $magnitude \propto distance^{1.5}$ threshold (dashed green line in Figure Error: Reference source not found) were reviewed interactively (next section).

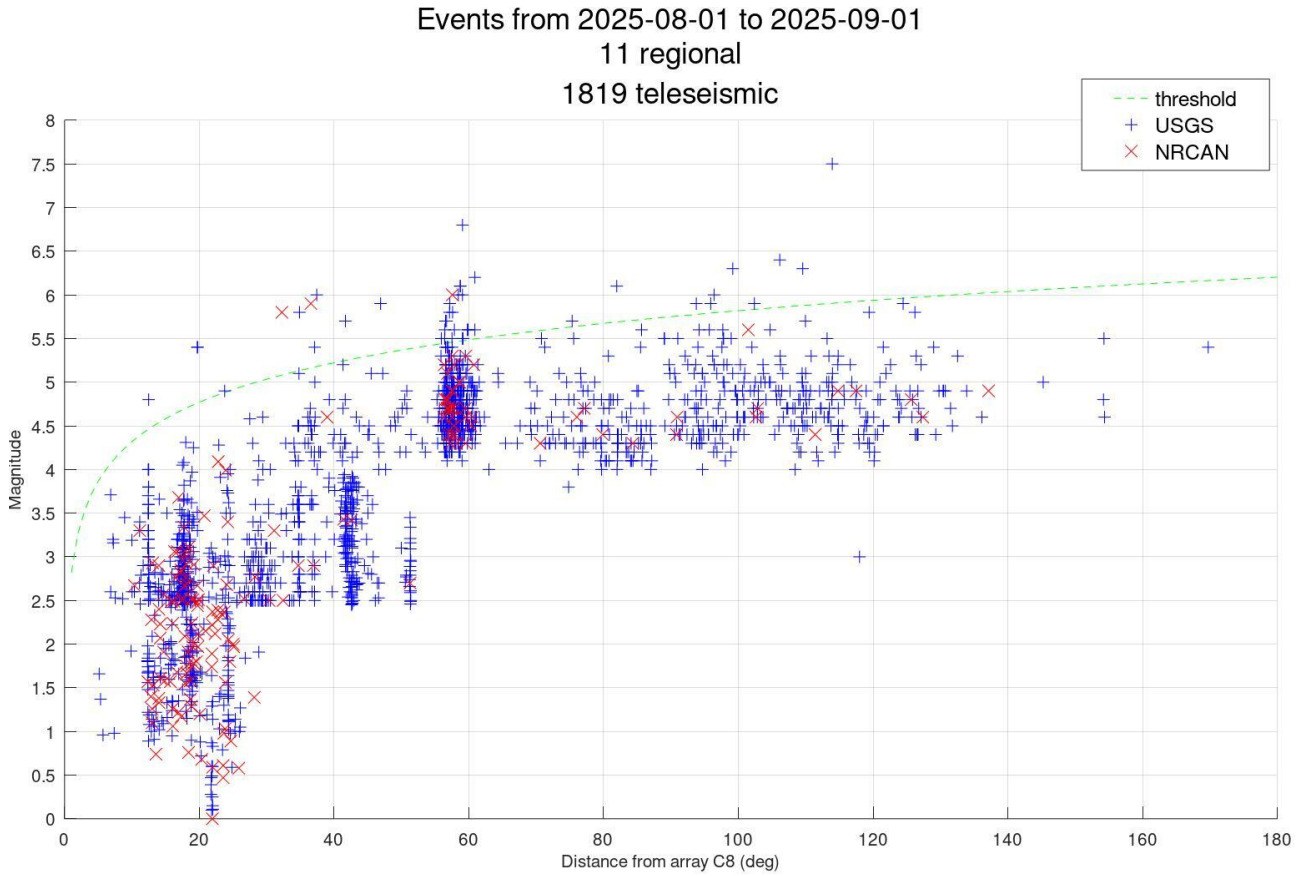


Figure 5. Magnitudes and distances from Aquistore for earthquake parameters downloaded from USGS and NRCan databases (legend). Dashed green line shows the detection threshold above which a manual review of events was performed.

## Teleseismic events (class 1)

Above the threshold line in Figure 5Error: Reference source not found, 35 teleseismic events (class 1 in Table 2) were identified in August 2025. To make clearer teleseismic earthquake displays, I increased the time intervals to include S-wave arrivals and lowered the frequency band.

Time zeros in Figure 6 plots are located at the times of P-wave arrivals at the Aquistore array predicted in the reference model IASP91, and blue bars near *time* = 0 are interactive picks of P-wave arrival times.

Note that although all records are shown in the following plots, records from station SV3S are often poor (noisy and low-amplitude) because of the faulty cable.

.

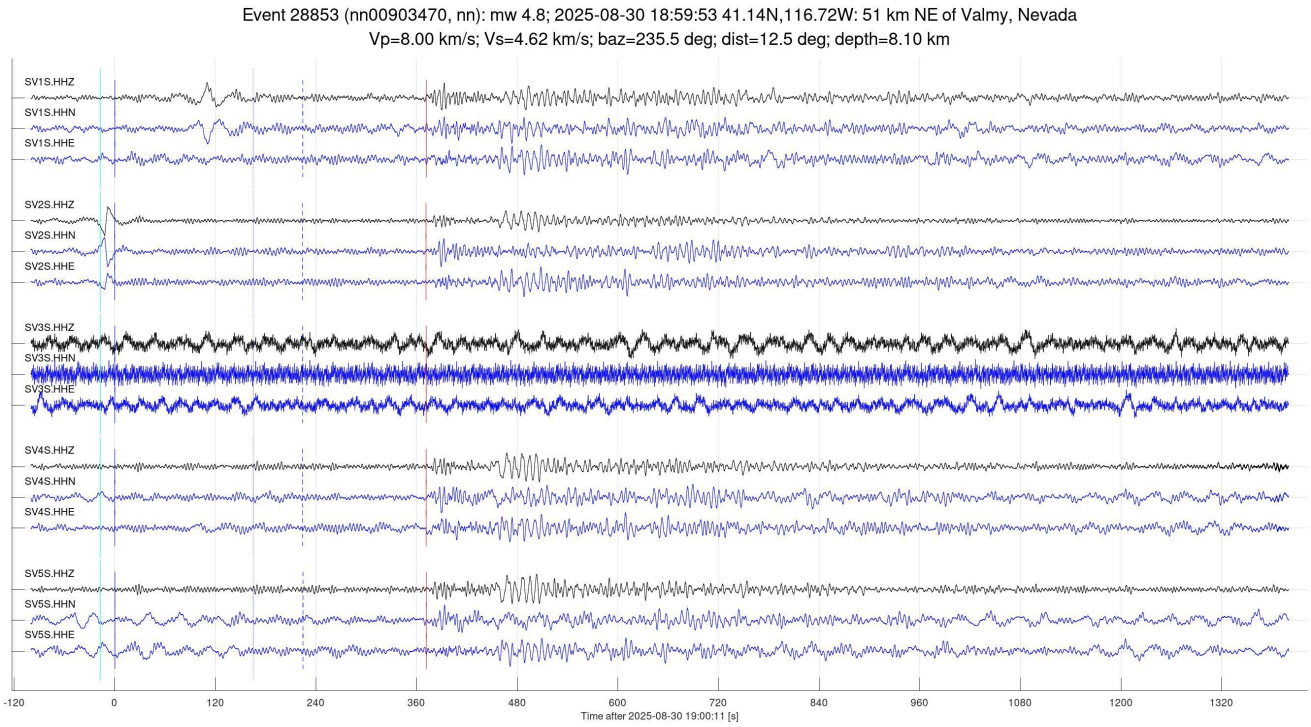


Figure 6. Sample teleseismic events detected at Aquistore in August 2025. Catalogue IDs, times, distances in degrees, source coordinates and localities, back-azimuths ('baz='), distances ('dist=') and source depths are shown in plot headings. Vertical-component records are shown in black, and horizontal components in blue. Colour bars above some records show single-channel STA/LTA values for accepted detections of these events.

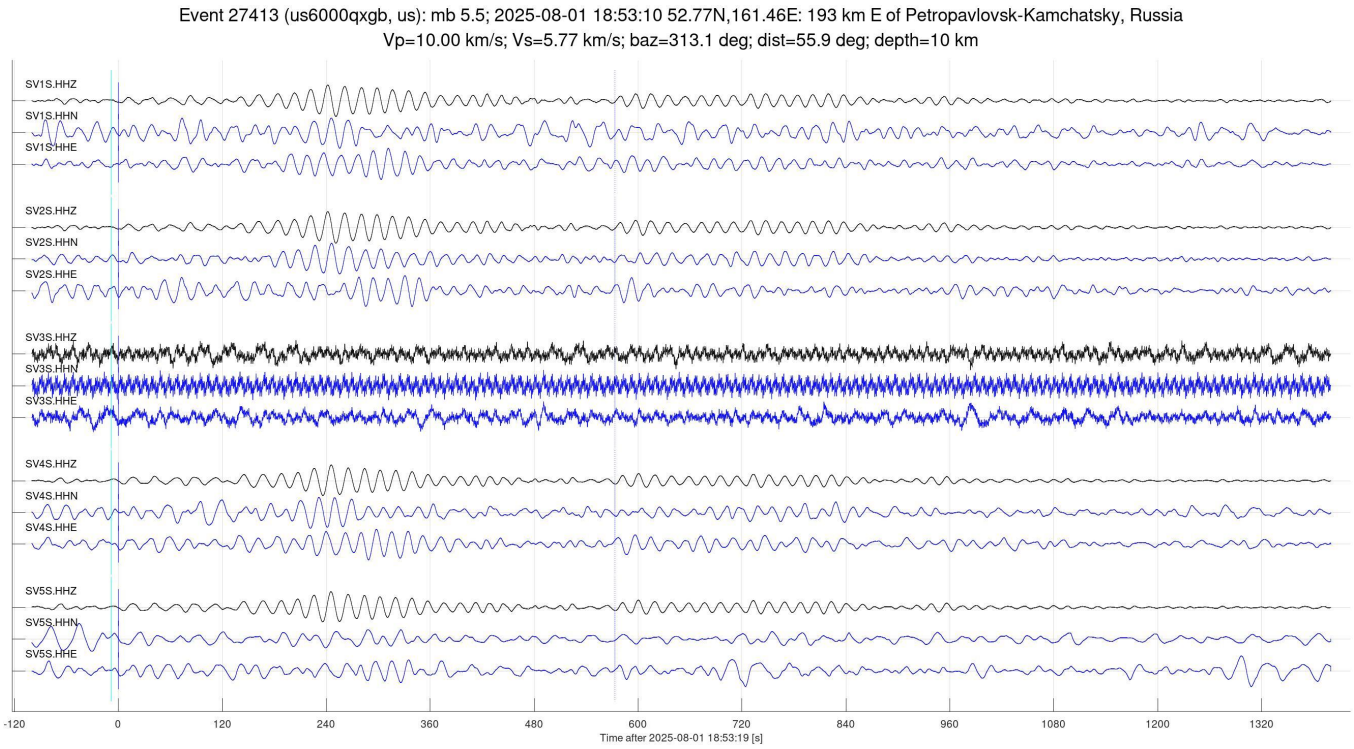


Figure 6, continued.

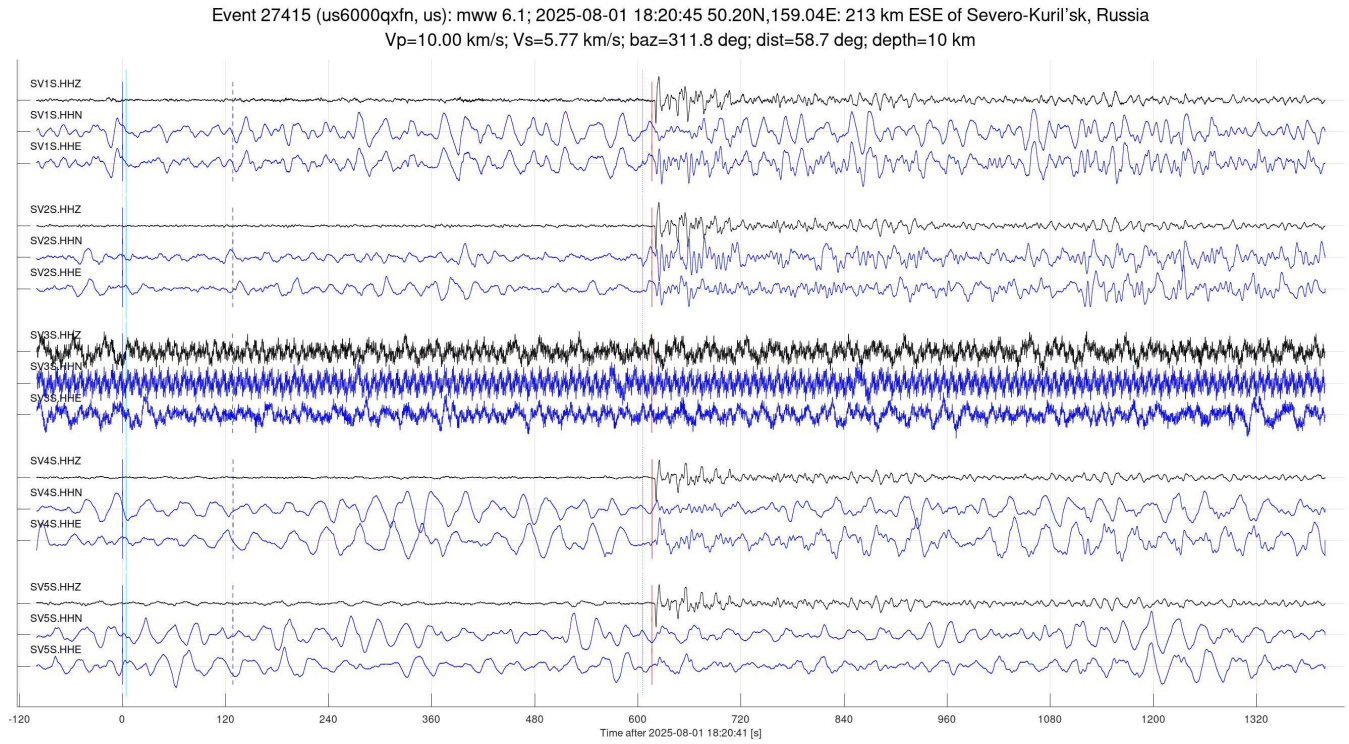


Figure 6, continued.

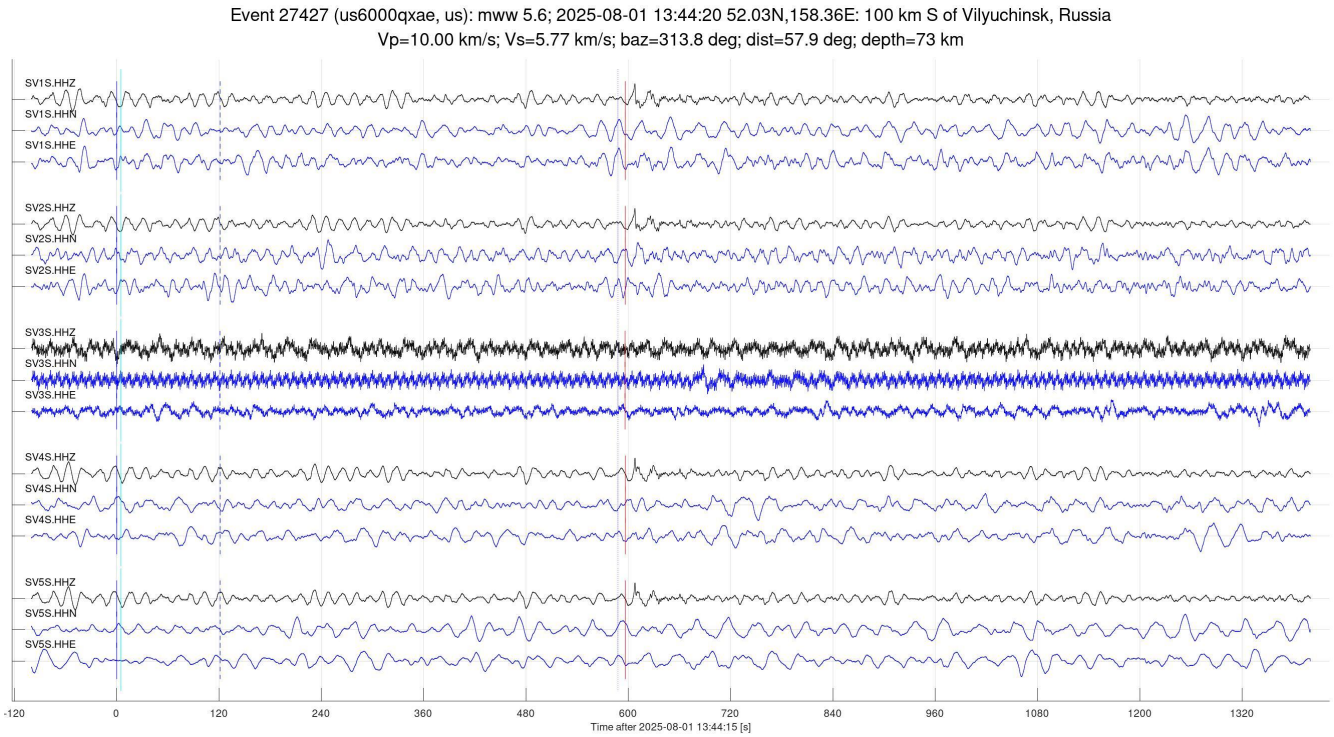


Figure 6, continued.

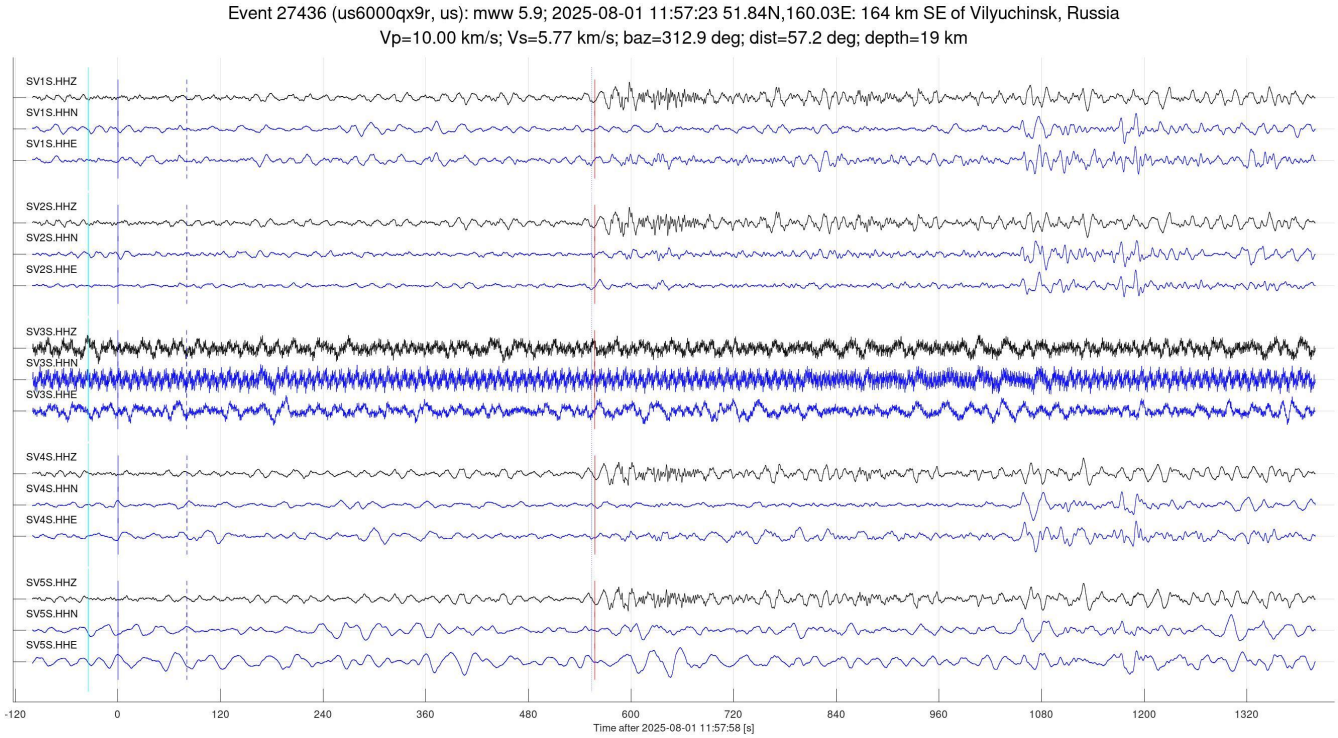


Figure 6, continued.

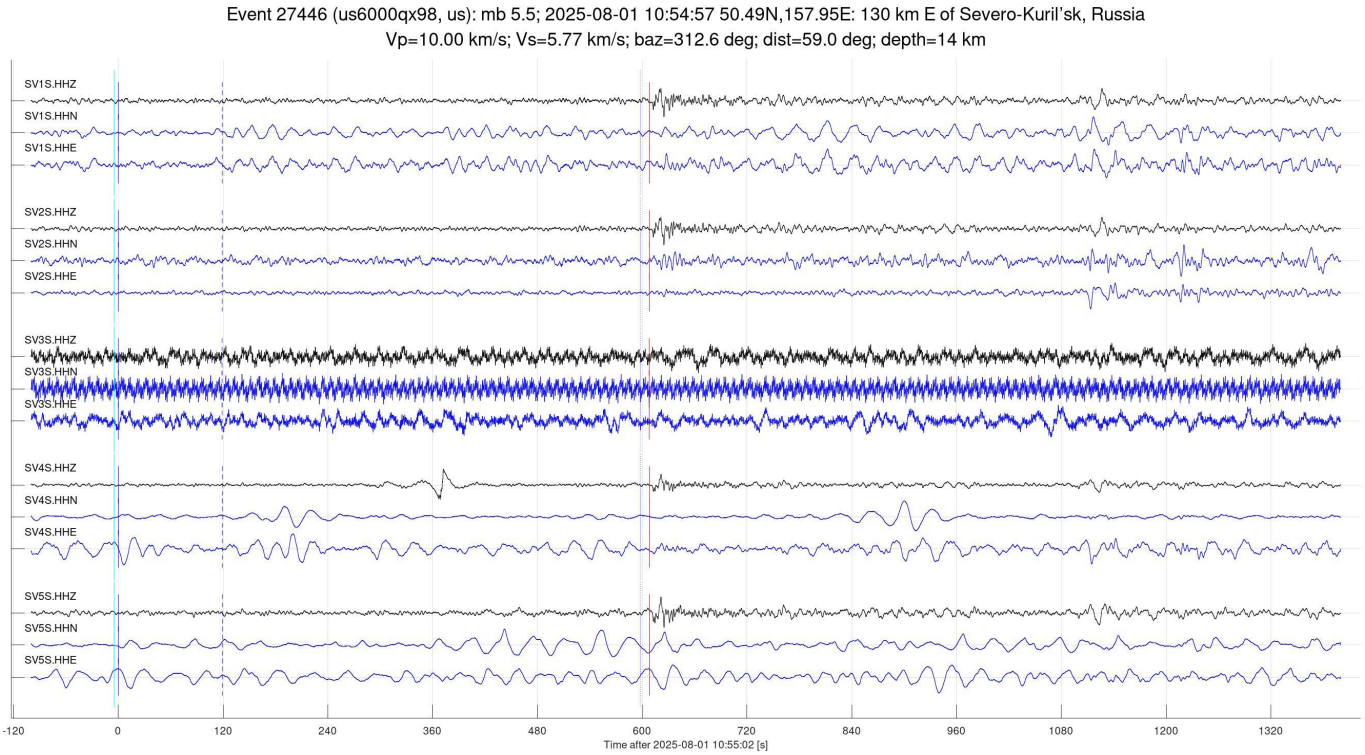


Figure 6, continued.

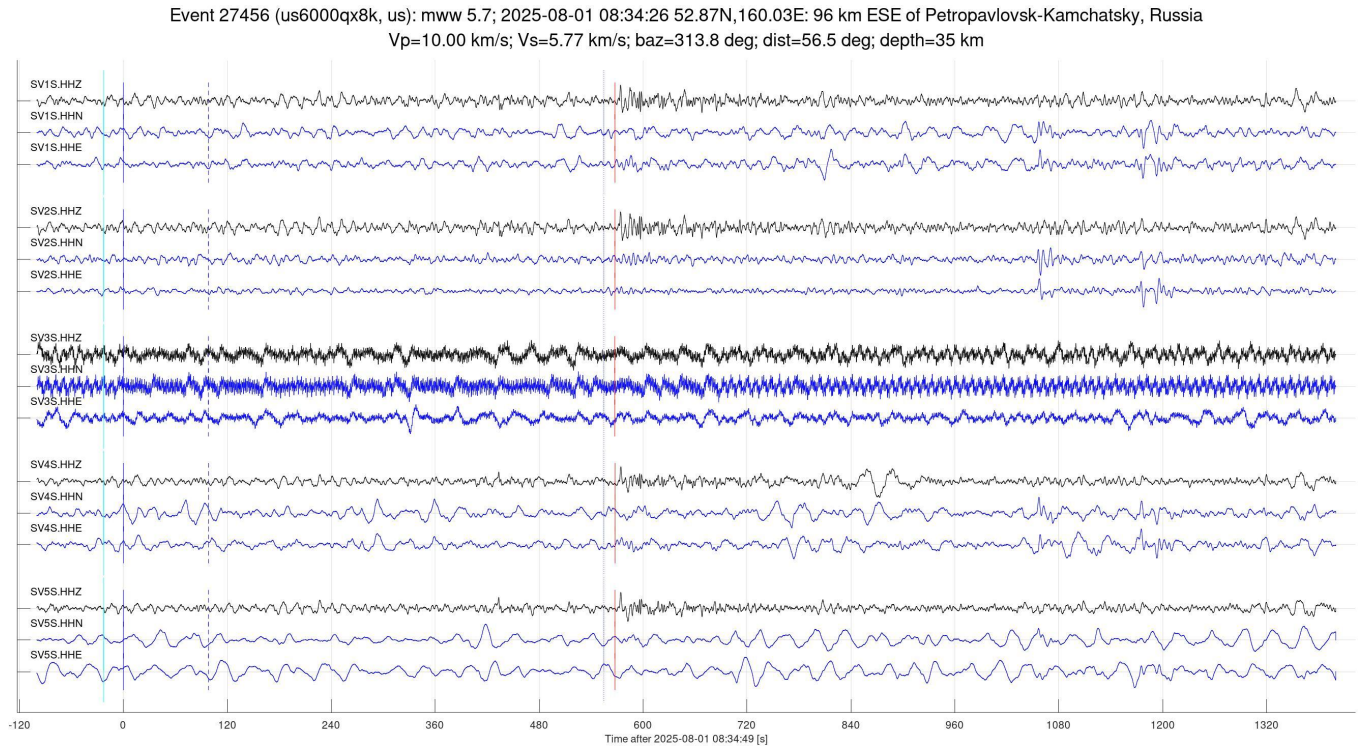


Figure 6, continued.

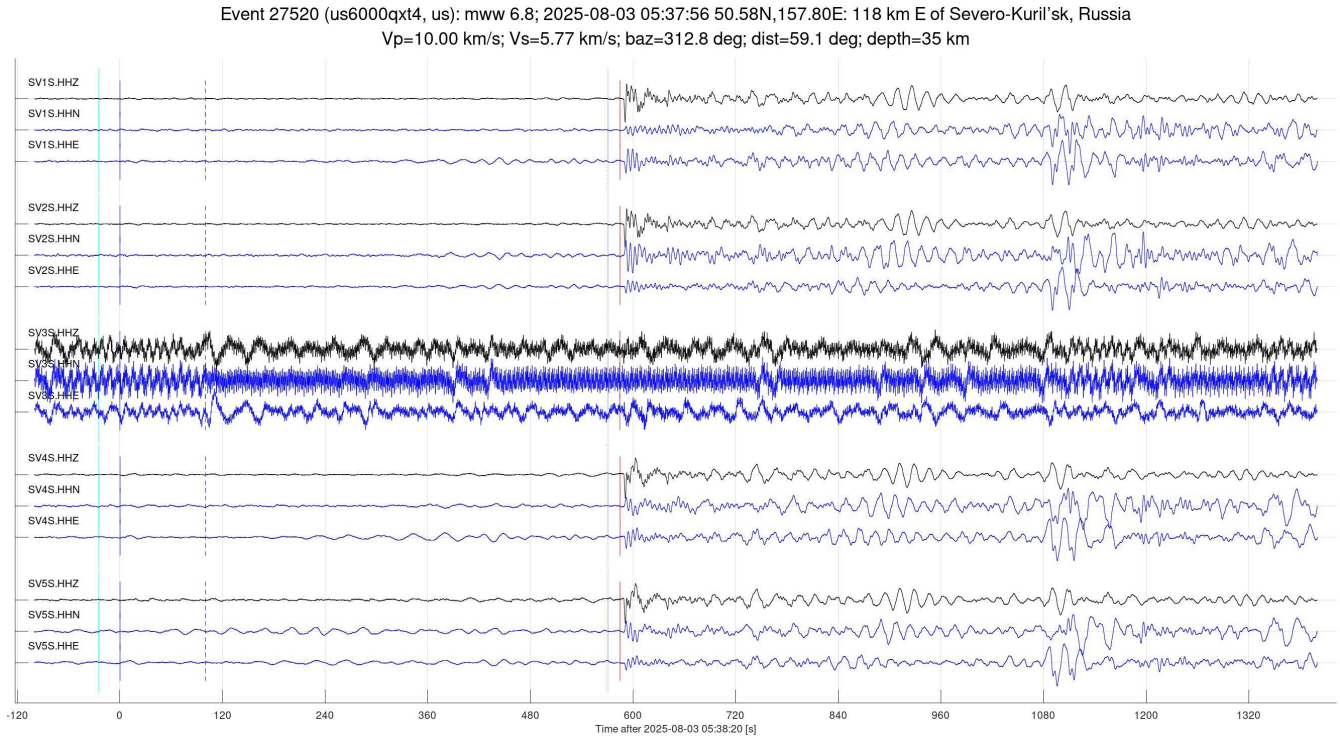


Figure 6, continued.

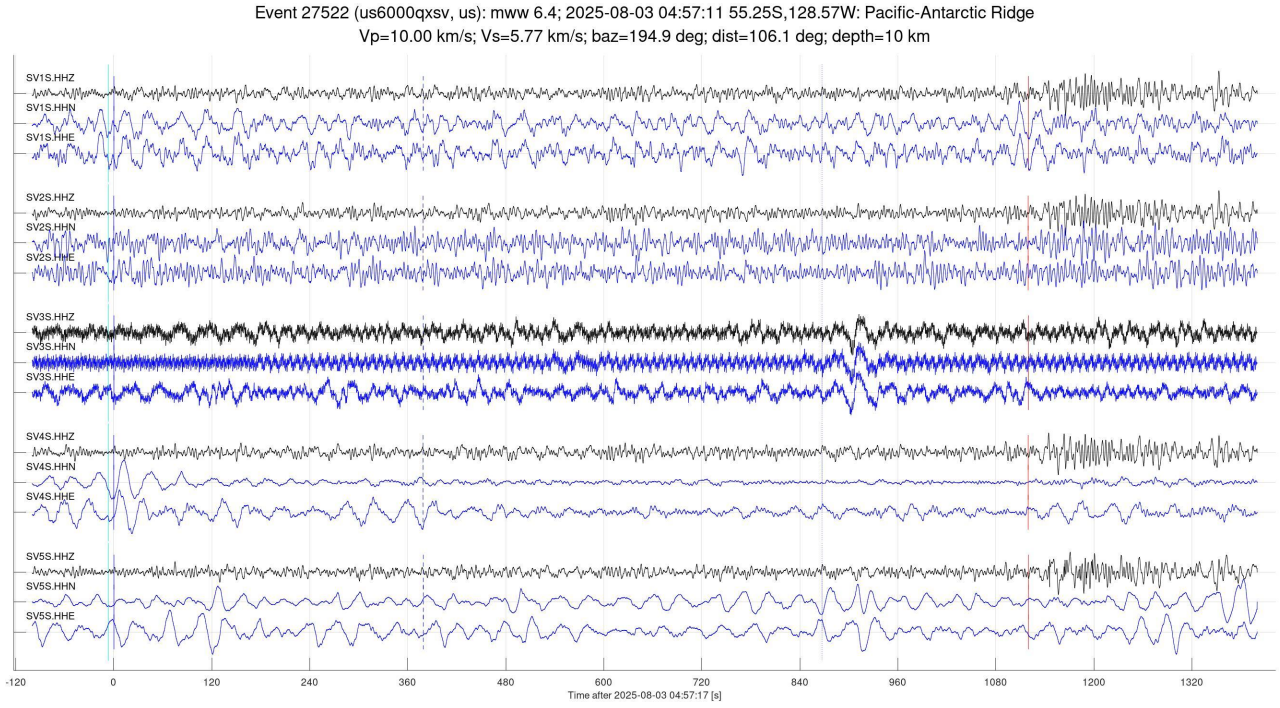


Figure 6, continued.

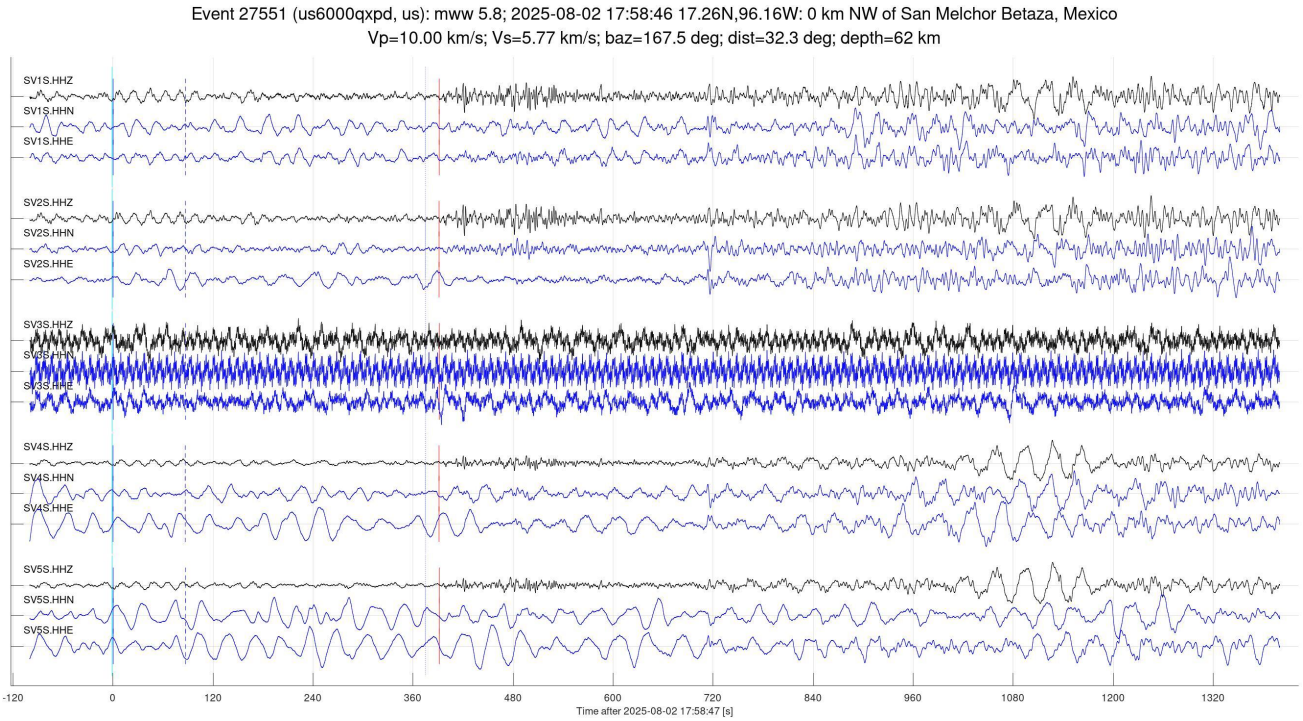


Figure 6, continued.

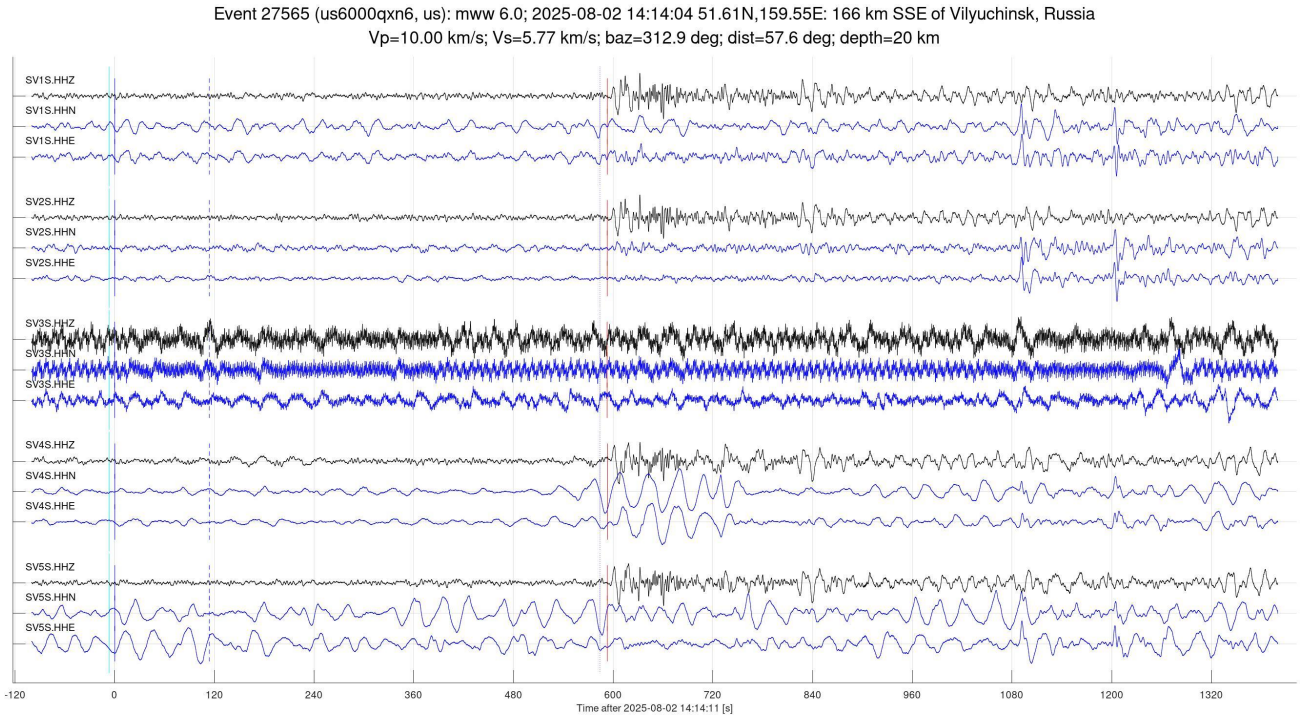


Figure 6, continued.

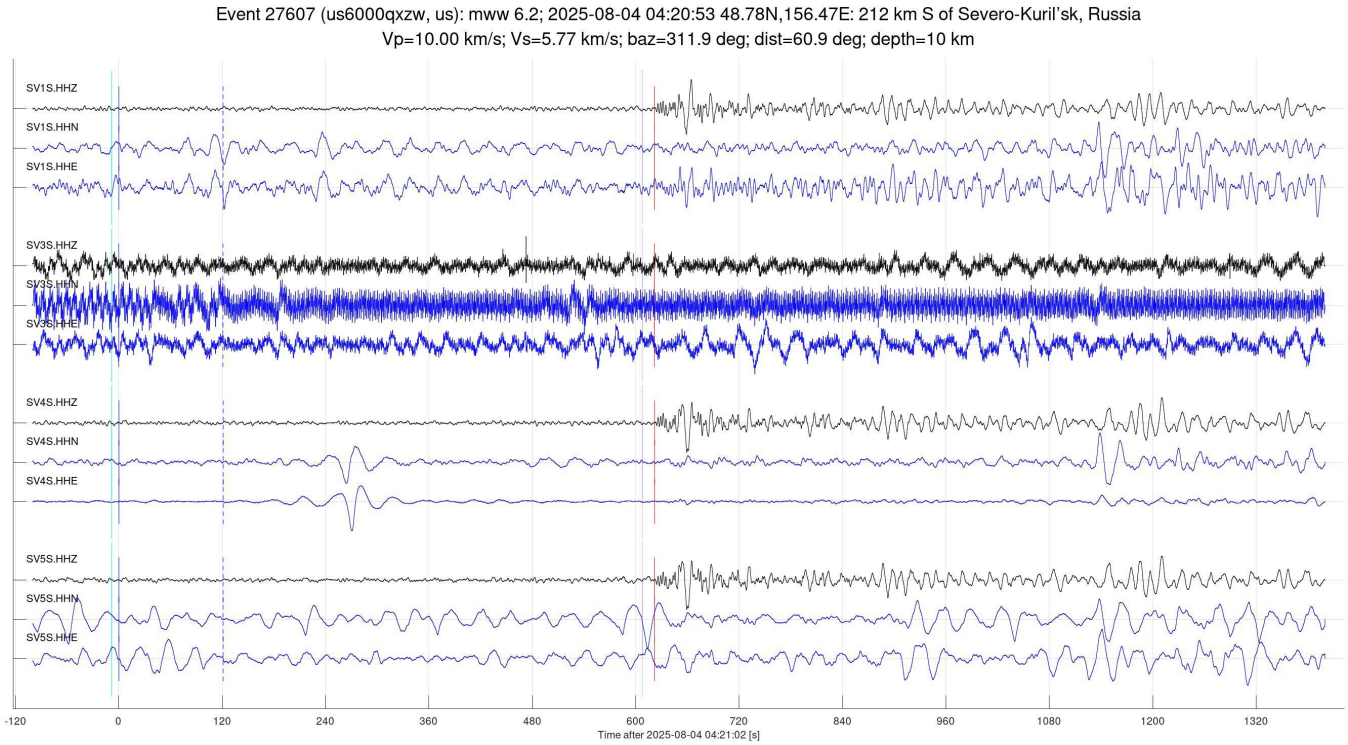


Figure 6, continued.

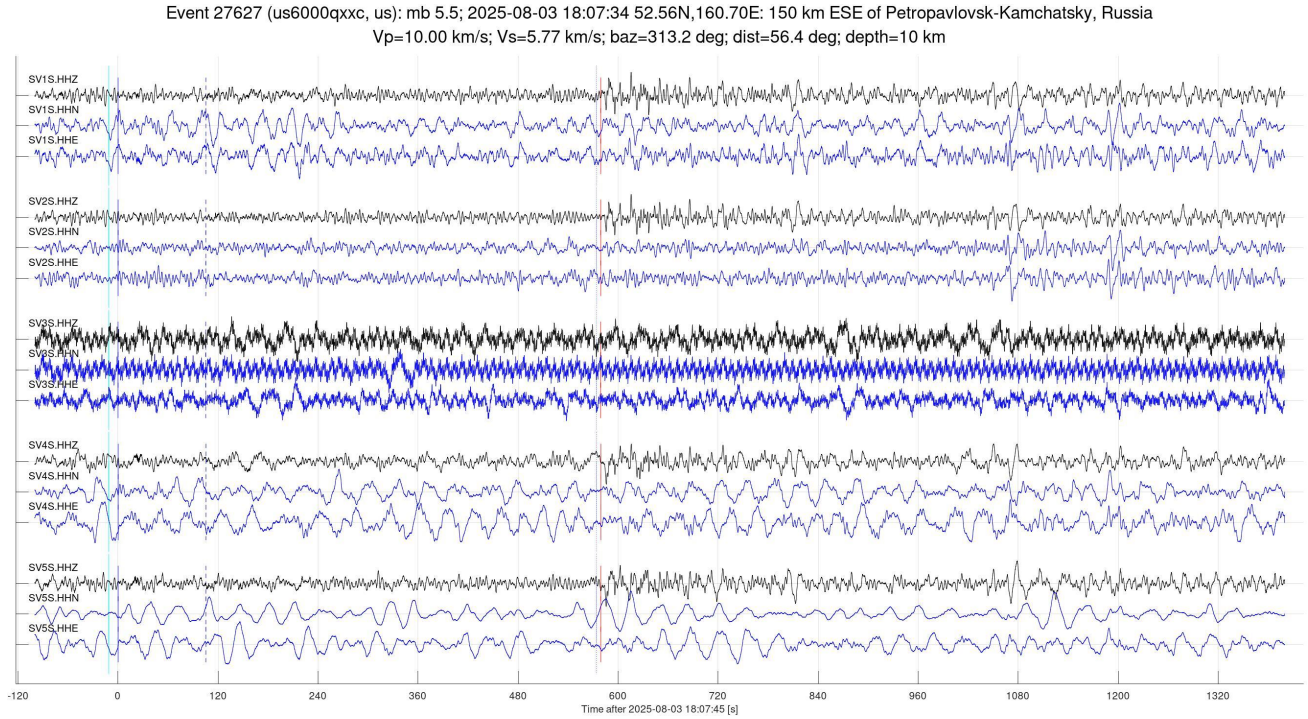


Figure 6, continued.

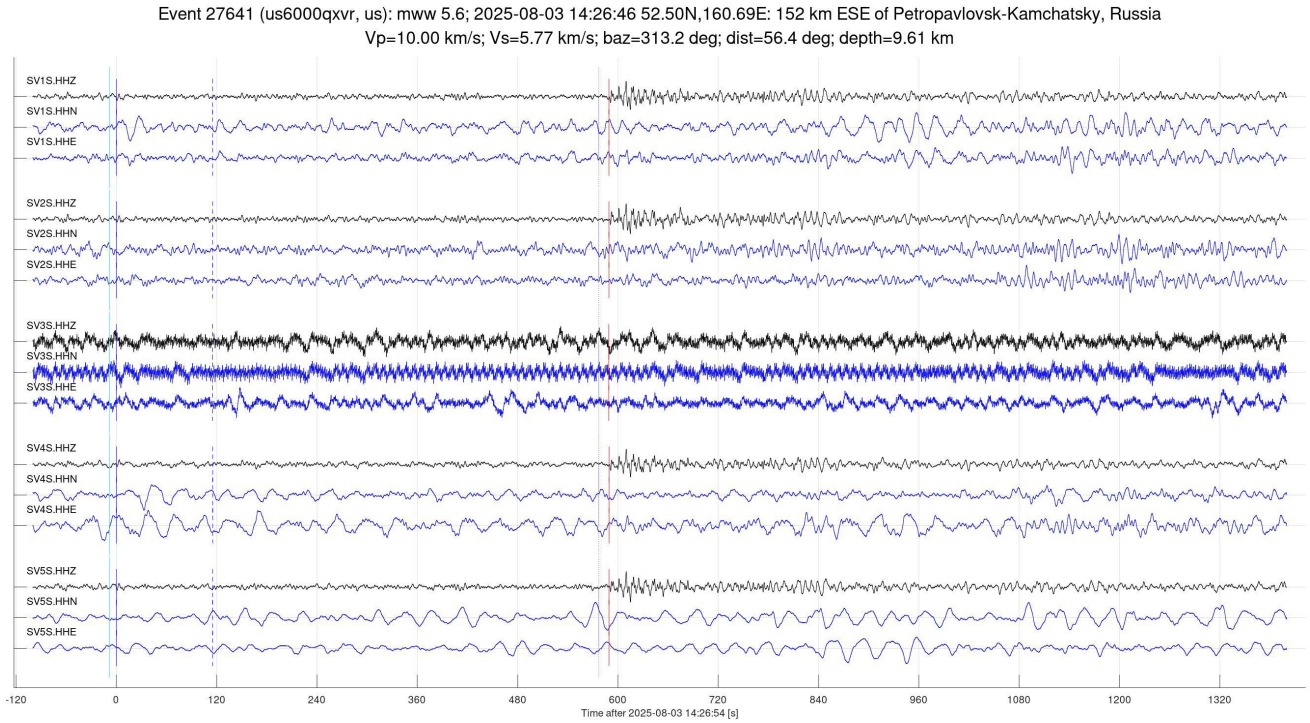


Figure 6, continued.

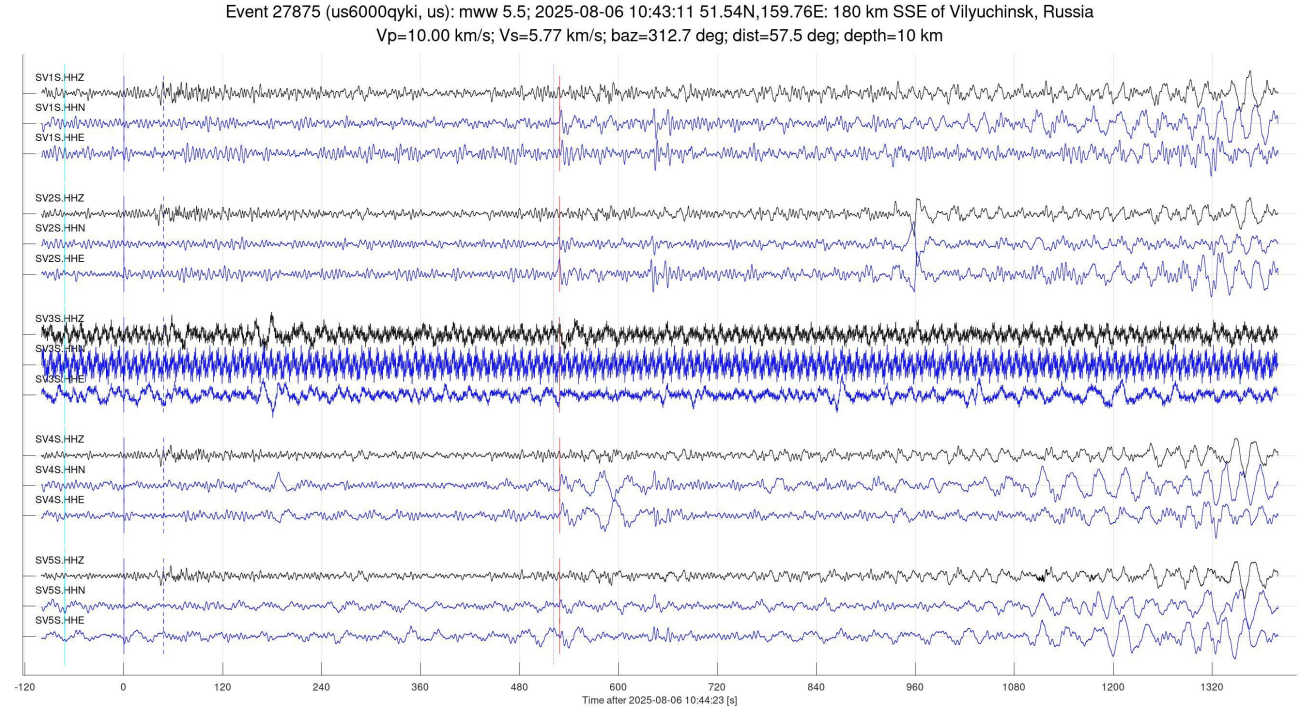


Figure 6, continued.

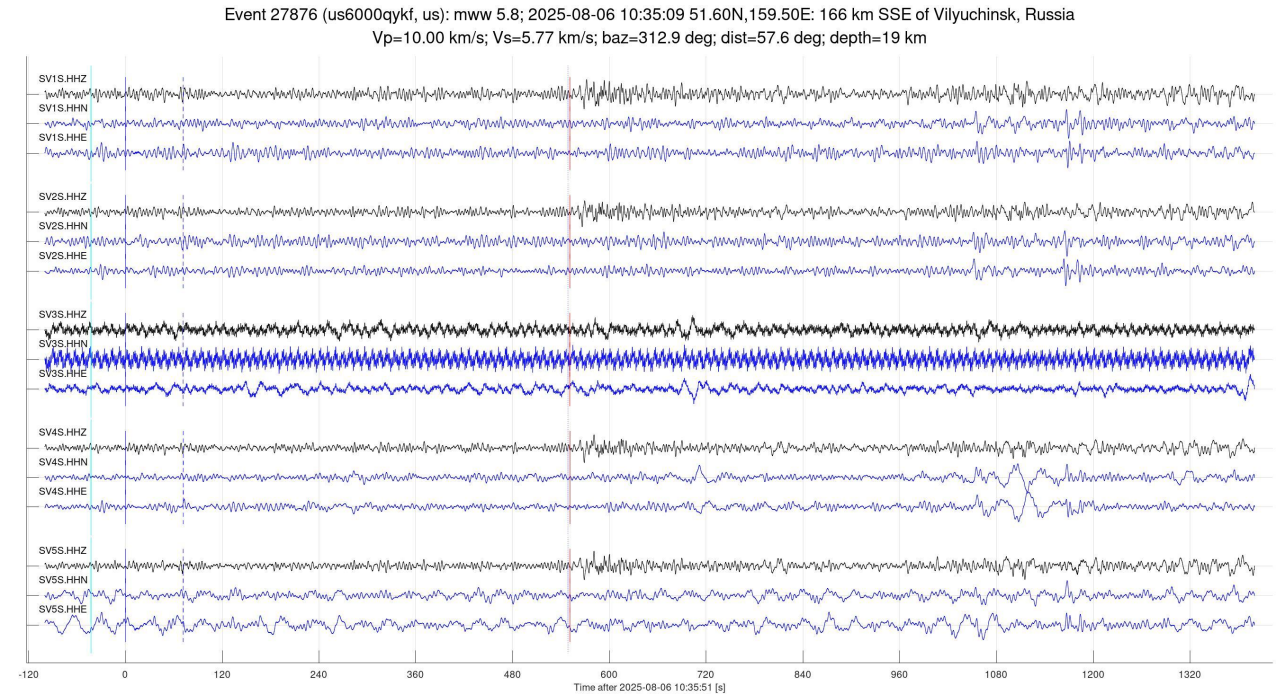


Figure 6, continued.

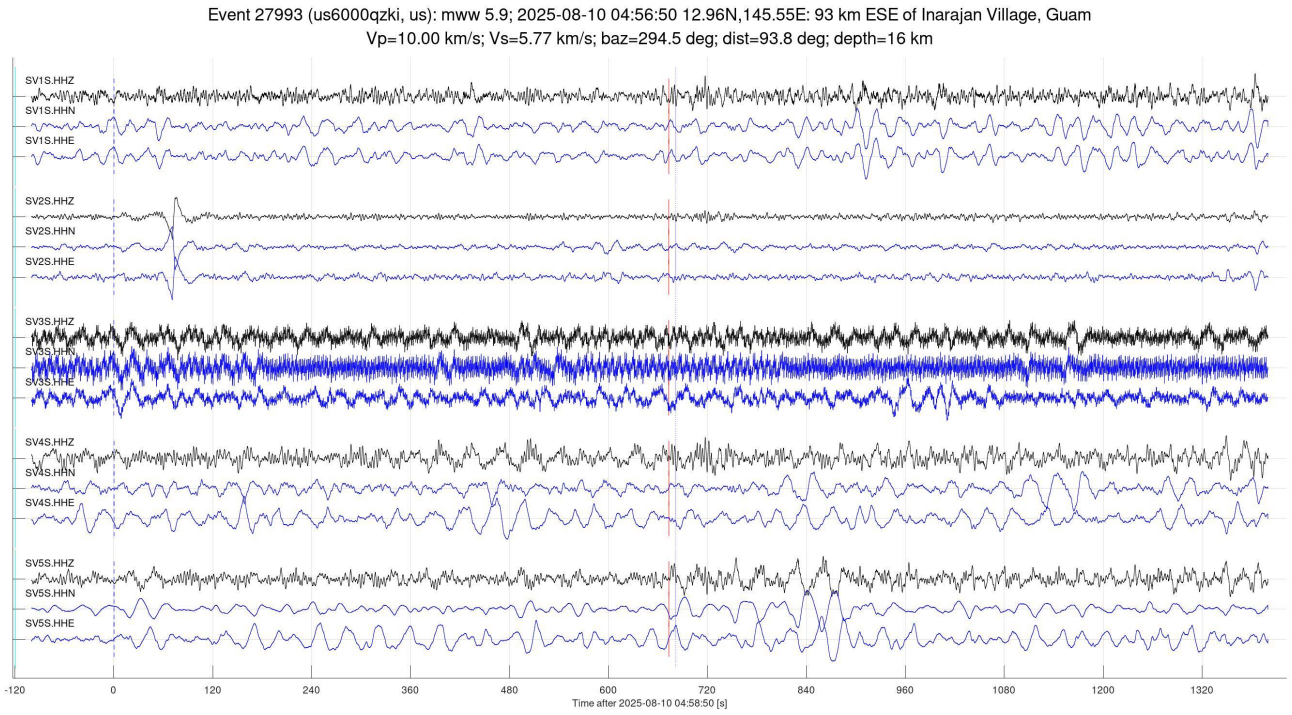


Figure 6, continued.

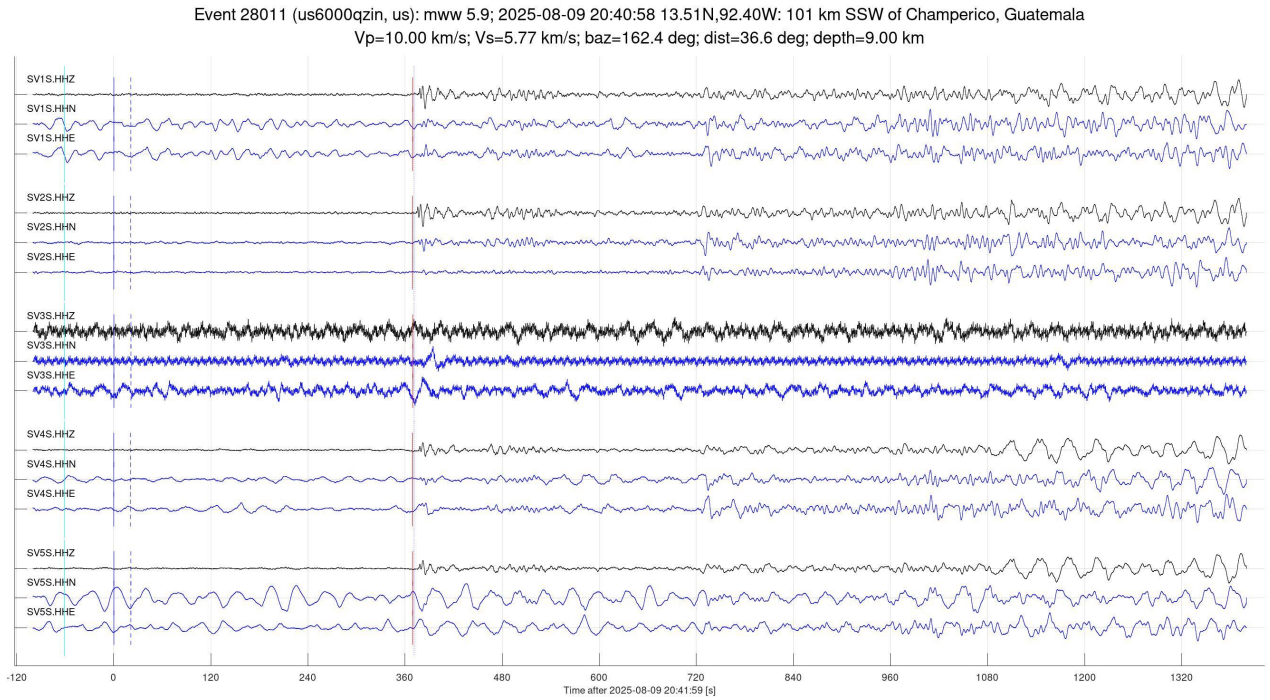


Figure 6, continued.

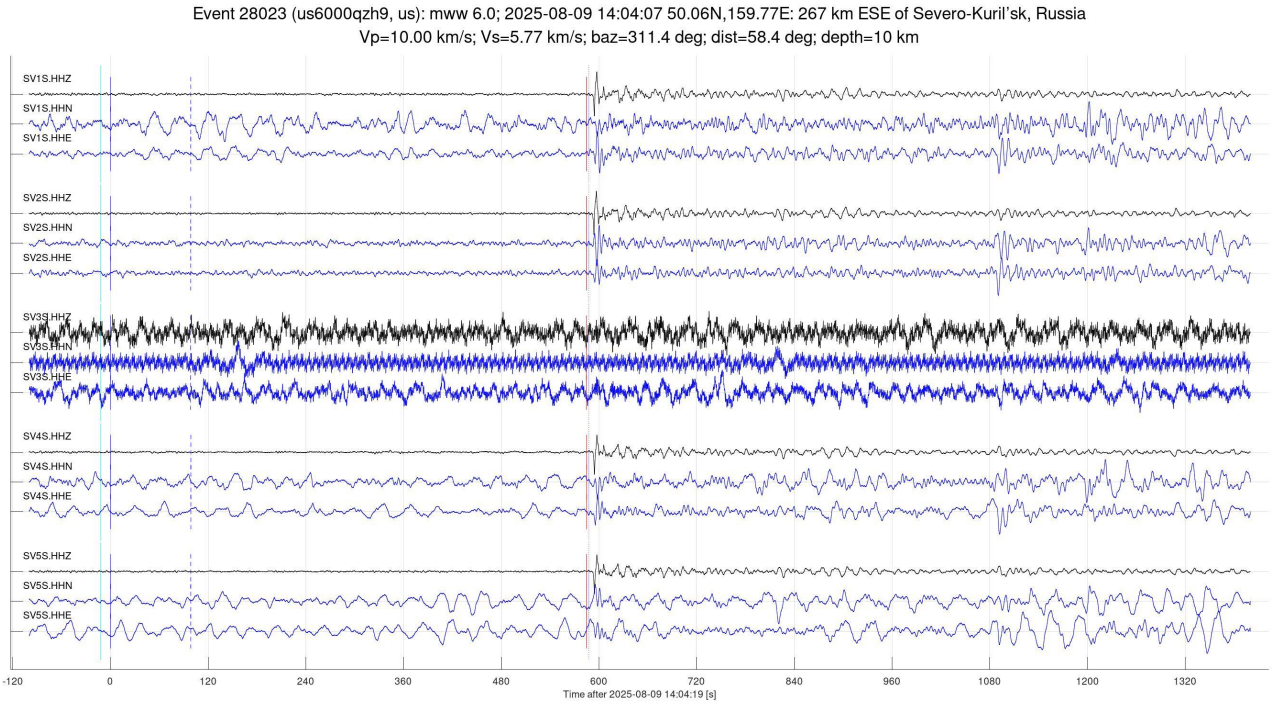


Figure 6, continued.

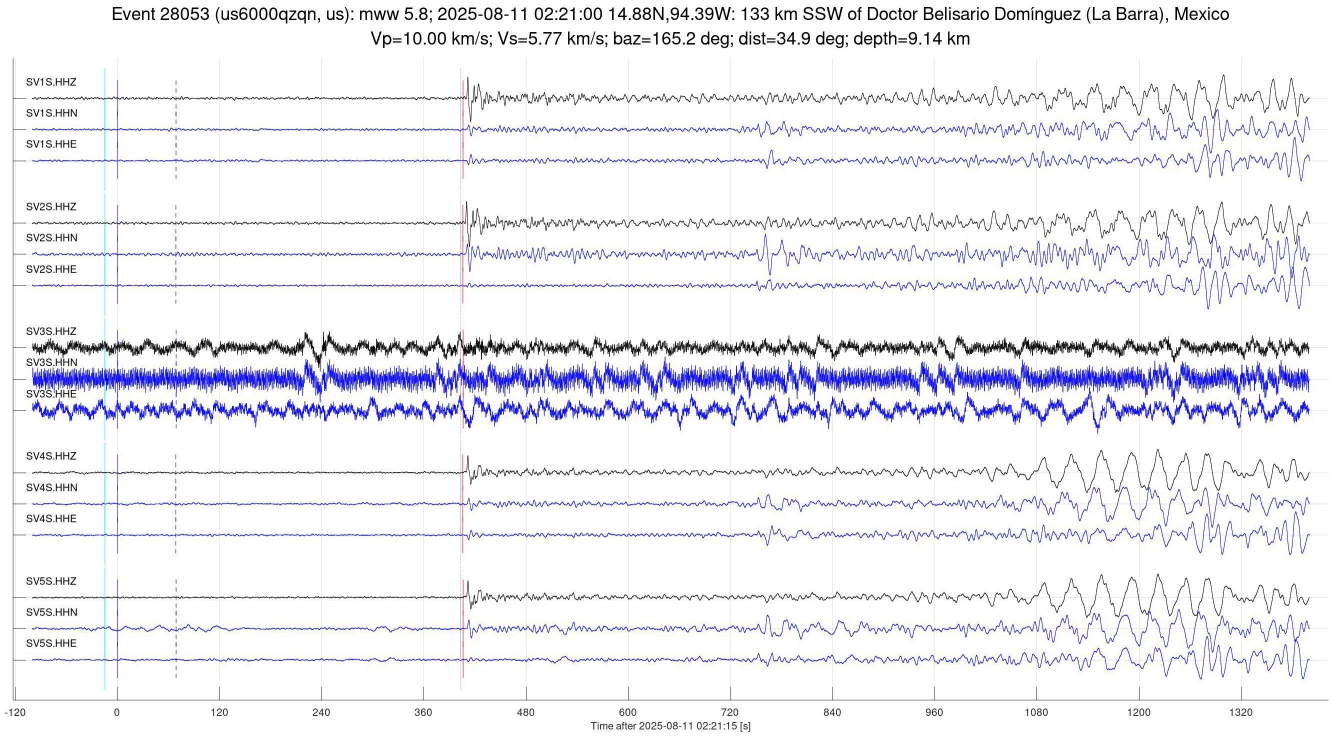


Figure 6, continued.

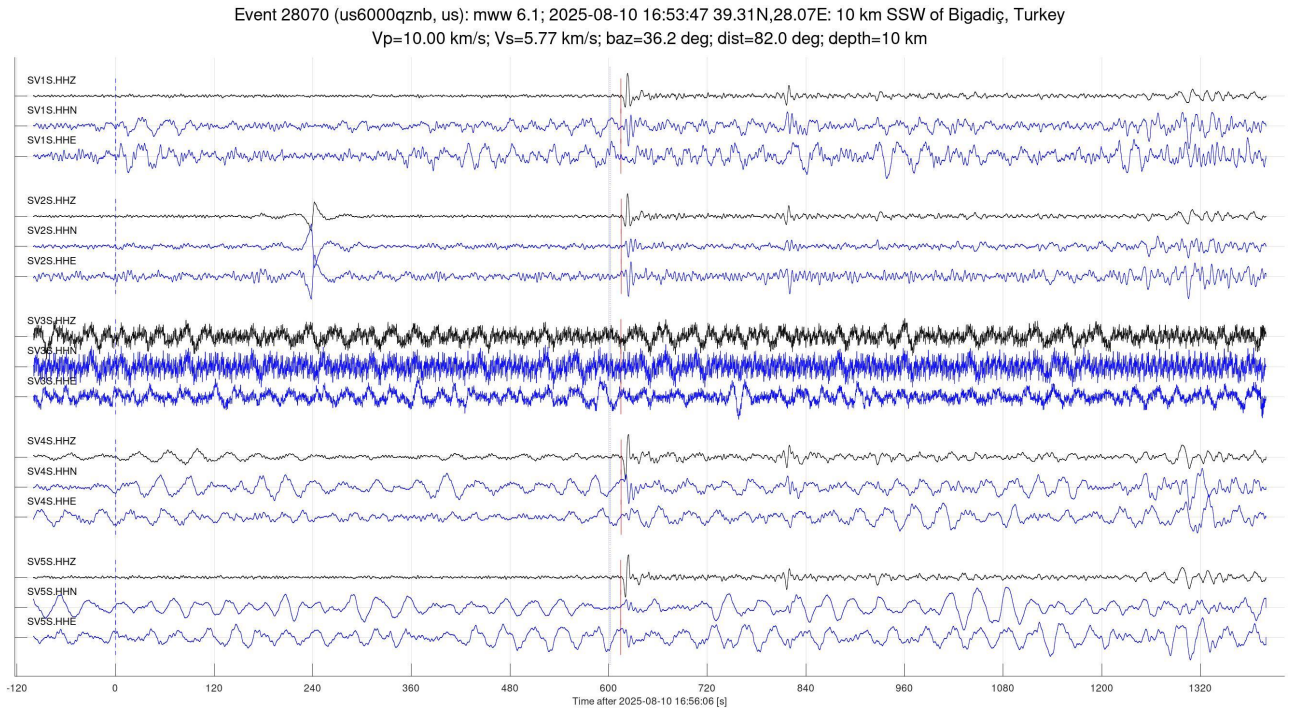


Figure 6, continued.

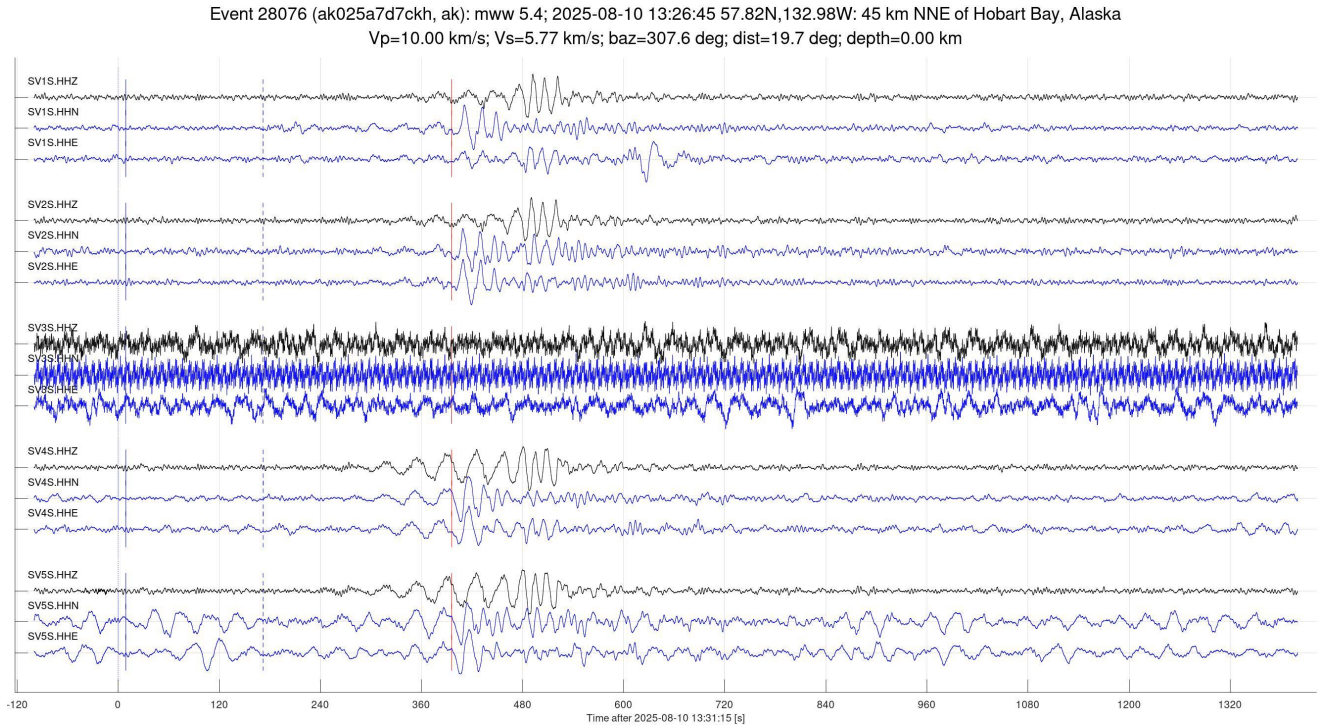


Figure 6, continued.

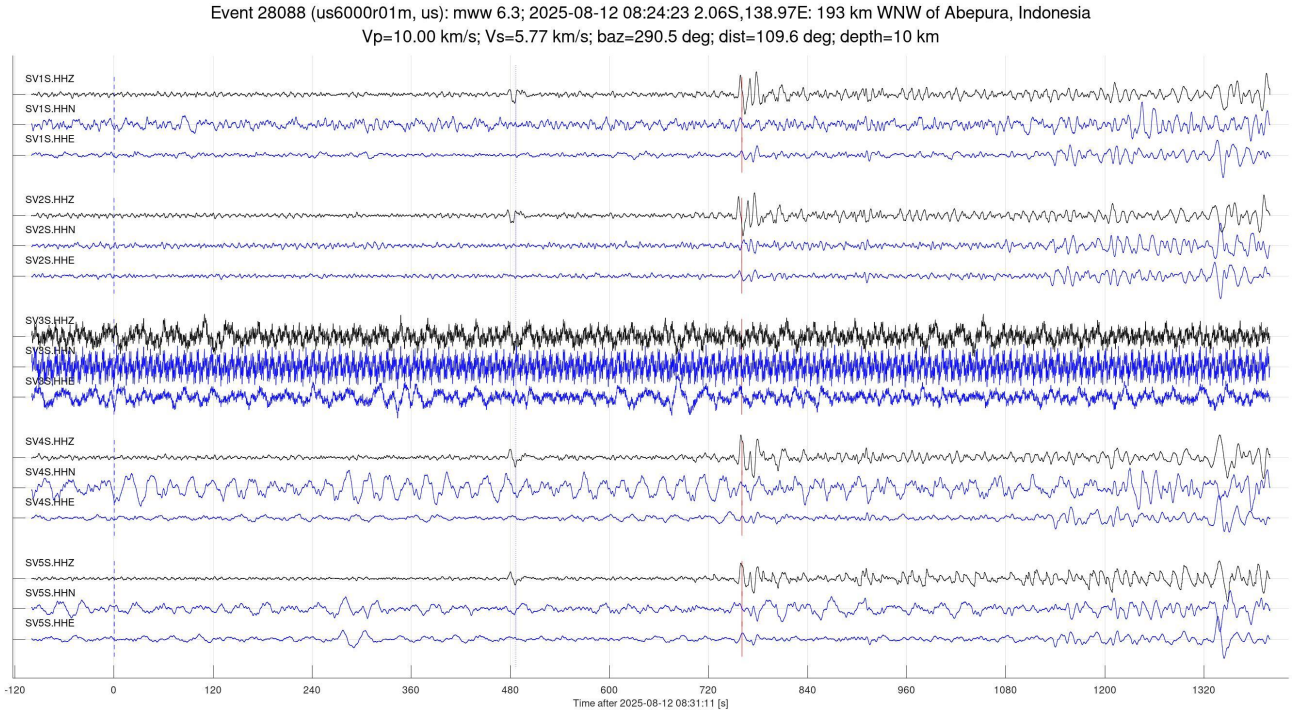


Figure 6, continued.

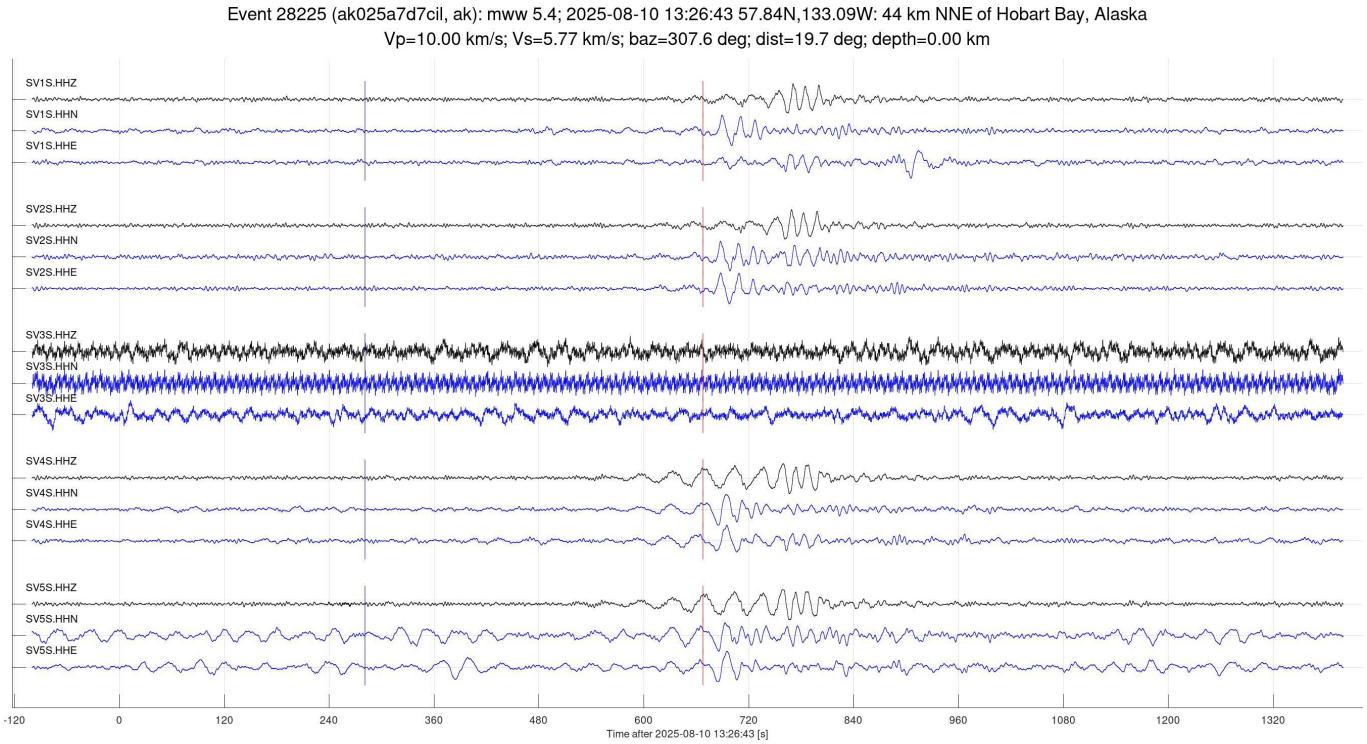


Figure 6, continued.

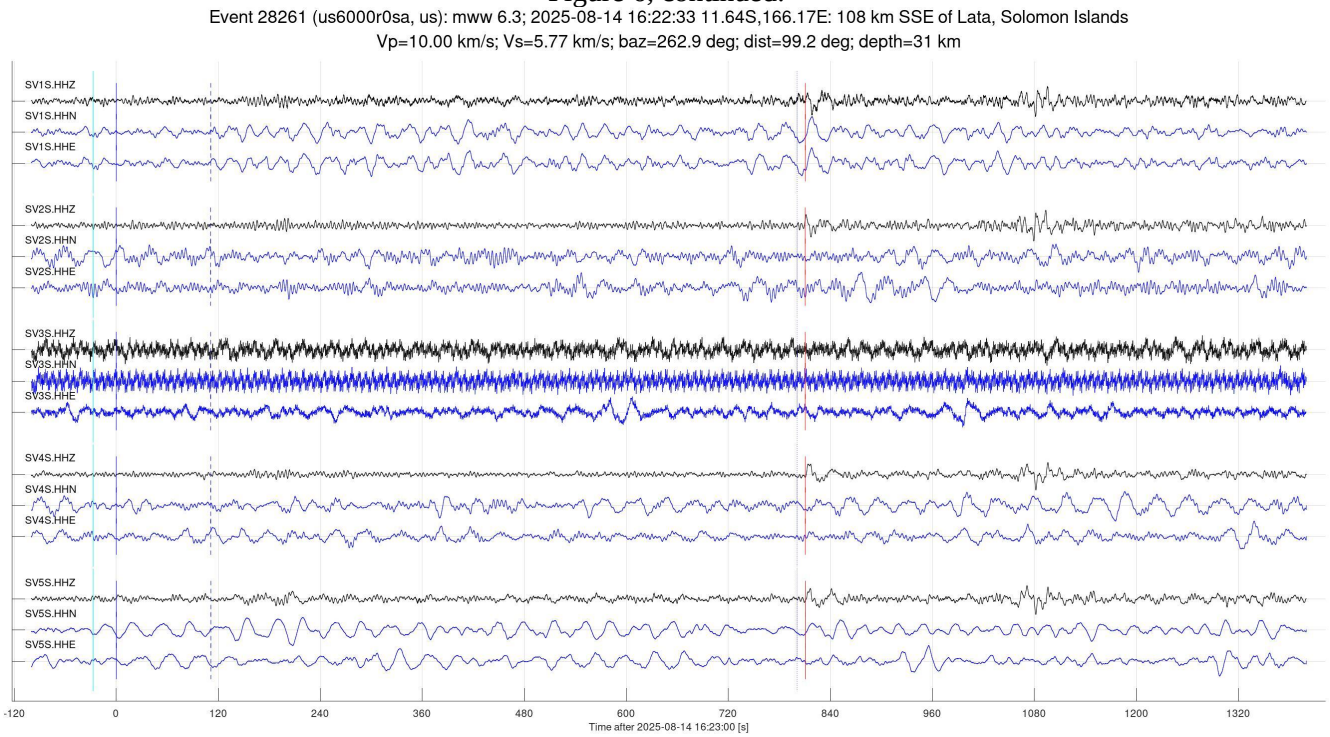


Figure 6, continued.

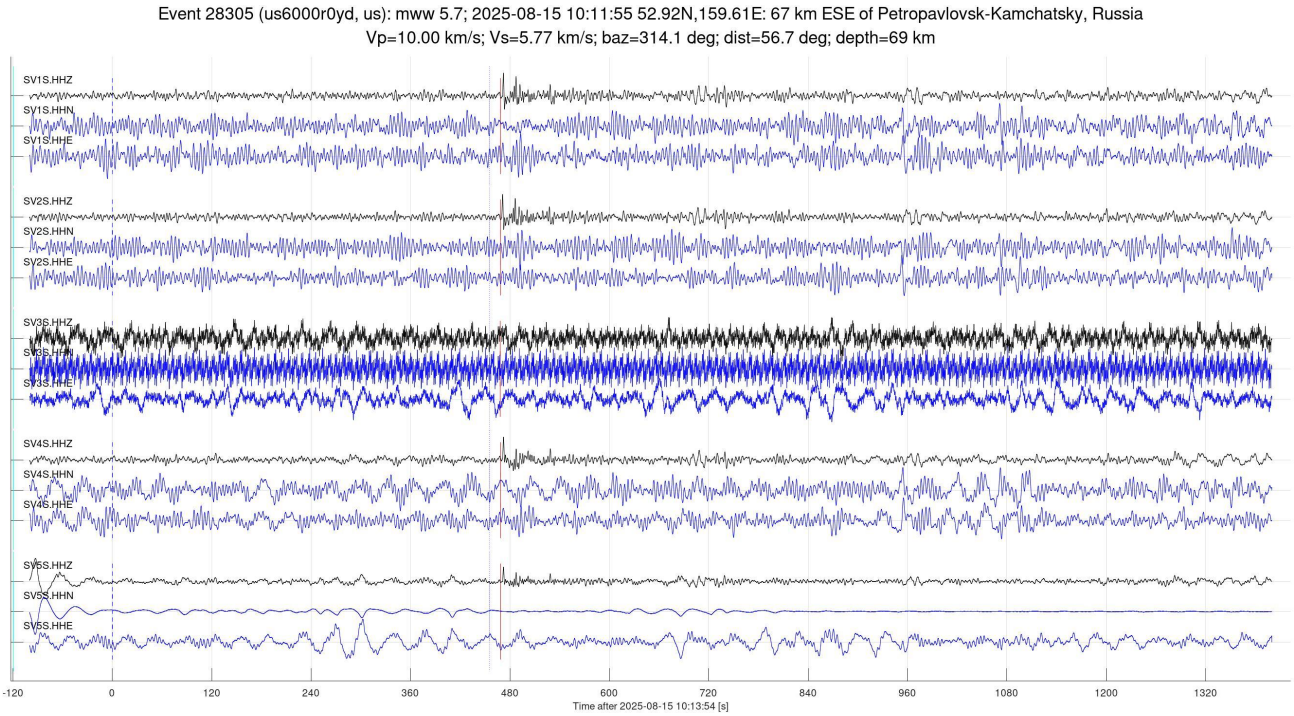


Figure 6, continued.

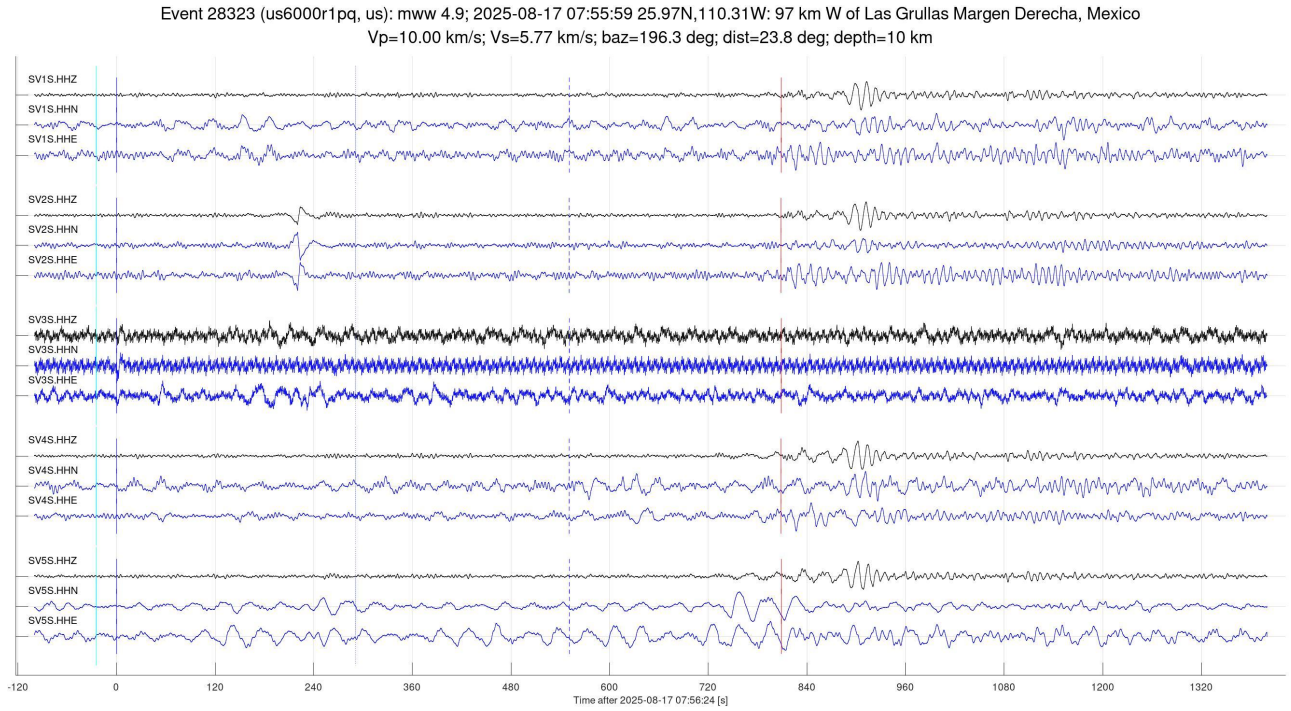


Figure 6, continued.

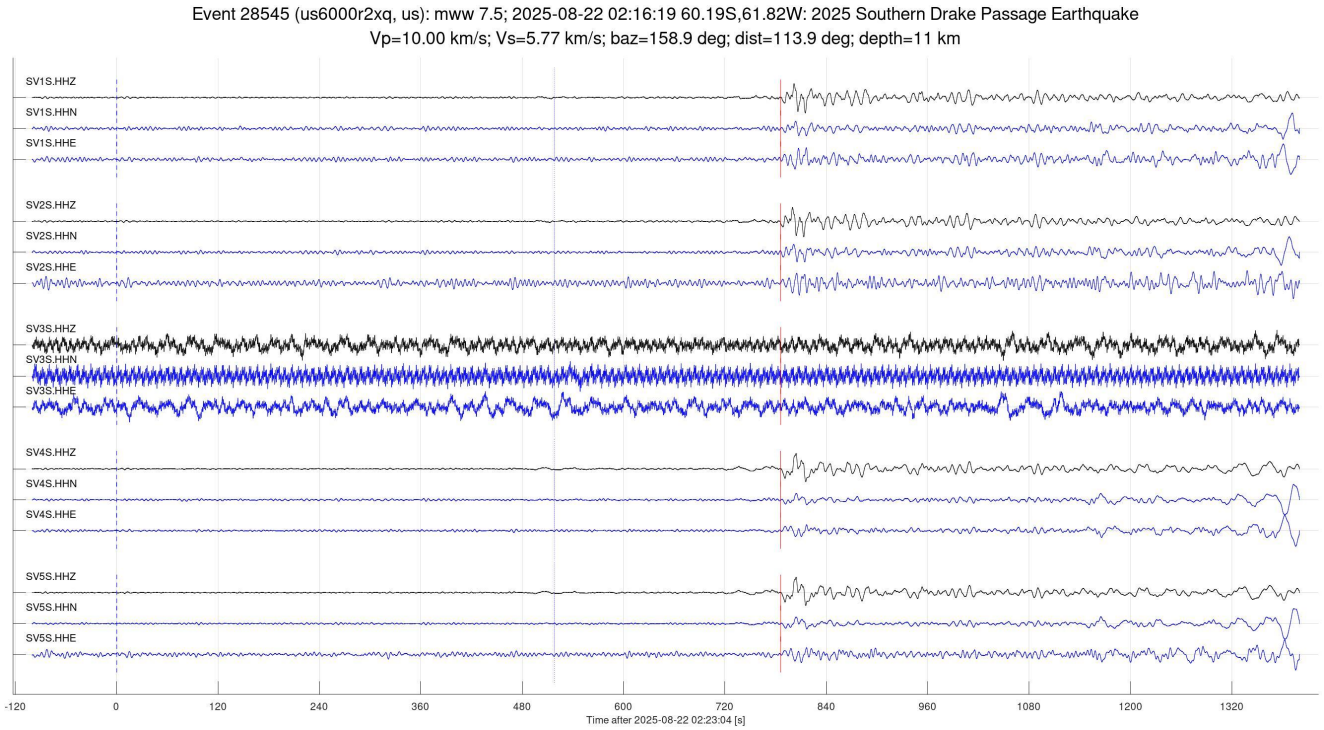


Figure 6, continued.

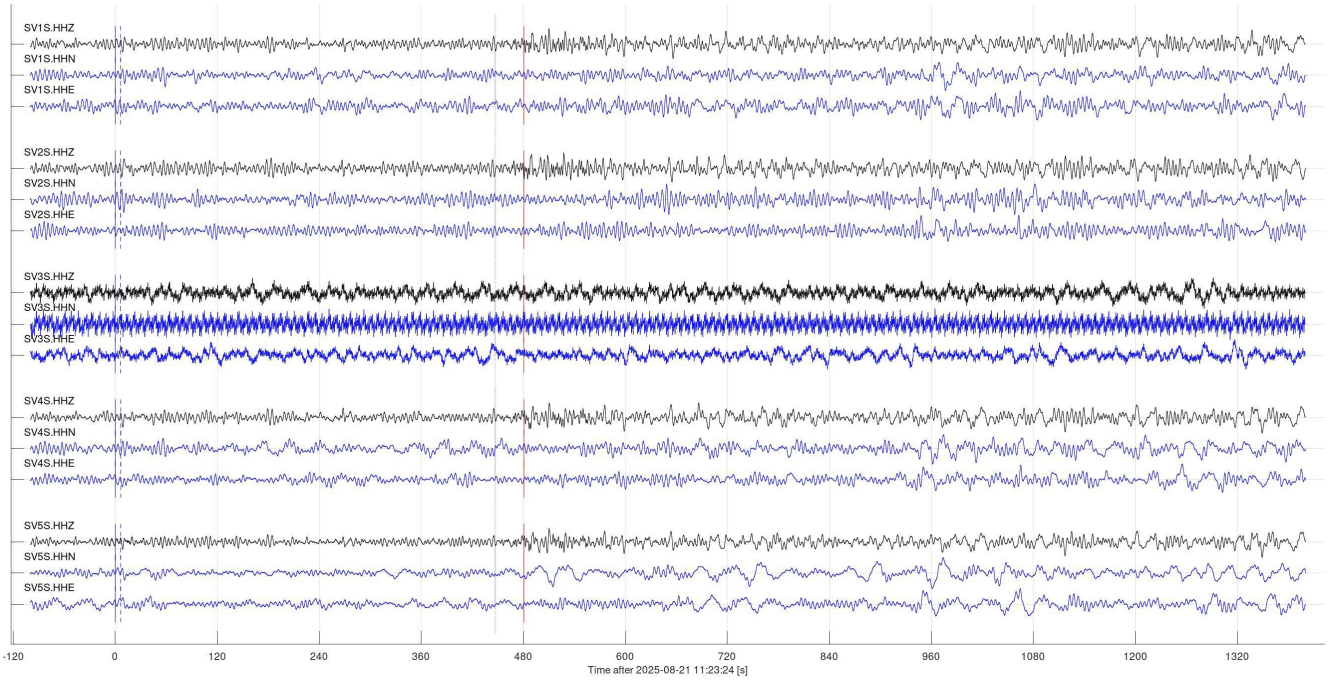


Figure 6, continued.

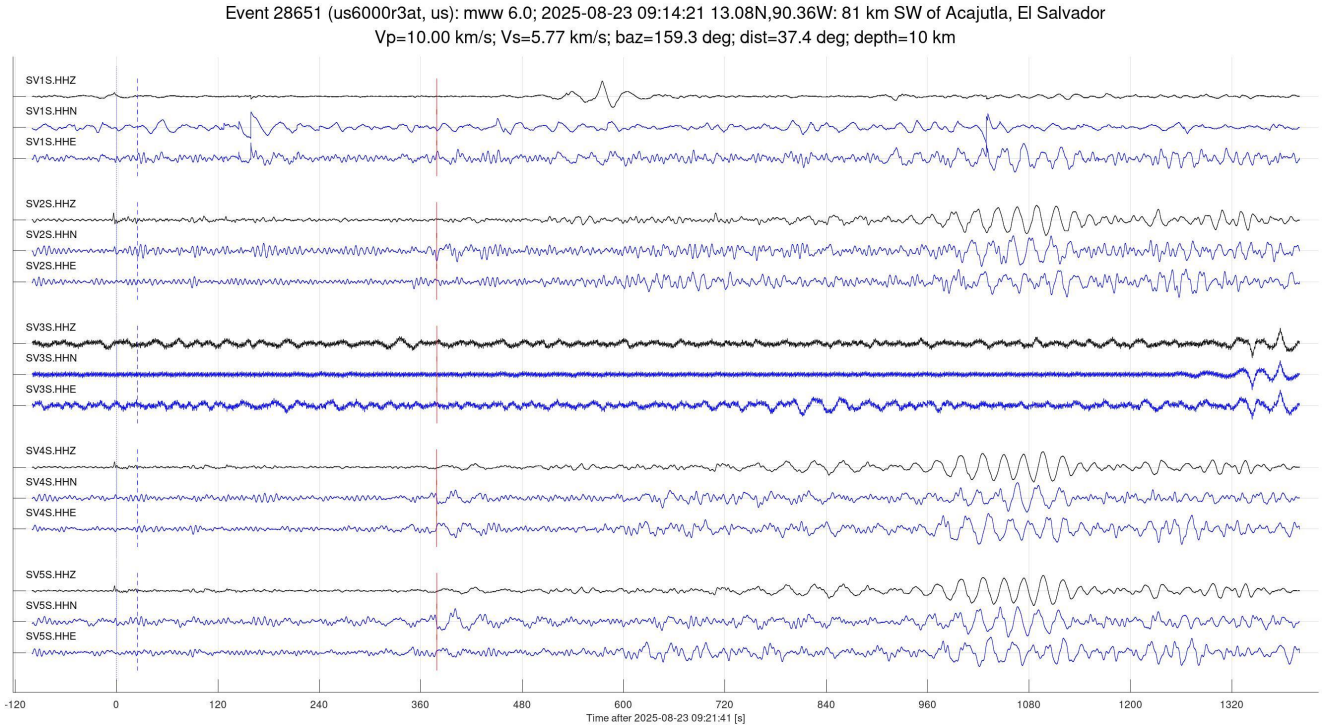


Figure 6, continued.

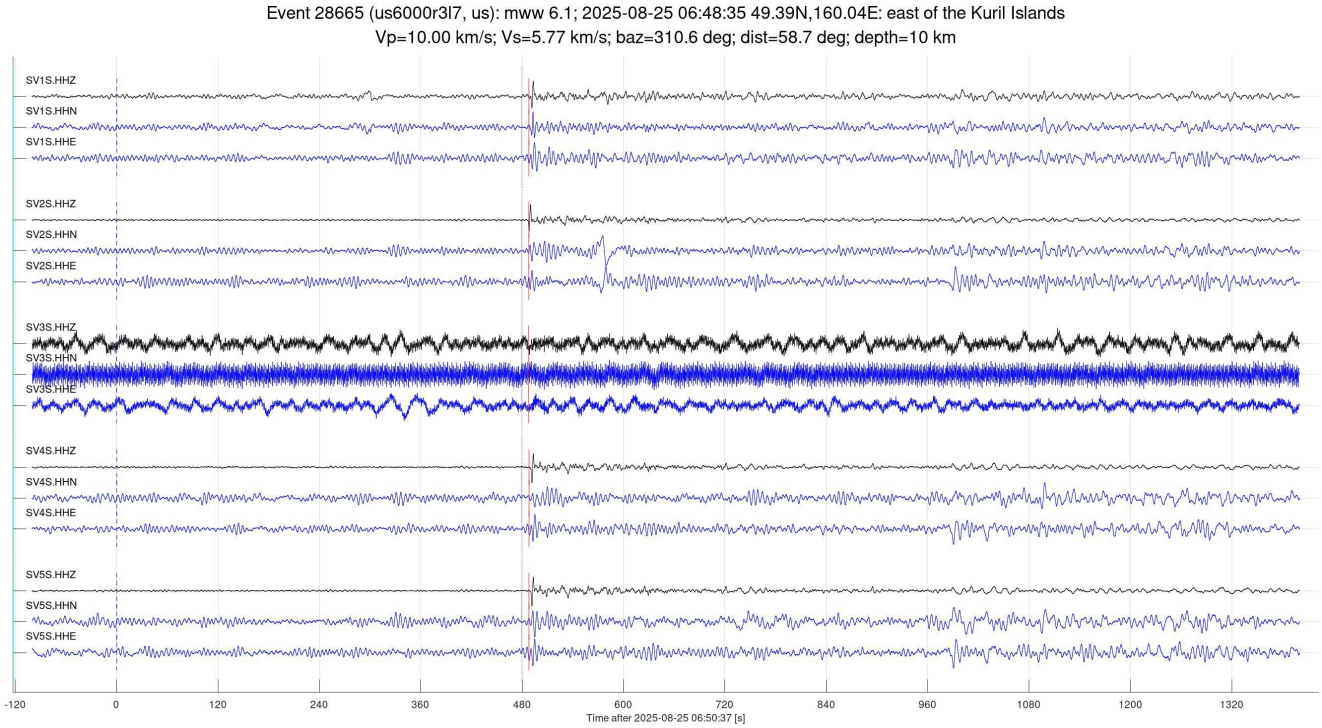


Figure 6, continued.

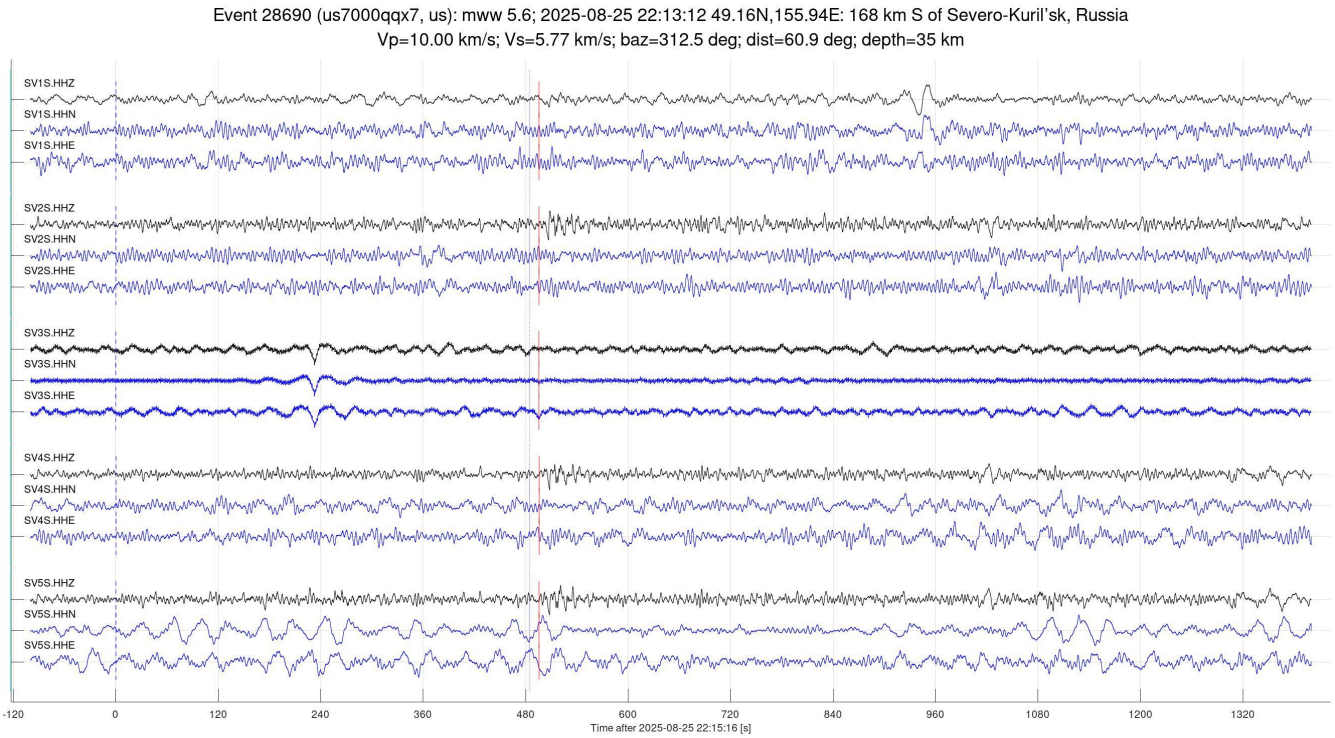


Figure 6, continued.

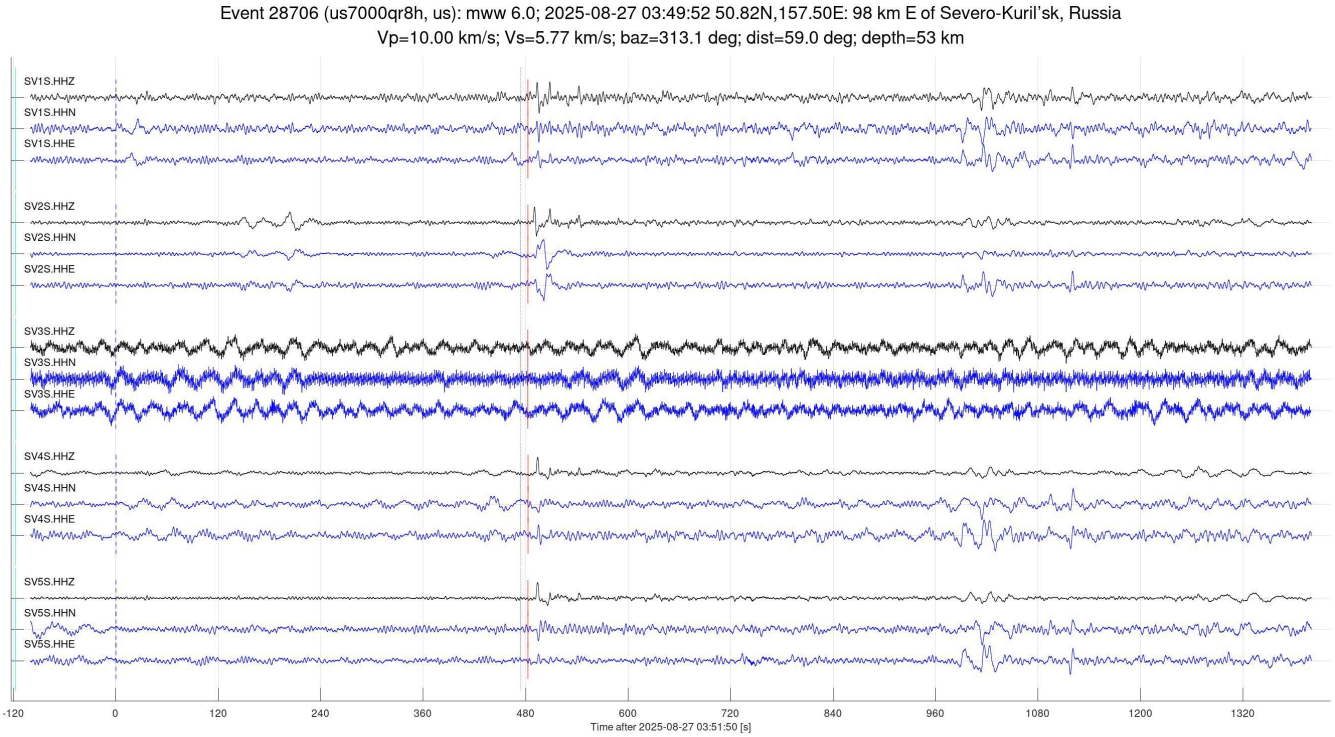


Figure 6, continued.

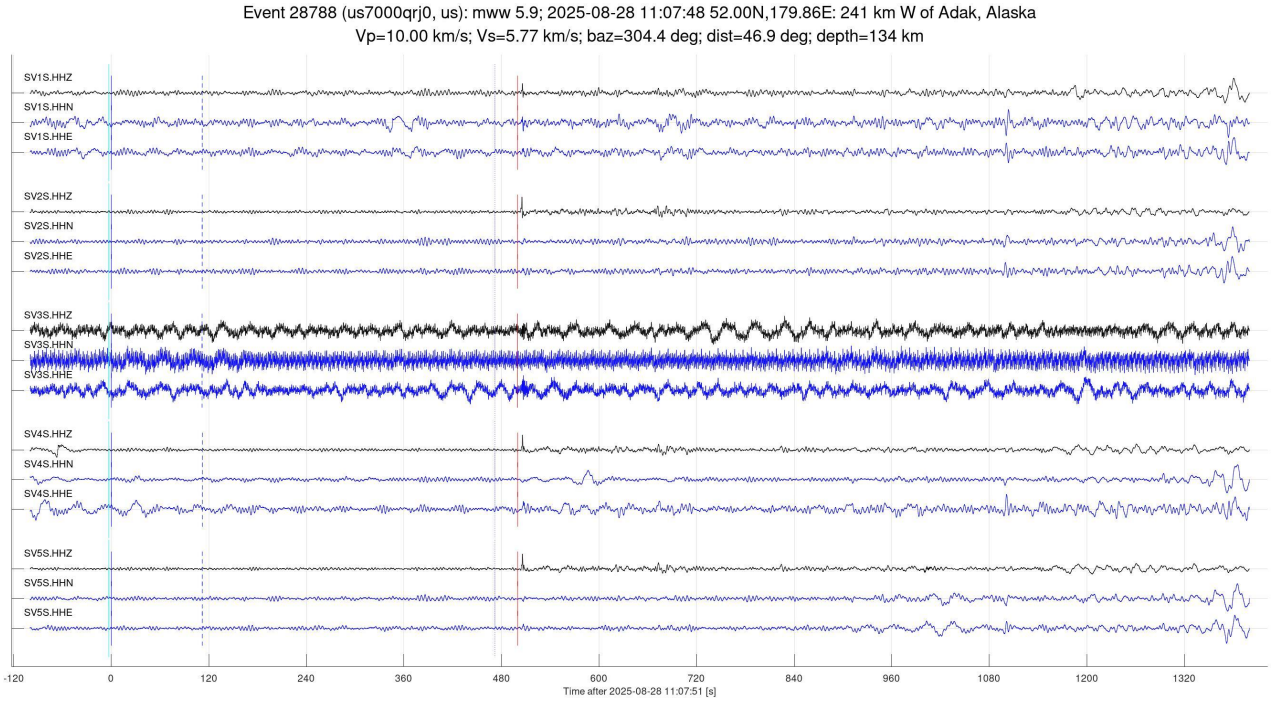


Figure 6, continued.

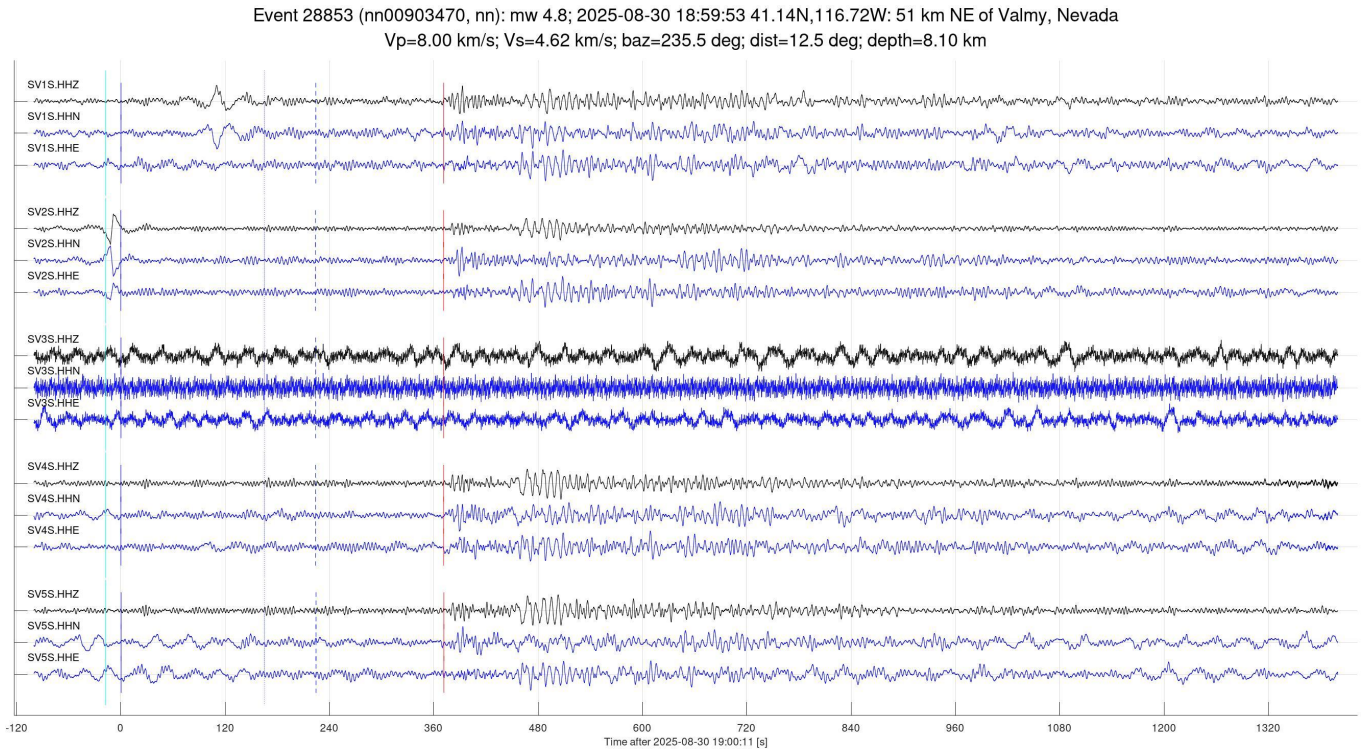


Figure 6, continued.

## Regional events (class 2)

One uncatalogued regional seismic events (class 2 in Table 2) was identified in the reporting period ().

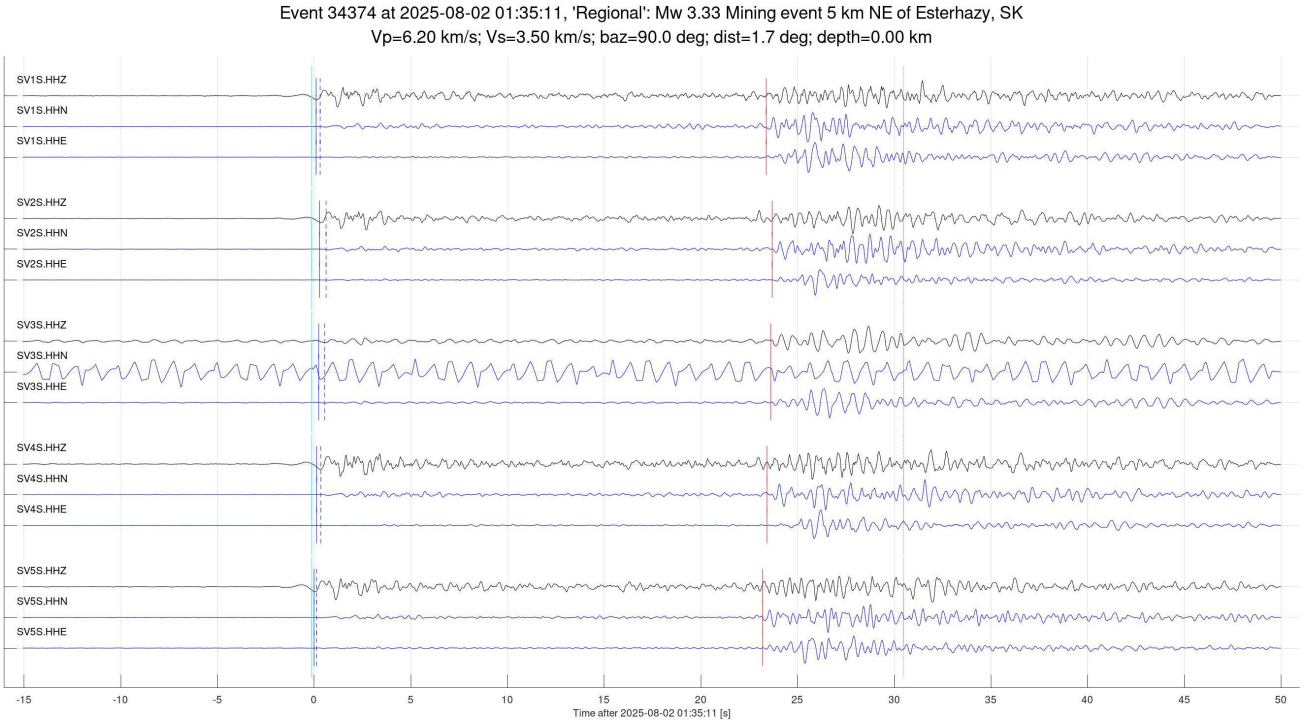


Figure 7. Seismic arrivals produced by mine blasts at the Estevan mine. Colours and labels are as in Figure 6.

## Local events (classes 3 and 4)

The following subsections summarize observations of event classes 3 and 4 in Table 2.

### Possible mine blasts at the Estevan mine (class 3a)

Thirteen detected events were identified as mine blasts in the area of Estevan coal mining (Figure 8). From these events, local P- and S-wave velocities, distances, and back-azimuths were roughly estimated. More accurate location work is in progress.

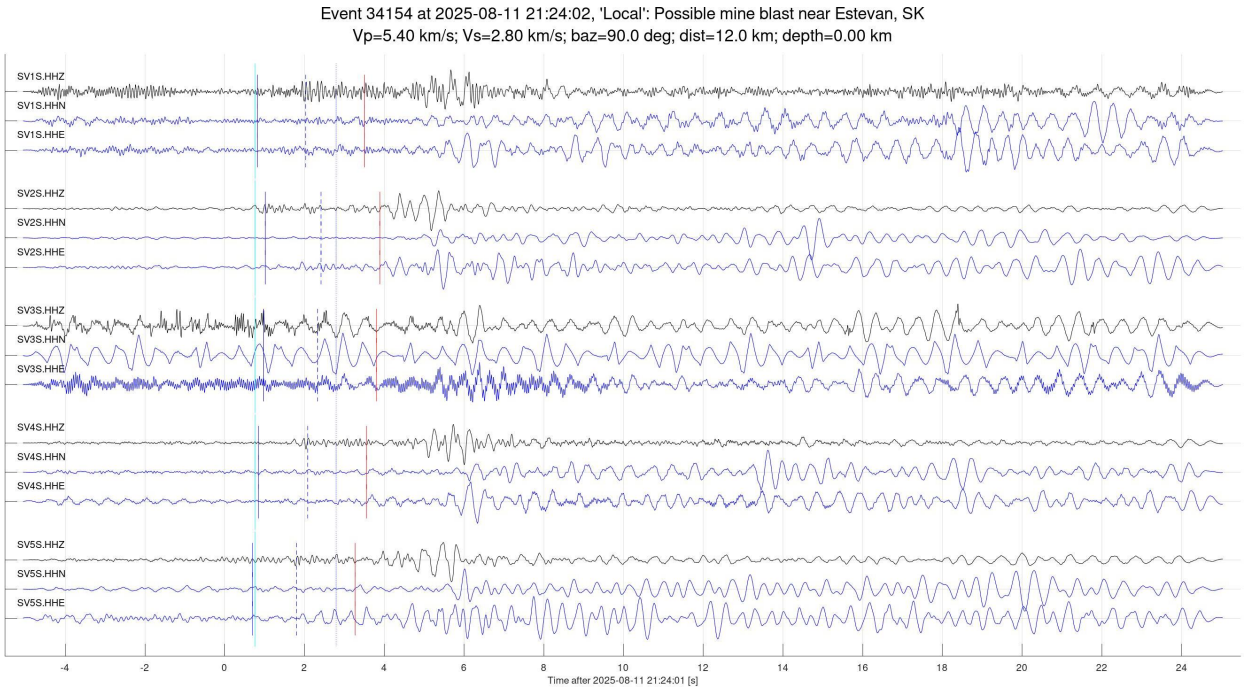


Figure 8. Seismic arrivals produced by mine blasts at the Estevan mine. Colours and labels are as in Figure 6.

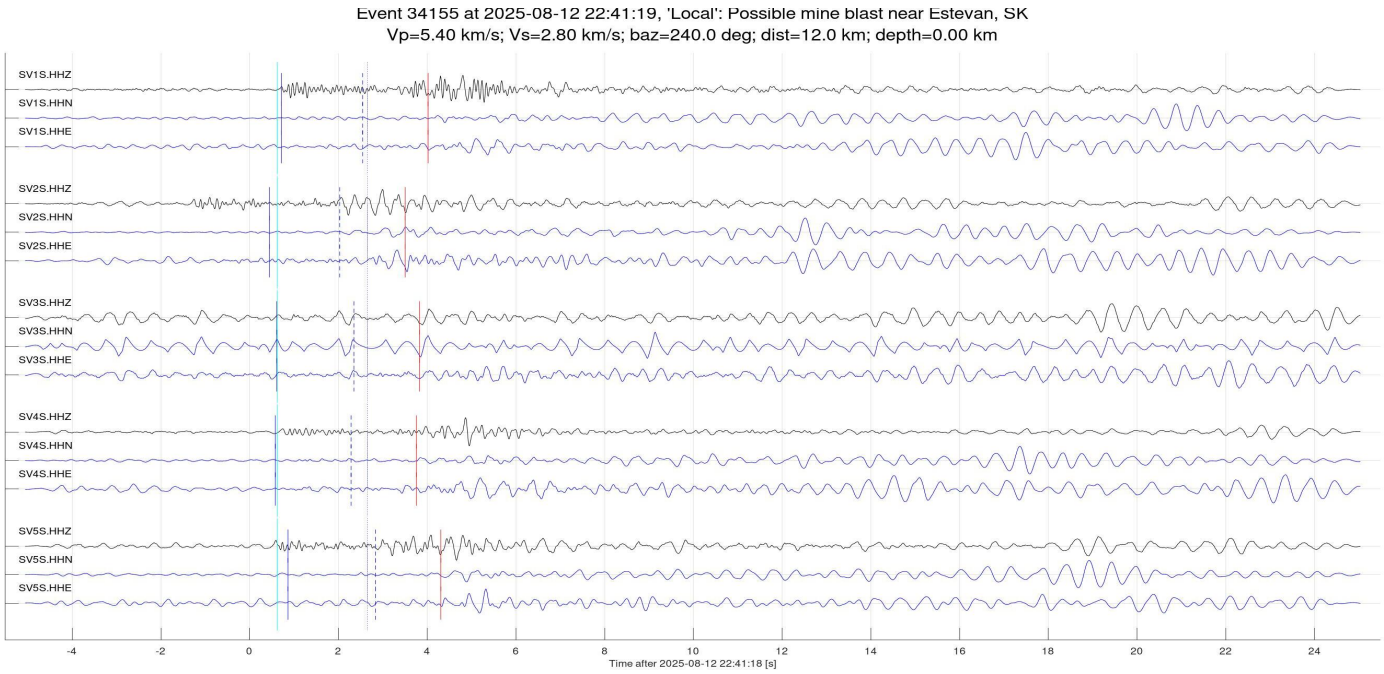


Figure 8, continued.

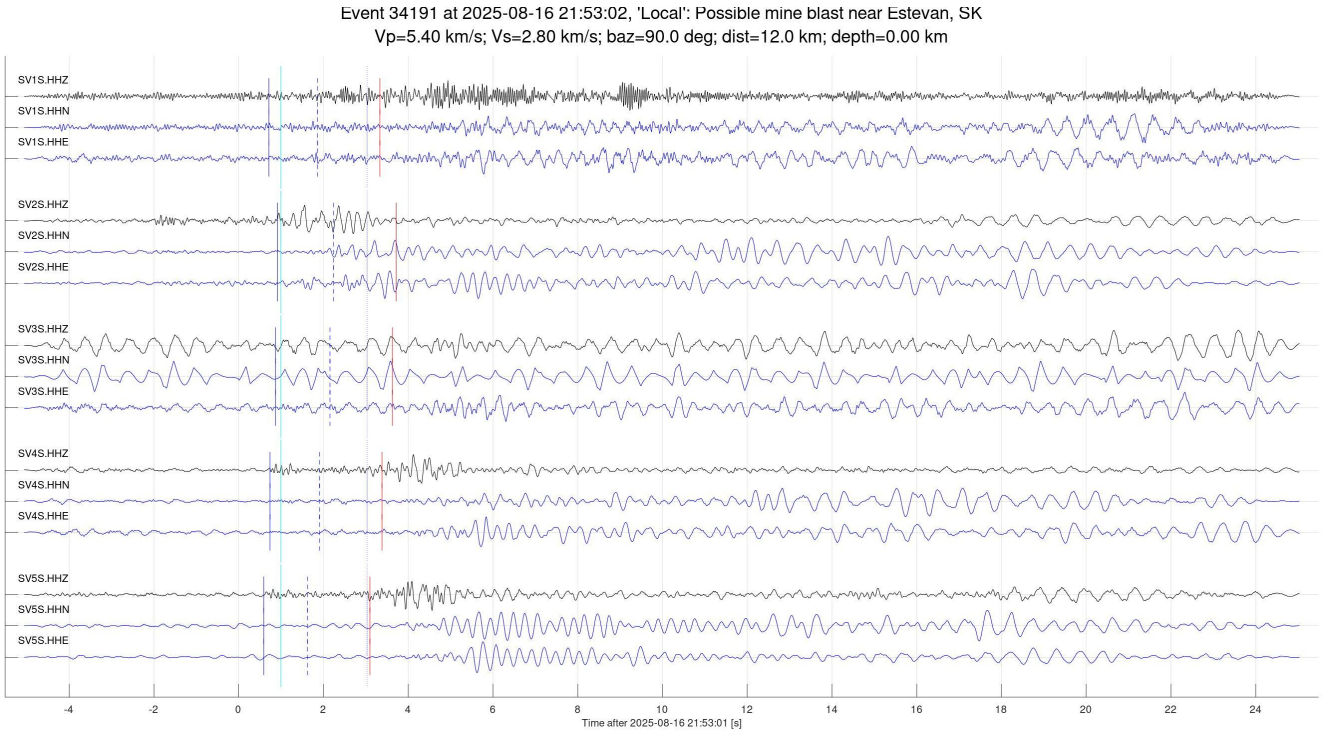


Figure 8, continued.

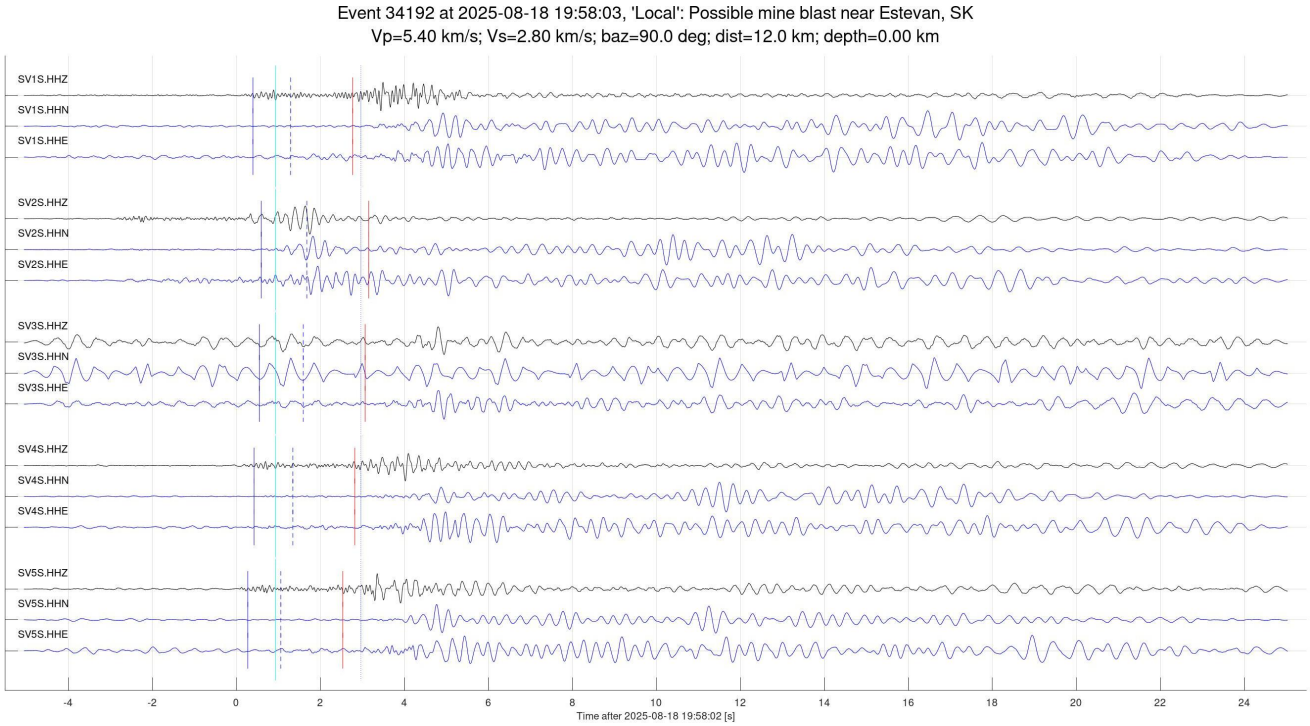


Figure 8, continued.

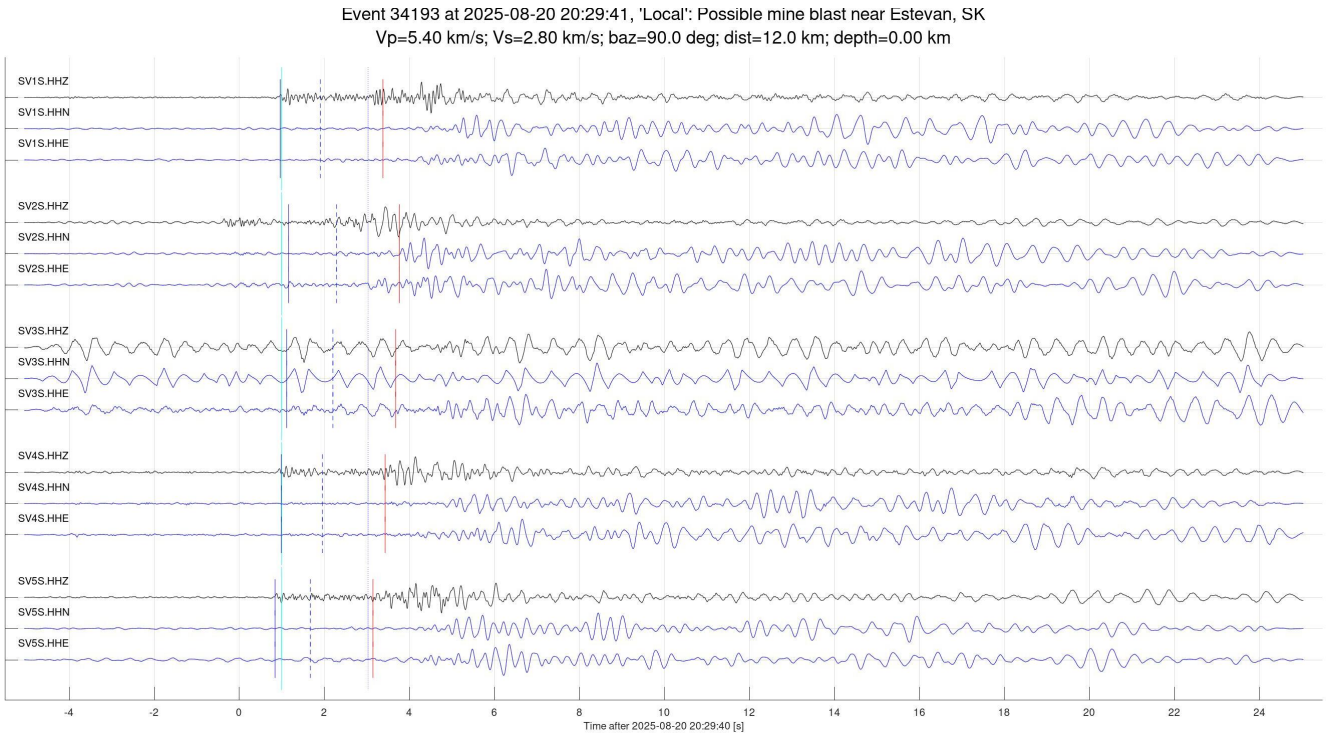


Figure 8, continued.

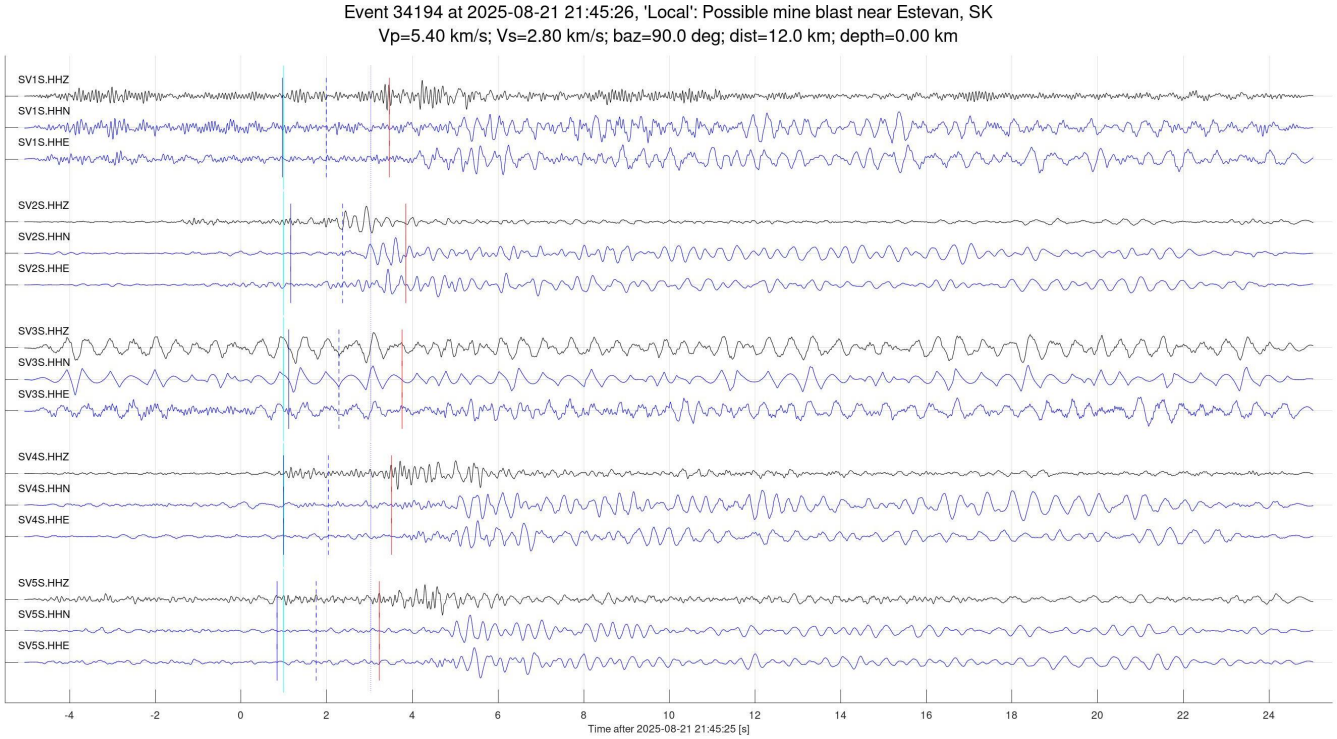


Figure 8, continued.

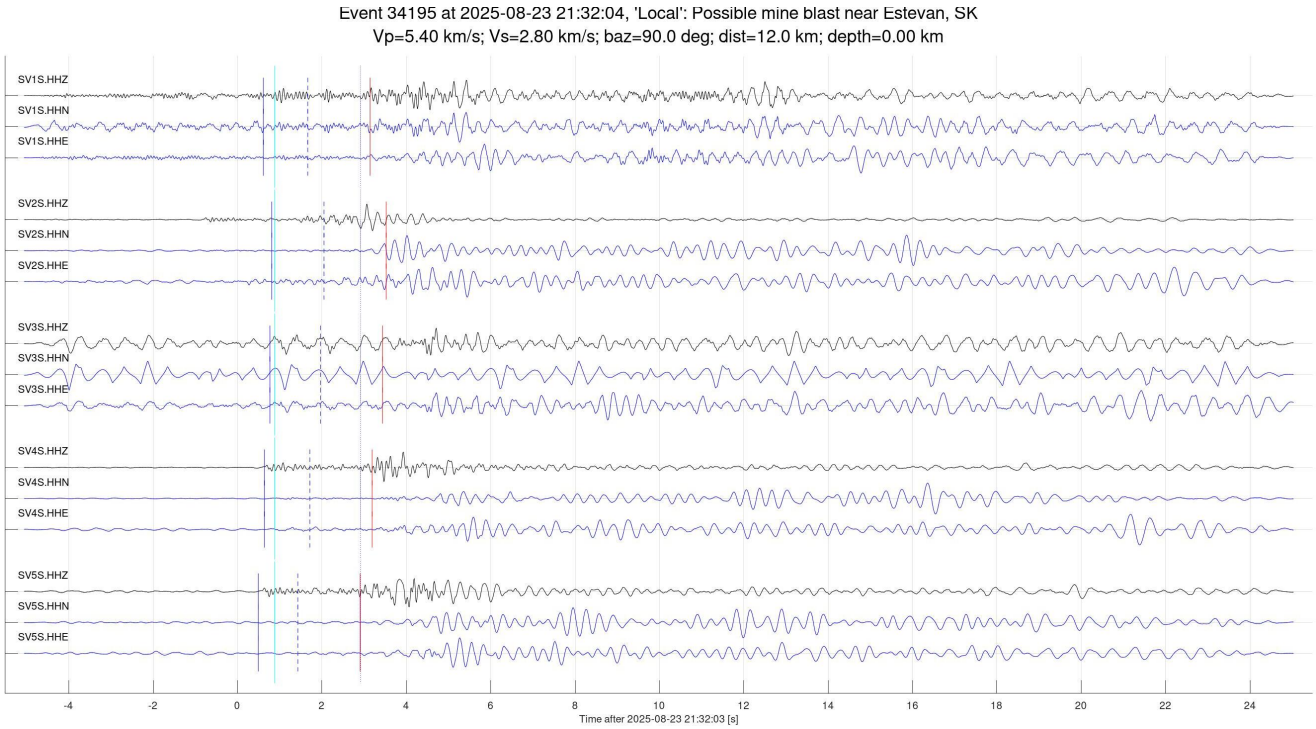


Figure 8, continued.

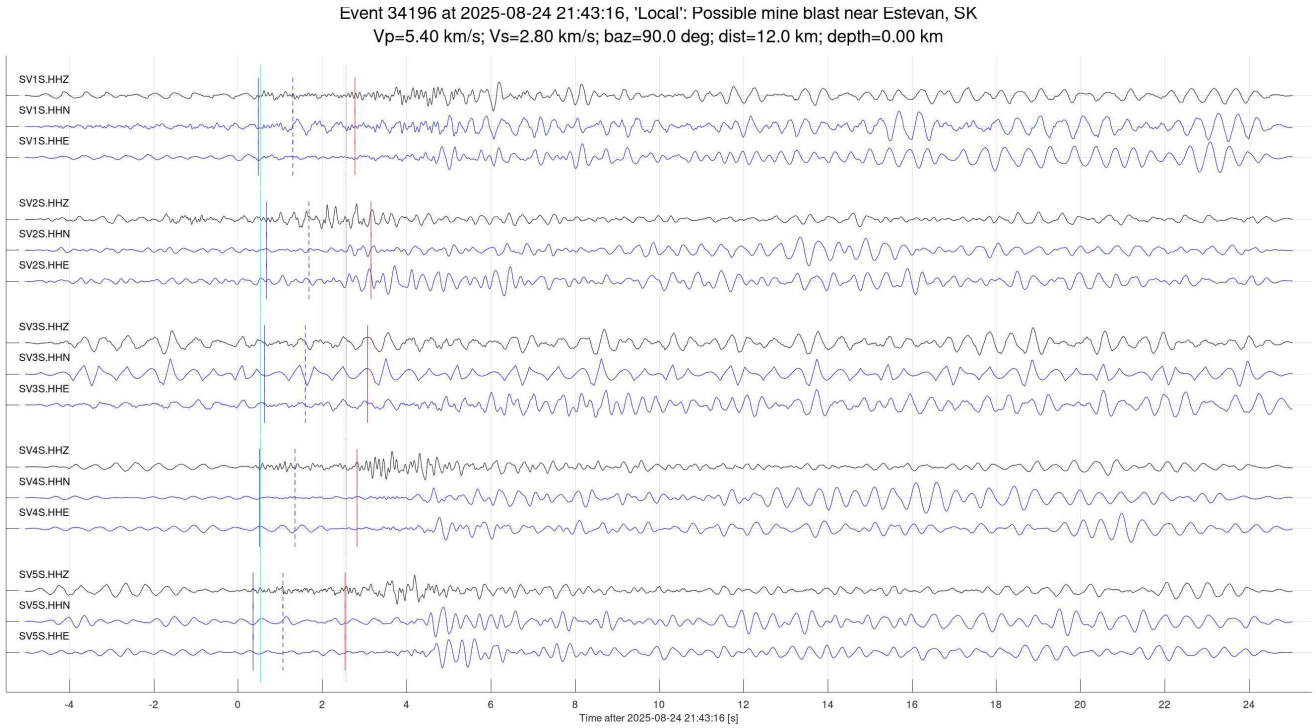


Figure 8, continued.

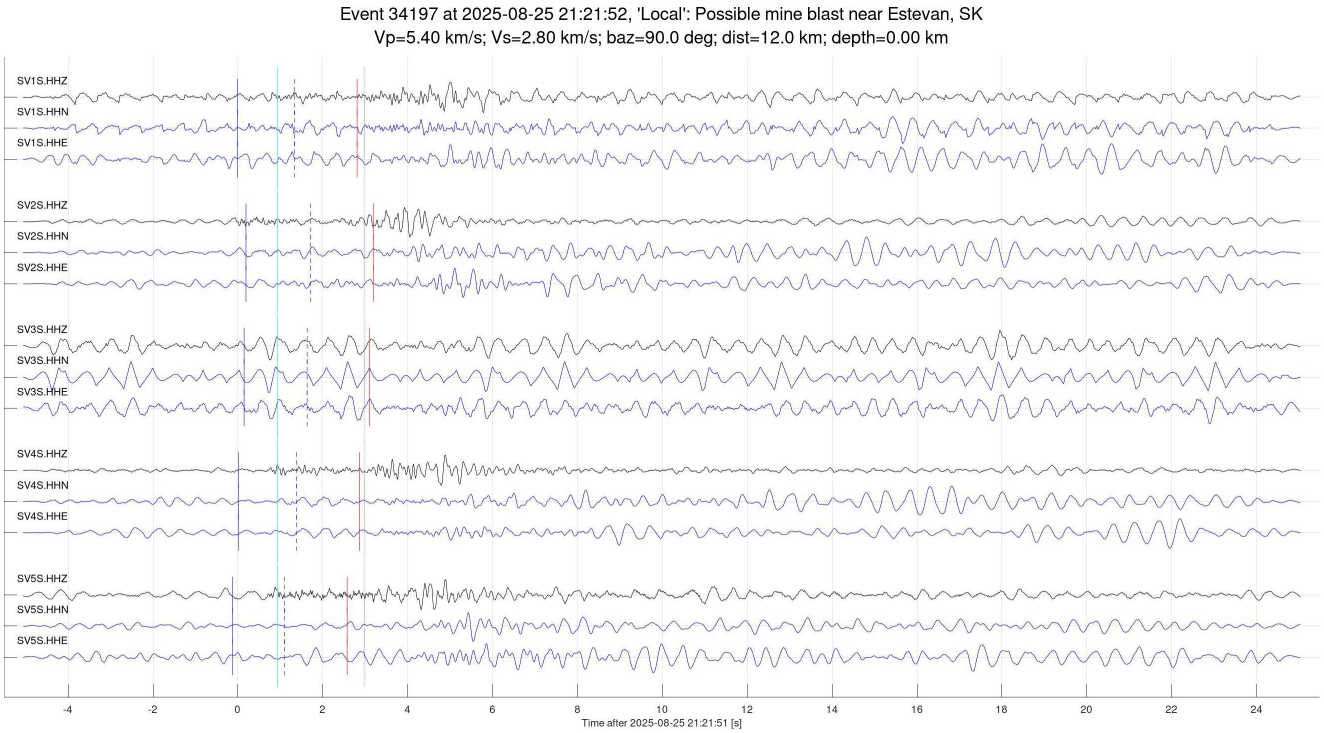


Figure 8, continued.

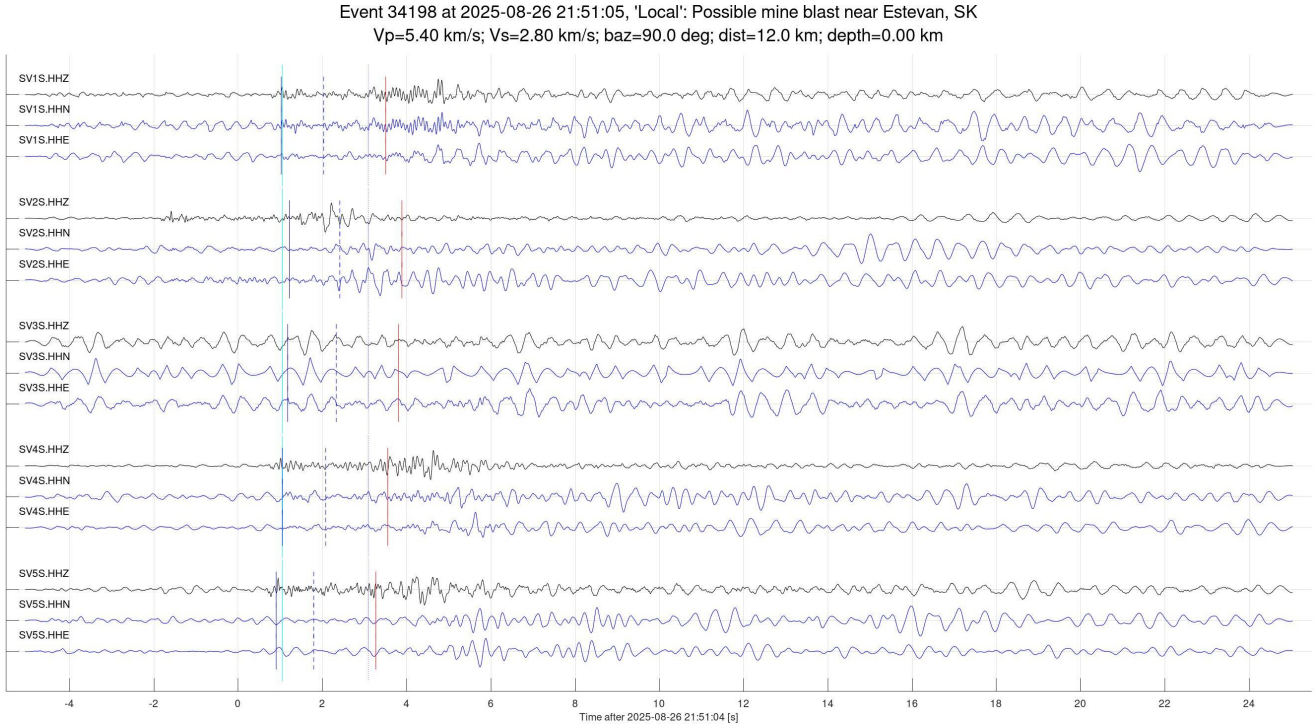


Figure 8, continued.

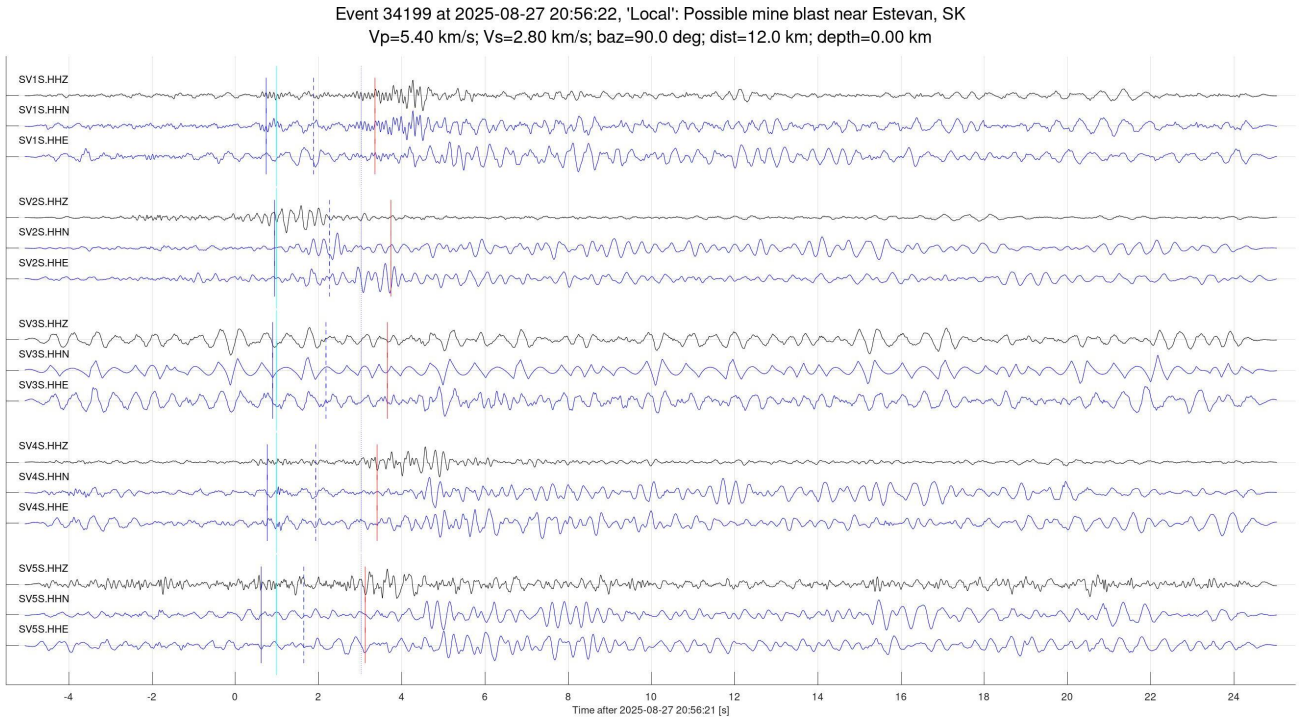


Figure 8, continued.

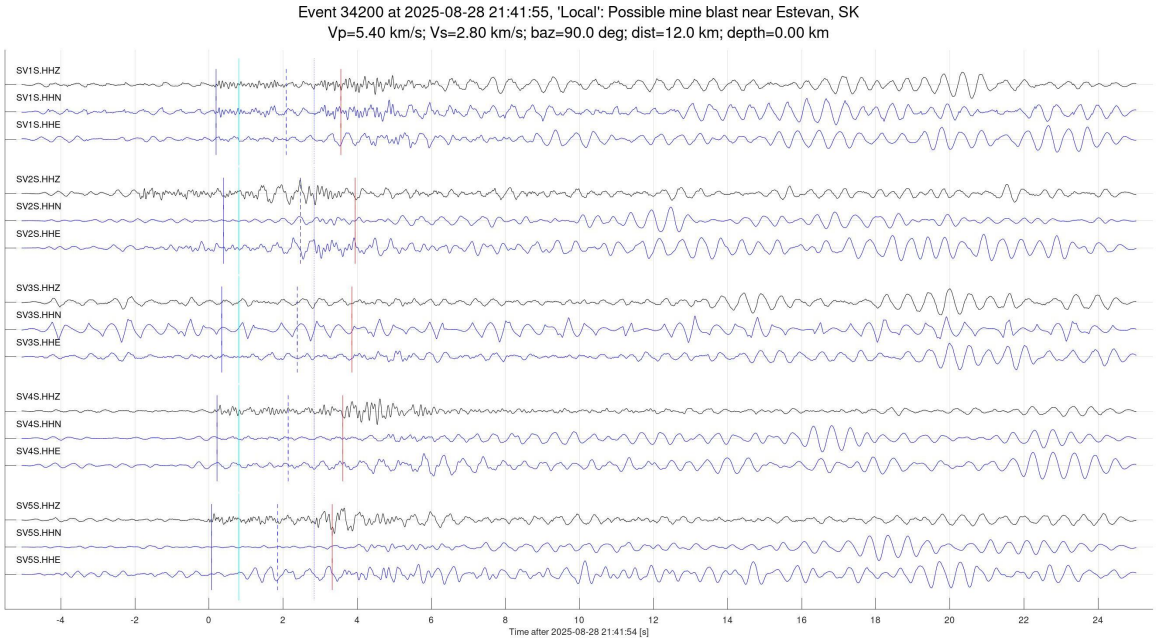


Figure 8, continued.

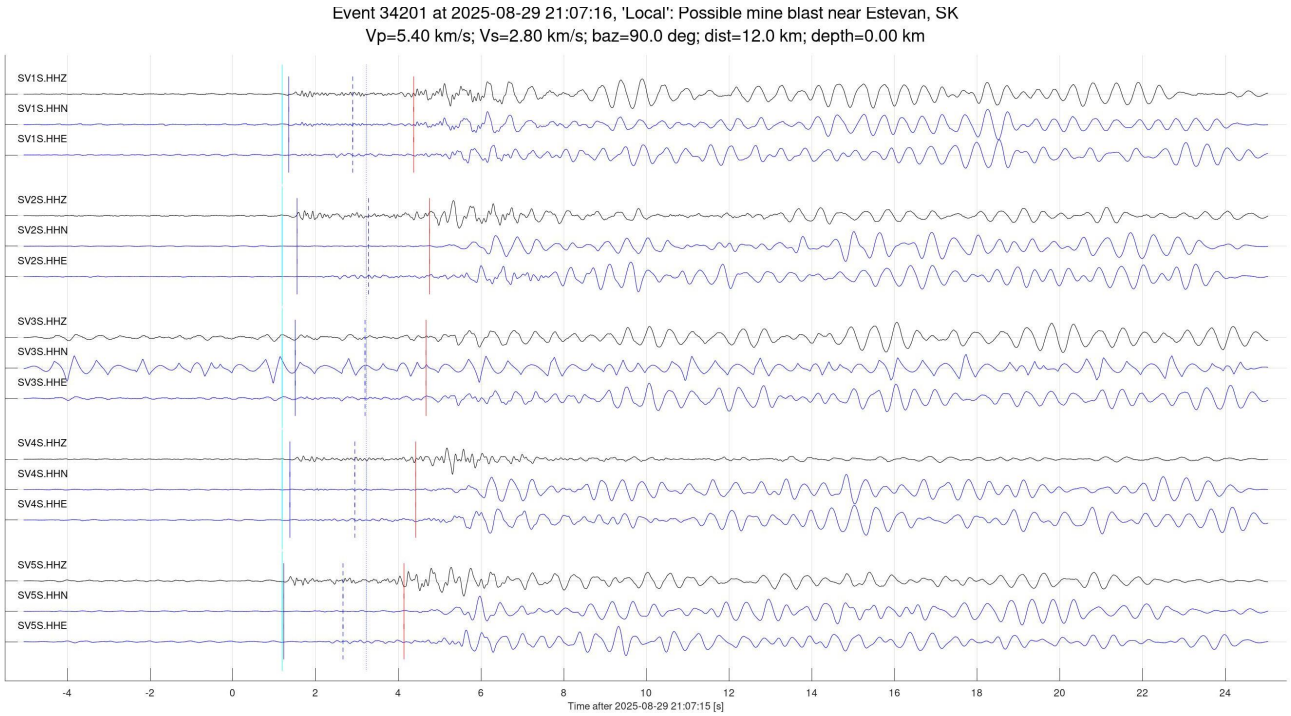


Figure 8, continued.

## Events related to mining operations (class 3b)

Numerous mining- and industrial-operations related seismic events were observed in the area. Figure 9 illustrates two of them, arbitrarily selected as appearing worth returning to later. Some of them (longer waveforms with strongly pronounced and lower dominant frequencies) may be produced by trains.

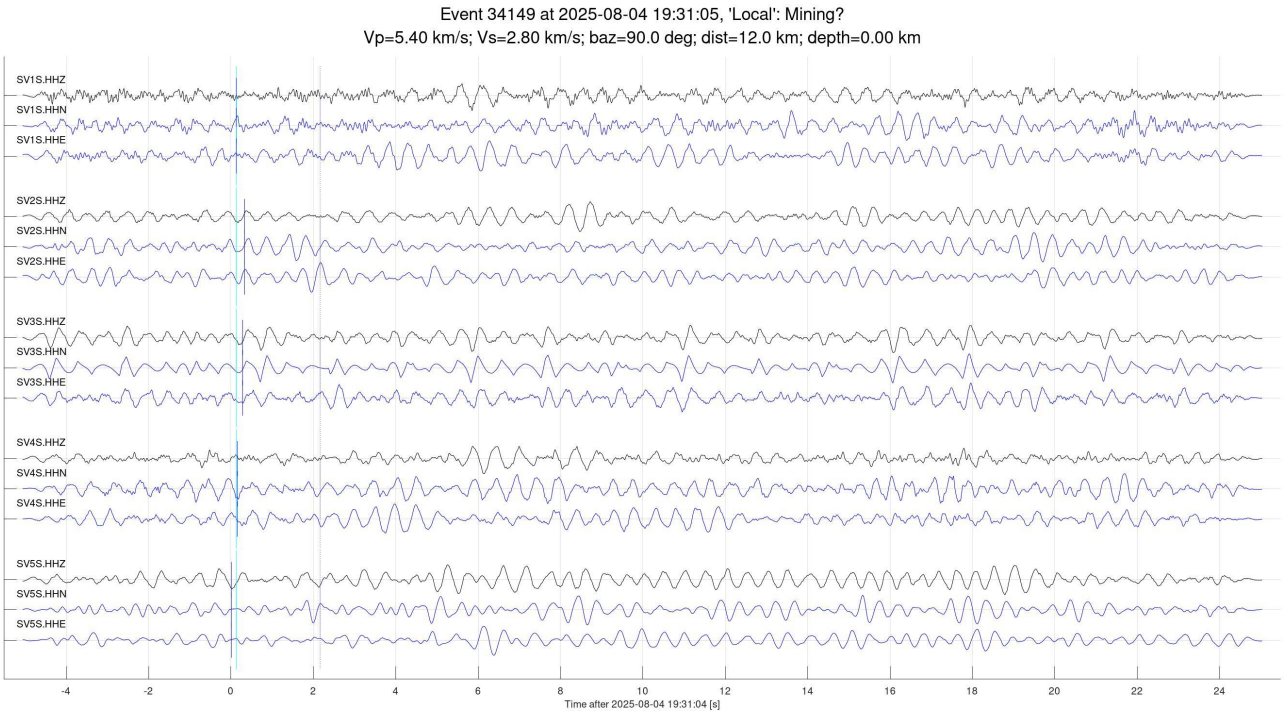


Figure 9. Sample events interpreted as due to mining activity in the area. Lines, color bars and labels are as in the preceding figures.

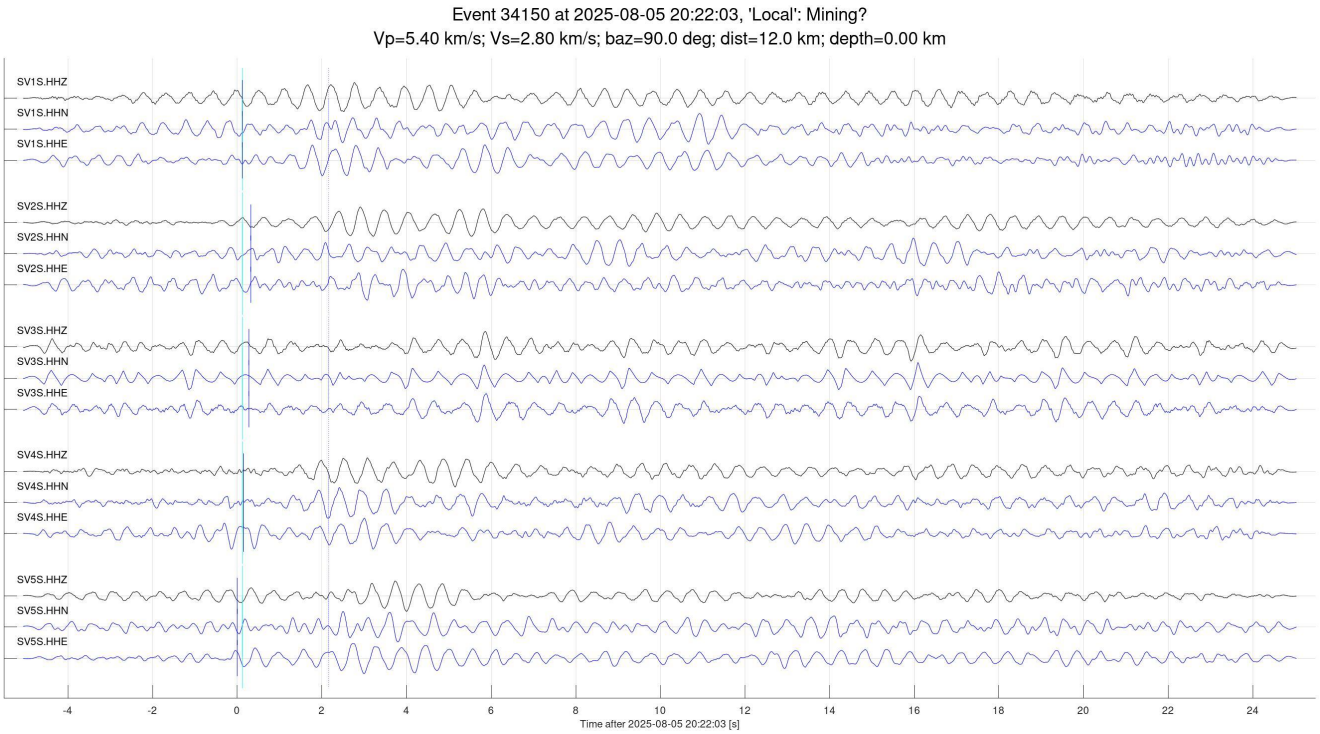


Figure 9, continued.

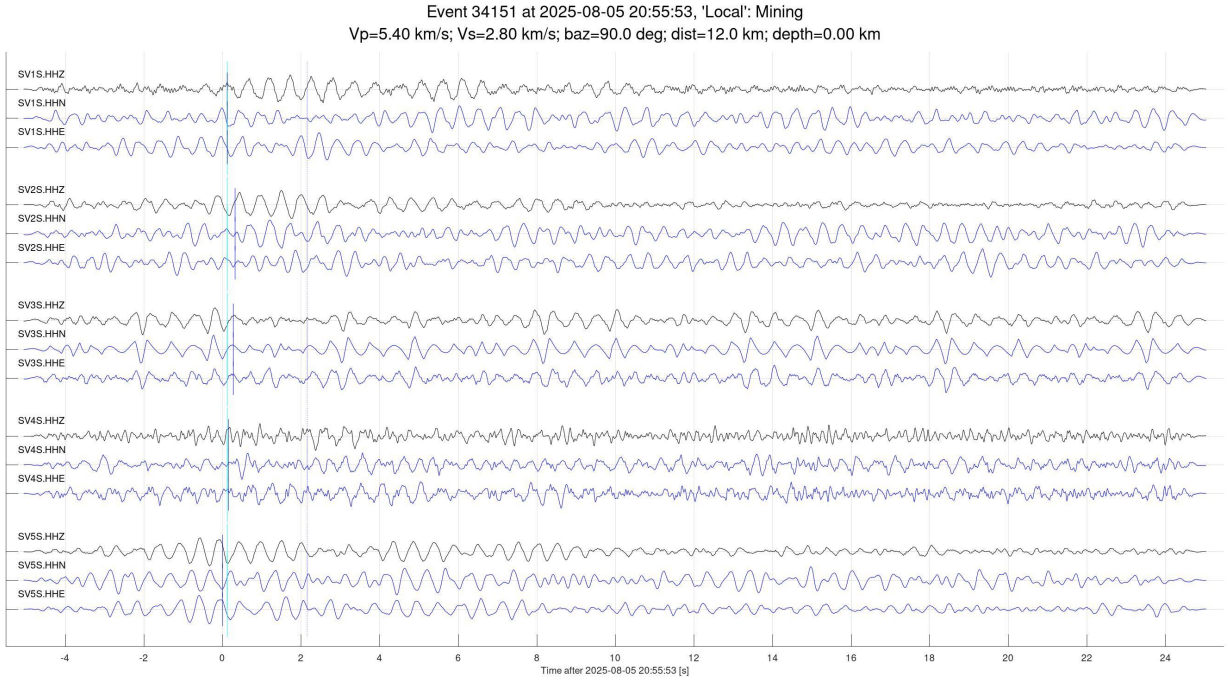


Figure 9, continued.

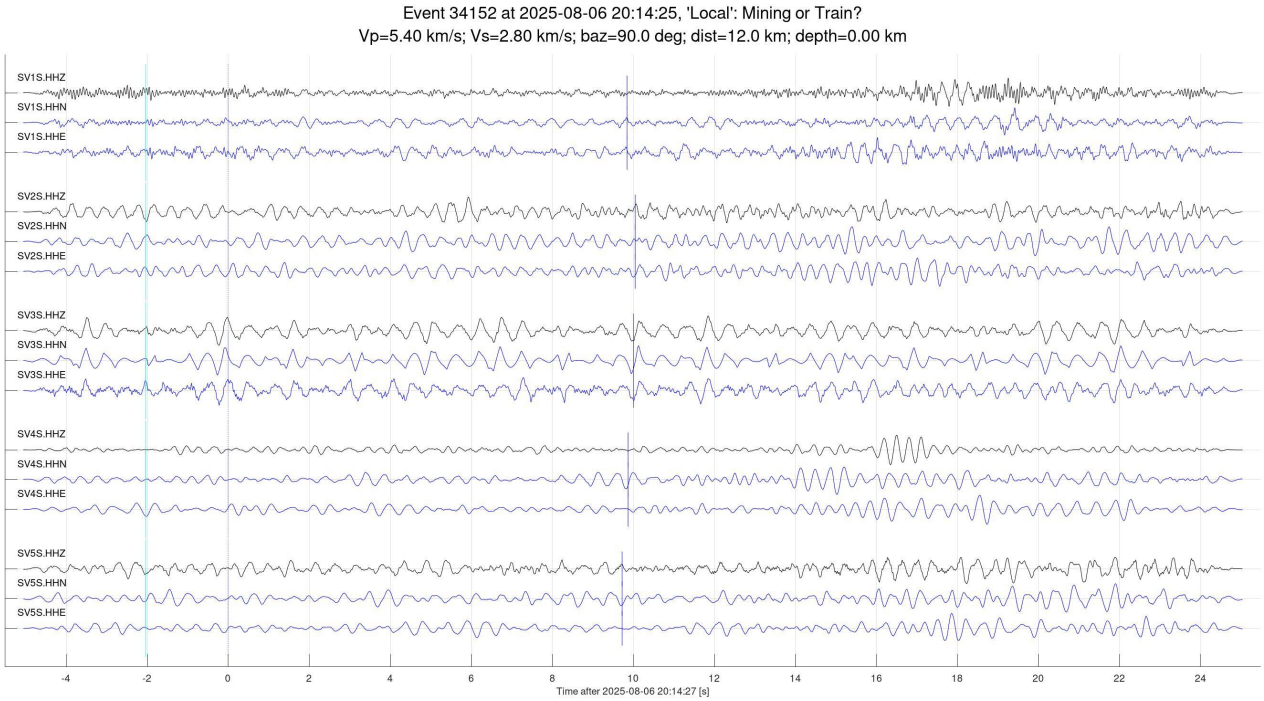


Figure 9, continued.

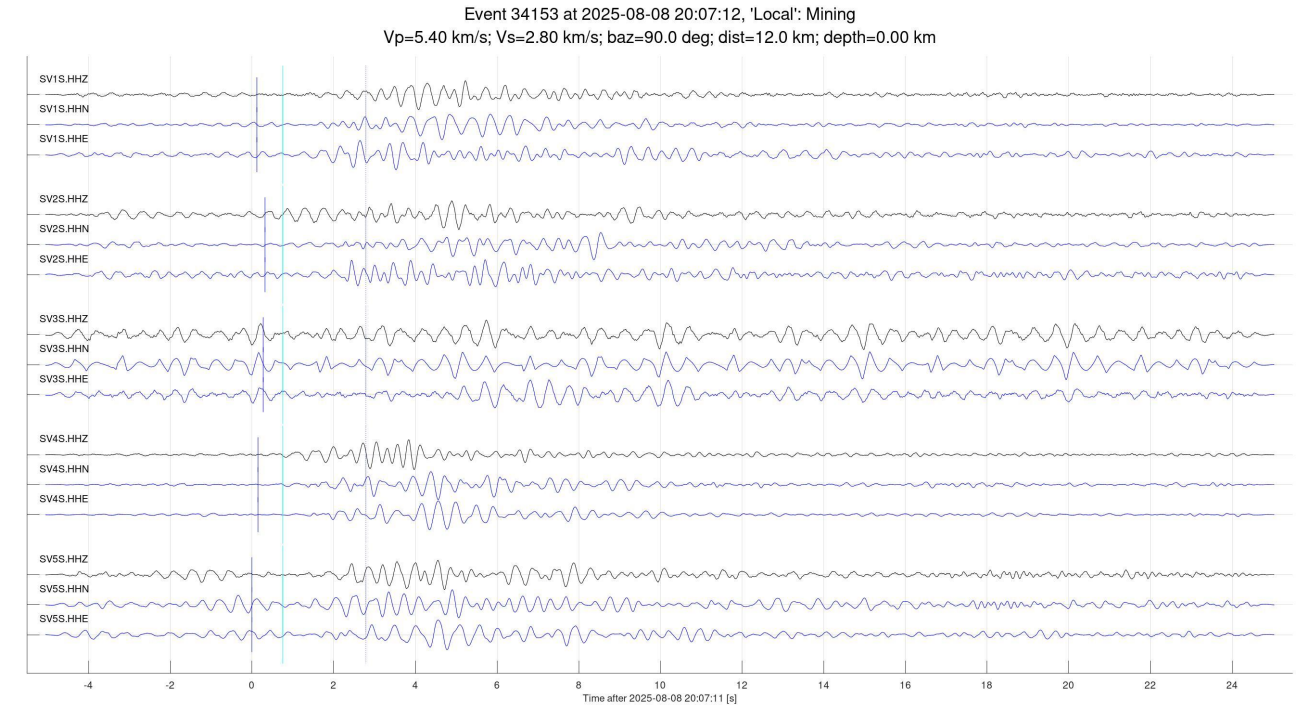


Figure 9, continued.

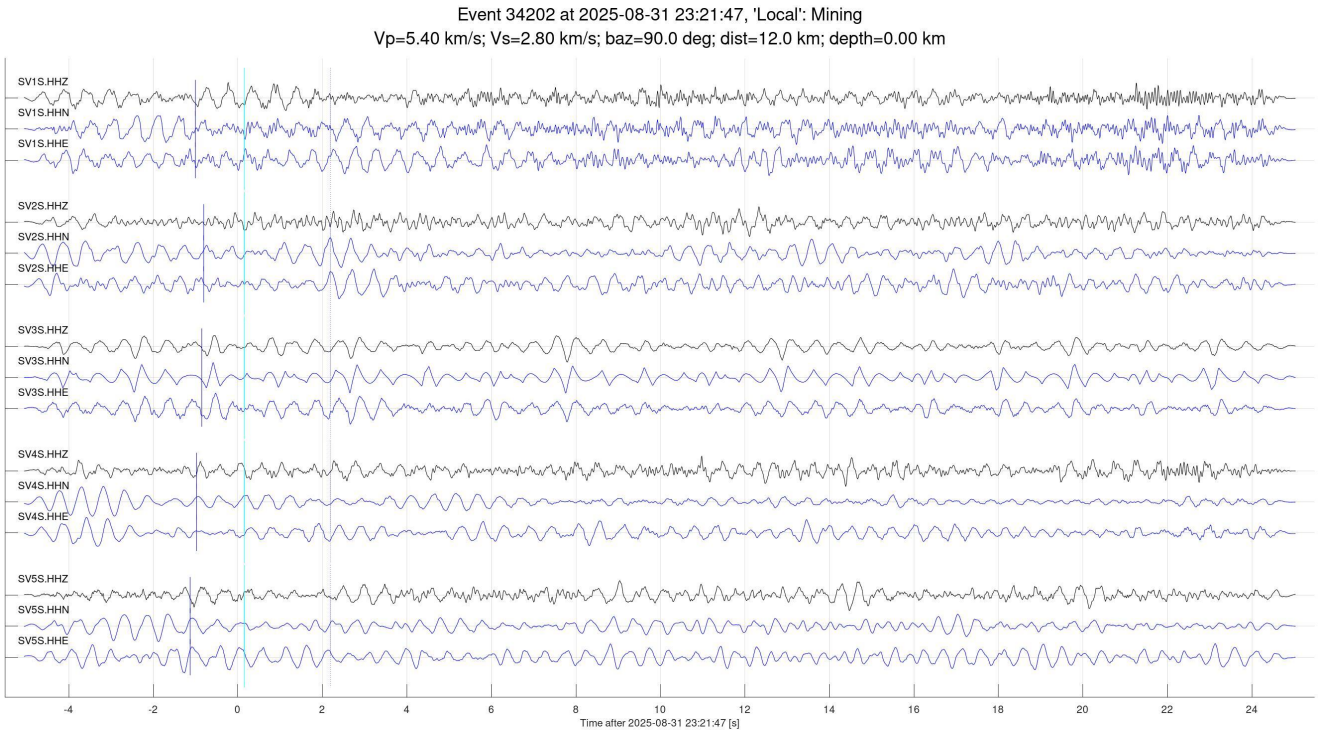


Figure 9, continued.

## Events in array proximity (classes 4a and 4b)

Six seismic events were identified as possibly occurring in the proximity of the array (class 4a) (Figure 9). All of these events likely originate in the near surface, which is suggested by strong differences in frequency content and large travel-time moveouts. However, with complex shapes of of the waveforms, noise, and using only four or five stations, it is difficult to determine the locations and depths of these sources and to differentiate between classes 4a and 4b.

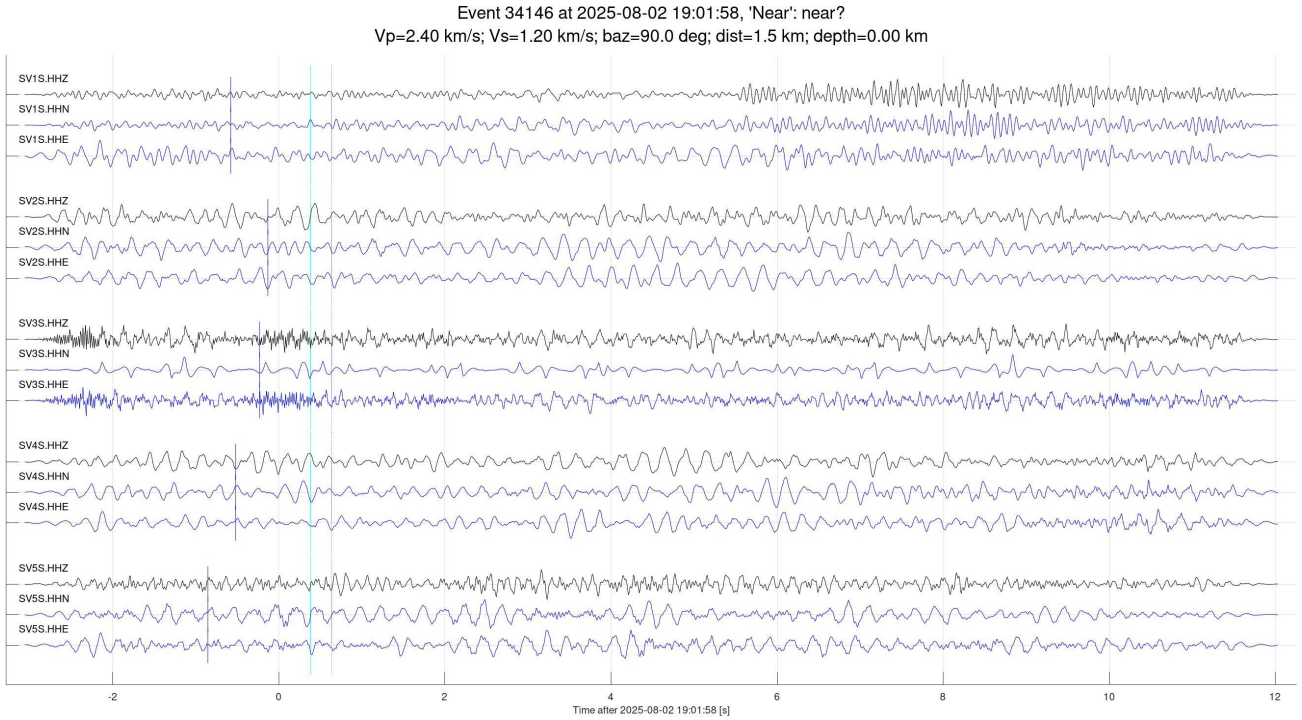


Figure 9. Events interpreted as occurring near surface in the proximity of the array (class 4a in Table 2). Lines, colour bars and labels are as in the preceding figures. Seismic velocity estimates shown in the headers (particularly P-wave) are from an averaged model and require further analysis.

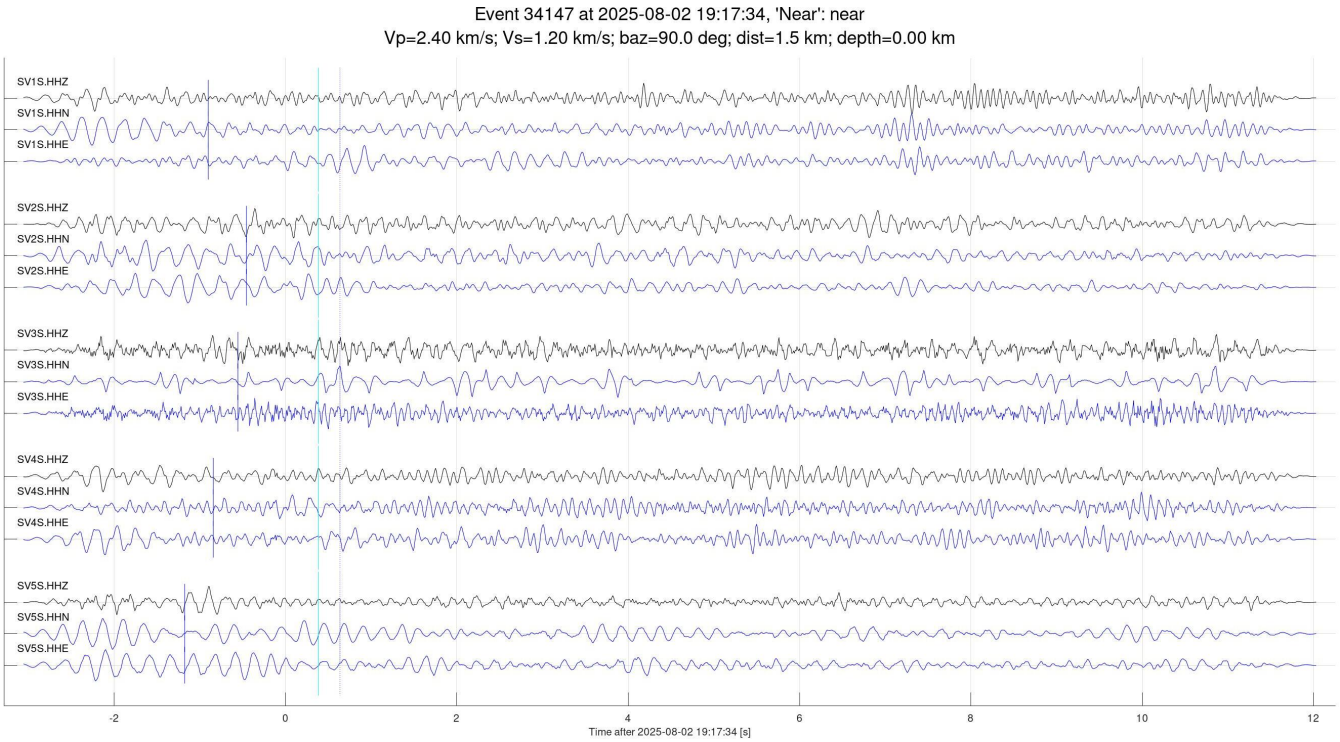


Figure 9, continued.

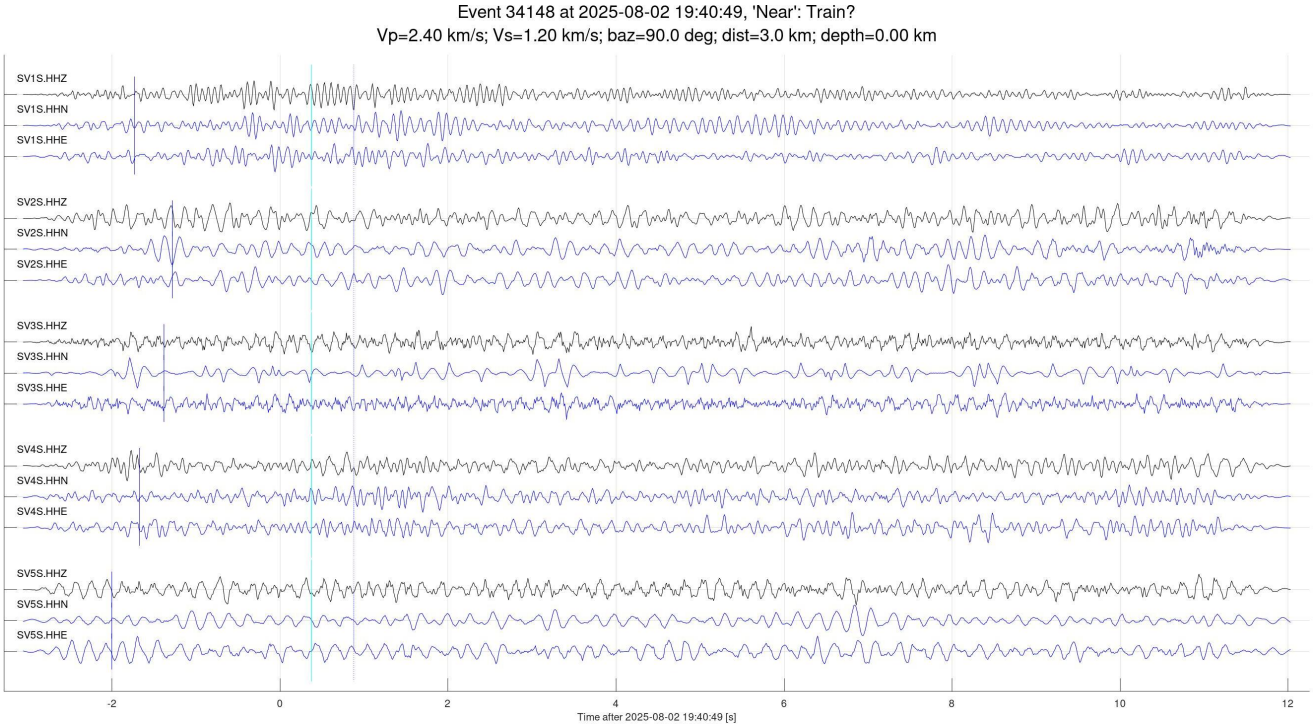


Figure 9, continued.

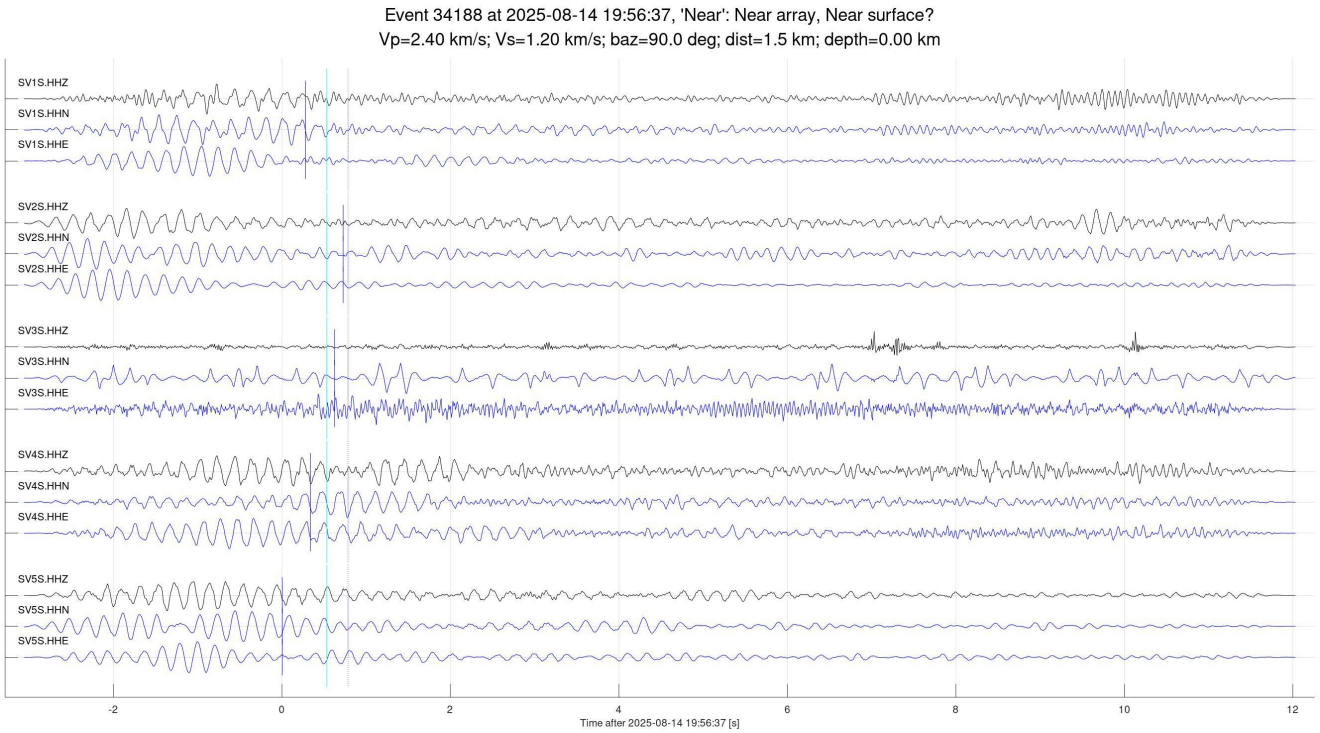


Figure 9, continued.

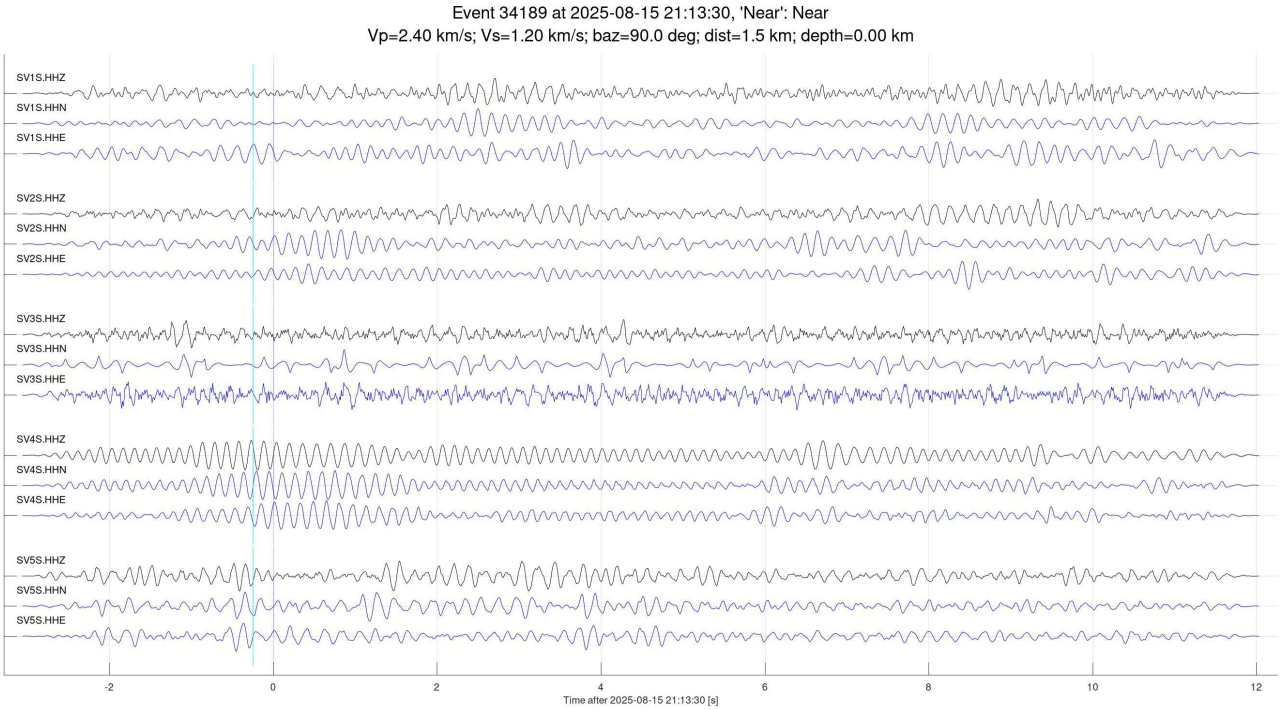


Figure 9, continued.

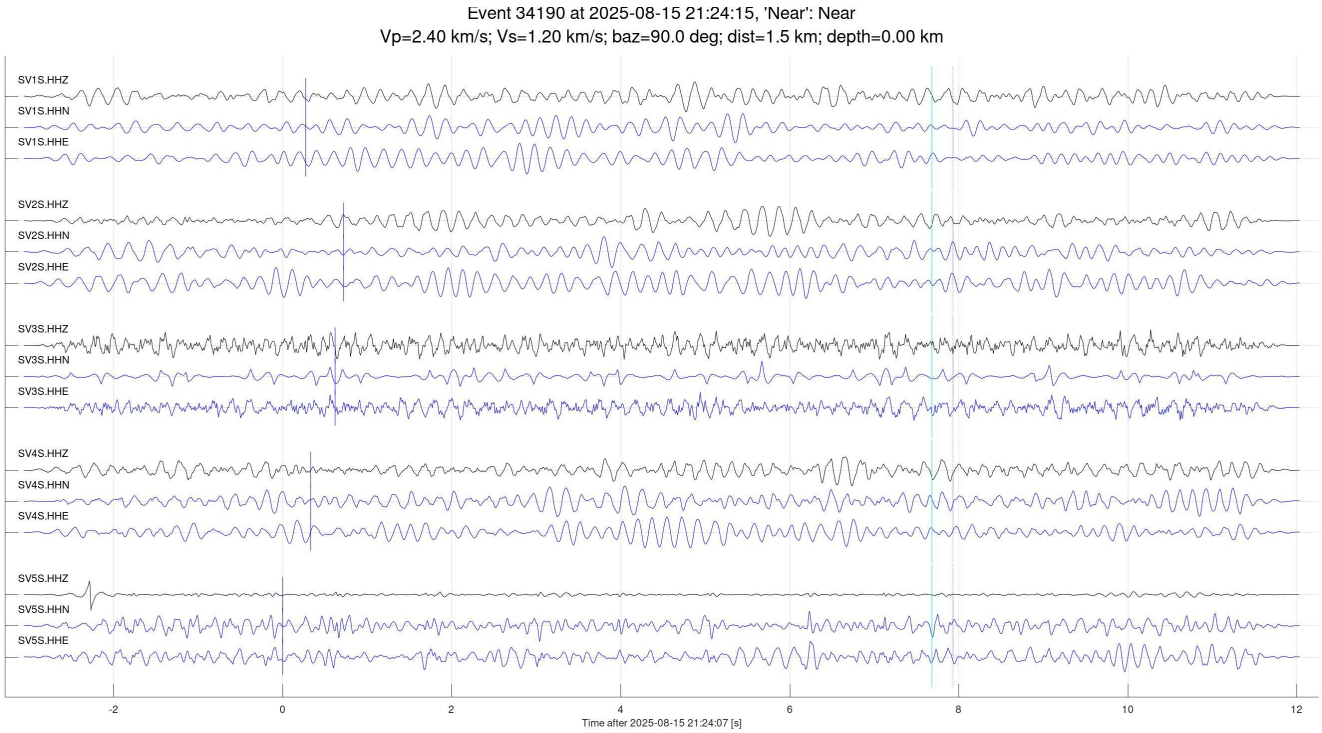

Figure 9, continued.

### *5. SEGY files*

Event time windows are provided in SEGY format in the attached zipped archive, separately for teleseismic and regional event detections. Subdirectory names and file naming convention and header formats are described in our reports for August and October 2024.

### *6. Conclusions and recommendations*

- The Aquistore array currently operates in a 4-station configuration, with station SV3S returning usable records only for strongest signals.
- 35 strong teleseismic events and 13 mine blasts were detected in August 2025. The large number of teleseismic detections is largely due to aftershocks of the big Kamchatka earthquake on July 29.
- Numerous local events were detected, likely related to mining operations or freight trains. These events were not catalogued or analyzed in detail.
- Several events occurring near-surface in the vicinity of the array were noted. No events occurring at the reservoir level were identified.